AN EXPERIMENTAL INVESTIGATION OF WIND EFFECT ON PENTAGONAL AND HEXAGONAL STAGGERED CYLINDERS

KAPIL GHOSH

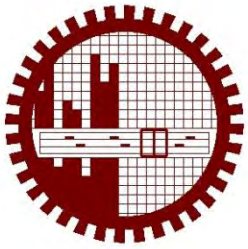

DEPARTMENT OF MECHANICAL ENGINEERING

BANGLADESH UNIVERSITY OF ENGINEERING AND TECHNOLOGY

DHAKA-1000, BANGLADESH

December, 2014

AN EXPERIMENTAL INVESTIGATION OF WIND EFFECT ON PENTAGONAL AND HEXAGONAL STAGGERED CYLINDERS

The thesis is submitted to the Department of Mechanical Engineering, Bangladesh University of Engineering & Technology (BUET), Dhaka, Bangladesh in partial fulfillment of the requirements for the degree of Master of Science in Mechanical Engineering.

THESIS PREPARED BY

Kapil Ghosh Student No: F0412102002

SUPERVISED BY

Professor Dr. Md. Quamrul Islam,
Department of Mechanical Engineering
Bangladesh University of Engineering &Technology (BUET)
Dhaka-1000, Bangladesh

Department of Mechanical Engineering
Bangladesh University of Engineering &Technology (BUET)
Dhaka-1000, Bangladesh

December, 2014

RECOMMENDATION OF THE BOARD OF EXAMINERS

The board of examiners hereby recommends to the Department of Mechanical Engineering, Bangladesh University of Engineering and Technology (BUET), Dhaka the acceptance of the thesis on "An Experimental Investigation of Wind Effect on Pentagonal and Hexagonal Staggered Cylinders". Submitted by Kapil Ghosh , Roll no: F0412102002, Session: April-2012, in partial fulfillment of the requirement for the degree of the Master of Science in Mechanical Engineering.

---------- Chairman

Dr. Md. Quamrul Islam
Professor
Department of ME, BUET, Dhaka.
(Supervisor)

---------- Member (Ex-Officio)

Dr. Md. Zahurul Haq
Head
Department of ME, BUET, Dhaka.

---------- Member

Dr. Mohammad Ali
Professor
Department of ME, BUET, Dhaka.

---------- Member

Dr. Mohammad Mamun
Professor
Department of ME, BUET, Dhaka.

---------- Member (External)

Dr. A. K. M. Sadrul Islam
Professor
MCE Department, IUT, Gazipur.

CERTIFICATE OF RESEARCH

This is to certify that the work presented in this thesis is an outcome of the investigation Carried out by the author under the supervision of Dr. Md. Quamrul Islam, Professor, Department of Mechanical Engineering, Bangladesh University of Engineering and Technology (BUET), Dhaka.

Prepared by

…….
Kapil Ghosh
Student No: F0412102002

Supervised by

…….
Dr. Md. Quamrul Islam,
Professor
Department of Mechanical Engineering
Bangladesh University of Engineering &Technology (BUET)
Dhaka-1000, Bangladesh

ABSTRACT

In this research work, an experimental investigation of wind effect on pentagonal and hexagonal staggered cylinders was carried out. The study was performed on both the single cylinder and the group consisting of three cylinders, arranged in staggered form, one pentagonal cylinder in the upstream and another two hexagonal cylinder in the downstream side. The test was conducted in an open circuit wind tunnel at a Reynolds number of 4.22 x 10^4 based on the face width of the cylinder across the flow direction in a uniform flow velocity of 13.5 m/s. At first experiment, the test was carried out on a single hexagonal cylinder at various angles of attack from 0° to 50° at a step of 10°. The surface static pressures at the different locations of the cylinder were measured with the help of inclined multi-manometers. Then the test was carried out on a single pentagonal cylinder at various angles of attack from 0° to 72° at a step of 9°. After that the group of three cylinders was taken into consideration for the study and the surface static pressures were measured for various transverse spacing of 2D, 3D, 5D and longitudinal spacing of 1D, 2D, 4D, 6D, 8D, where D is the width of the cylinder across the flow direction. In each case, the wind velocity was kept constant at 13.5 m/s. The pressure coefficients were calculated from the measured values of the surface static pressure distribution on the cylinder. Later the drag and lift coefficients were obtained from the pressure coefficients by the numerical integration method. The results will enable the engineers and architects to design buildings more efficiently. Since the results were expressed in the non-dimensional form they might be applied for the prototype building.

ACKNOWLEDGEMENTS

I wish to express my sincerest gratitude and indebtedness to Dr. Md. Quamrul Islam for his guidance and supervision throughout the entire period of the experimental investigation. His encouragement and invaluable suggestions are gratefully acknowledged.

The author is also gratefully acknowledging her deepest gratitude to Professor Dr. Mohammad Ali, Department of Mechanical Engineering, for his Constructive suggestion and advice during several phases of this problem.

Sincere thanks are offered to the staffs of the machine shop and special thanks to Mr. Md. Abul Kalam Azad, instructor of Fluid Mechanics Laboratory of Mechanical Engineering Department of BUET, Dhaka for their kind cooperation in constructing, fabricating and assembling different parts and components of the experimental set-up.

LIST OF CONTENTS

LIST OF FIGURES

NOMENCLATURE

A	Frontal area of the Cylinder
I	Net force
F_D	Drag force
F_L	Lift force
C_L	Coefficient of lift
C_D	Coefficient of drag
C_p	Coefficient of pressure
P	The static pressure on the surface of the cylinder
P_o	The ambient pressure
ρ	The density of the air
U_∞	The free stream velocity
V	Wind speed
Z	Height
dp/dn	The pressure gradient
ώ	The angular velocity of the earth
X	The latitude velocity of the earth
ΔP	Pressure difference
Δh_w	The manometer reading
γ_w	The specific weight of manometer liquid (water)
h_a	The air head
γ_a	The specific weight of air
α	The angle of attack

CHAPTER-1
INTRODUCTION

1.1 General

Wind is air in motion relative to the earth. The primary cause of wind is trace to earth‟s rotation and differences in terrestrial radiation. The radiation effects are mainly responsible for convection current either upwards or downwards. The wind generally blows horizontal to the ground at high speeds. Since vertical components of the atmospheric motion are relatively small, the term „wind‟ denotes almost exclusively the horizontal wind while „vertical‟ winds are always identified as such. The wind speeds are assessed with the aid of anemometers or anemographs, which are installed at the meteorological observations at heights generally varying from 10 to 30 meters above ground.

The subjects of wind load on buildings and structures are not a new one. In the 17^{th} century, Galileo and Newton have considered the effect of wind loading on buildings, but during that period, it did not gain popularity. The effect of wind loading on buildings and structures has been considered for design purposes since late in the 19^{th} century; but starting from that time up to about 1950, the studies in this field have not been considered seriously. Building and their components are to be designed to withstand the code specified wind loads. Calculating wind loads is important in the design of wind force resisting system, including structural members, components, and cladding against shear, sliding, overturning, and uplift actions.

In recent years, much emphasis has been given on “The study of wind effect on buildings and structures” in the different corners of the world. Even researchers in Bangladesh have taken much interest in this field. Till now, little attention has been paid to the flow over the bluff bodies like square cylinders, rectangular cylinders, hexagonal cylinders, octagonal cylinders etc. and some information is available concerning the flow over them in staggered condition, although this is a problem of considerable practical significance. With the progressing world, Engineering problems regarding wind loads around a group of skyscrapers, chimneys, towers and the flow induced vibration of tubes in heat exchangers, bridges, oil rigs or marine structures need detailed investigation of flow patterns and aerodynamic characteristics.

Arising from the increasing practical importance of bluff body aerodynamics, over the past few decades‟ sufficient effort has been given in research works concerning laboratory

simulations, full-scale measurements and more recently numerical calculations and theoretical predictions for flows over bodies of wide variety of shapes. A number of failures of bridges, transmission towers, buildings and housings over the last one hundred years prompted researchers to do research work in this field. Some of the pioneer researchers in the field are Smeaton (1759), Vogt (1880), Irminger (1891), Eiffel (1900) and Stanton (1907).

Irminger in 1891 published results of measurements on models, which was probably the first-ever wind tunnel test and Eiffel in the period up to 1900, following completion of the famous tower, conducted pioneer studies on the flow velocities and tower movements from a laboratory at the top of the tower.

The study of wind effect was first limited to loading on buildings and structures only, possibly because of its most dramatic effects are seen in their collapses. In mid-sixties, researchers started the study of less dramatic, but equally important environmental aspects of flow of wind around buildings. These include the effects on pedestrians, weathering, rain penetration, ventilation, heat loss, wind noise and air pollution etc. The pioneer researcher in this field is Lawson, T.V. [17] of the University of Bristol. A number of works of the environmental aspects of wind was being studied at the Building Research Establishment at Garson and the University of Bristol, UK.

It is true that researchers from all over the world have contributed greatly to the knowledge of flow over bluff bodies as published by Mchuri, F. G. [35] but the major part of the reported works are of fundamental nature involving the flow over single body of different profiles. Most of the researchers have conducted works either on single cylinder with circular, square, octagonal, hexagonal or rectangular sections etc. or in a group with them for various flow parameters. However, the flow over a combination of pentagonal and hexagonal cylinders has not been studied extensively especially in-groups to date, although this is a problem of practical significance. It is believed that the study on the cylinder with pentagonal and hexagonal section will contribute to find the wind load on the single and group of pentagonal and hexagonal buildings and the results will be useful to the relevant engineers and architects.

1.2 Nature of the Wind

Very strong winds are generally associated with cyclonic storms, thunderstorms, dust storms or vigorous monsoons. A feature of the cyclonic storms over the Bangladeshi region is that they rapidly weaken after crossing the coasts and move as depressions or lows inland. The influence of a severe storm after striking the coast does not in general exceed about 60 kilometers, though sometimes, it may extend even up to 120 kilometers. Very short duration hurricanes of very high wind speeds called Kal Baisaki or Norwesters occur fairly frequently during summer months over North East Bangladesh. The wind behavior is discussed in this section in brief. The characteristics of the wind, which are more or less related to the present study, have been taken into consideration for discussion in a nutshell.

1.2.1 Wind Velocity

High wind velocity is responsible for the failure of building and structures and it can cause unpleasant side effects also. Strong winds often have special names, including gales, hurricanes and typhoons. The wind speeds recorded at any locality are extremely variable and in addition to steady wind at any time, there are effects of gusts, which may last for a few seconds. Because of the inertia of the building, short period gusts may not cause any appreciable increase in stress in main components of the building and structure. The response of a building to high wind pressures depends not only upon the geographical location and proximity of other obstructions to airflow but also upon the characteristics of the structure itself.

Winds are named by the direction they come from. Thus a wind from south, blowing toward the north is called a south wind. Windward refers to the direction a wind comes from, leeward to the direction it blows toward. When a wind blows more frequently from one direction than from any other it is called a prevailing wind. Wind speed increases rapidly with height above the ground level, as frictional drag declines. Wind is commonly not a steady current but is made up of a succession of gusts, slightly variable in direction, separated by lulls. Close to the earth the gustiness is developed due to irregularities in the wind are caused by the conventional currents. All forms of turbulence play a part in the process of transporting heat, moisture and dust into the air aloft.

There are various parameters, which control the flow behavior as mentioned by Castro, J.P. [7] They are (i) vortices in front of the building, (ii) opening through buildings, (iii) spacing of rows, (iv) wakes of buildings, (v) long straight streets, (vi) narrowing streets, (vii) corners

and (viii) courtyards. The mean wind speed varies with height. The variation of wind speed has been expressed by Davenport, A. G. [14] as

$$V = V_c(Z/Z_c)^a \quad (1.1)$$

Where, V is the mean wind speed at a height Z, V_c is the mean wind speed at the gradient height Z_c. The value of V_c depends upon the geographical locality, but Z_c is a function of terrain. Values of Z_c and the exponent "a' suggested by Davenport, A. G. [14] are as follows:

For open terrain with very few obstacles : a = 0.16, Z_c = 300m

For terrain uniformly covered with obstacles 10-15 in height: a = 0.28, Z_c = 430m

For terrain with large and irregular objects : a = 0.40, Z_c = 560m

1.2.2 Generation of Wind

The source of wind energy is the sun that emits solar radiation, which causes differential heating of the earth surface and the atmosphere. In the atmosphere there is a general convective transport of heat from lower to higher latitudes in order to make the earth's radiation imbalance as mentioned by Lanoville, A. [28] It is for this reason that the atmosphere is a restless medium in which circulation of all sizes is normal. Wind is simply air moving in a direction that is essentially parallel with the earth's surface. The atmosphere is fixed to the solid-liquid earth in gravitational equilibrium and so moves with the earth in its west to east rotational movement. Wind, therefore is air movement in addition to that associated with rotation. In large-scale circulation covering several thousand miles, horizontal motion greatly exceeds vertical motion. Thus, a wind that takes several days to cross an ocean may move up or down only a few miles. The vertical component of movement is much greater in small-scale circulation such as thunderstorms and tornadoes. In a thunderstorm, air may ascend to the top of the atmosphere in about an hour.

Wind is complex in origin. Usually, its direct cause lies in differences between atmospheric densities resulting in horizontal differences in air pressure. That is, it represents nature attempt to rectify pressure inequalities. When these horizontal pressure differences develop, a gradient of pressures exists. But in spite of the direct part played by pressure differences, the ultimate source of average for generating and maintaining winds against the drag is mainly from the differences in heating and cooling between high and low latitudes.

1.2.3 Forces Governing Winds

Four forces operate to determine the speed and direction of winds: (i) pressure gradients force, (ii) coriolis force, (iii) frictional force, (iv) centrifugal force.

i) Pressure Gradient Force

This sets the air in motion and causes it to move with increasing speed along the gradient. The magnitude of the force is inversely proportional to the isobar spacing. Since the gradient slopes downward from high to low pressure, direction of airflow is from high to low pressure along the pressure gradient. But due to the rotation of the earth, the trajectory of an air particle moving from high to low pressure is very indirect, except close to the equator.

ii) Coriolis Force

This is the deflecting force of the earth's rotation that affects only the direction of wind. Except at the equator, winds and all other moving objects, no matter what their direction, are deflected to the right of the gradient in the northern hemisphere and to the left in the southern hemisphere. The force acts at right angles to the direction of motion. Coriolis force is stronger in higher latitudes. When pressure gradient is balanced by the Coriolis force, wind blows parallel with the isobars and it is called geotropic wind. The geotropic wind V_c can be estimated from the expression as suggested by Davenport, A. G. [14].

$$V_c = (dp/dn)\,(2\rho\omega \sin x) \tag{1.2}$$

Where (dp/dn) is the pressure gradient, ω is the angular velocity of the earth, x is the latitude and ρ is the air density. Outside the atmosphere friction layer may be extended up to 1000m above the earth's surface. Winds actually do blow in a direction almost parallel with the isobars with low pressure on the left and high pressure on the right in the northern hemisphere.

iii) Frictional Force

This affects both wind speed and direction. Friction between the moving air and the earth's land-sea surface tends to slow the movement of air. Because of the frictional effects of the land-sea surface upon air flowing over it, surface air does not flow essentially parallel with the isobars as it does aloft, but instead crosses them at an oblique angle. The greater the friction, the wider is the angle the wind direction makes with the isobars. Winds over irregular land surfaces usually form angles varying from 20^0 to 45^0 with the isobars. But over oceans, the angle may be as little as 10^0.

iv) Centrifugal Force

This force comes into picture only when air moves in a curved path. Centrifugal force is a major factor only when the wind is strong and the radius of curvature small as they are in tropical hurricanes, tornadoes and the centers of a few usually well-developed cyclonic storms. The flow of air which is necessary to balance pressure force, Coriolis force and centrifugal force in absence of frictional force is called gradient wind. This happens at heights greater than 500 m or so.

1.3 Wind Loading on Structures

The effect of wind on the structure as a whole is determined by the combined action of external and internal pressures acting upon it. In all cases, the calculated wind loads act normal to the surface to which they apply. The pressures created inside a building due to access of wind through openings could be suction (negative) or pressure (positive) of the same order of intensity while those outside may also vary in magnitude with possible reversals. Thus the design value shall be taken as the algebraic sum of the two in appropriate/concerned direction. Furthermore, the external pressures (or forces) acting on different parts of a framework do not correlate fully. Hence, there is a reduction in the overall effect.

The development of modem materials and construction techniques has resulted in the emergence of a new generation of structures. Such structures exhibit an increased susceptibility to the action of wind. Accordingly, it has become necessary to develop tools enabling the designer to estimate wind effects with a higher degree of refinement than has been previously required. It is the task of the engineer to ensure that the performance of structures subjected to the action of wind will be adequate during their anticipated life from the standpoint of both structural safety and serviceability. To achieve this end, the designer needs information regarding (i) the wind environment, (ii) the relation between that environment and the forces it induces on the structures, (iii) the behavior of the structure under the action of forces.

The action of wind on building considering the load effect may be classified into two major groups; the static effect and the dynamic effect. There are many other effects like generation of noise the risk of the hazard, the penetration of rain and uncomfortable wind for the pedestrians etc. but they are not usually considered for structural design. Since all wind

loadings are time-dependent because of varying speeds and direction of winds, wind loading is never steady. For this reason, static load is referred to the steady (time-variant) forces and pressures tending to give the structure a steady displacement. On the other hand, dynamic effect has the tendency to set the structure oscillating. A steady wind load on a building is very difficult to achieve. In fact, always wind loads are of a fluctuating nature because of varying speeds and directions of winds. The type of wind and the stiffness and roughness of the structure determine the nature of loading on a building. When a building is very stiff the dynamic response of the structure may be neglected and only the static leads may be considered. This is because the natural frequency of an extremely stiff building is too high to be excited by wind. In the present study the effect of static loading is taken into account due to the steady wind. Since natural winds are continually fluctuating, it is generally assumed that these fluctuations are so irregular and random that the response of a structure will not differ from that due to a steady wind of the same average speed. Very recently the dynamic response of building has been considered for study because of the modern tendency to build more slender and lighter structures.

1.4 Necessity of the Study

Housing and mankind is the basic primary need next to food and clothing, clear air and portable water being very essential for existence. In Bangladesh, strong wind is an annual natural hazard due to its geographical location. On the other hand, most of the existing houses and those which are going to be built in the next few decades are likely to be non-engineered, mostly with thatched roofs and are vulnerable to wind. Strong wind is causing immense losses of rural dwellers by making their houses collapse fully or partially by lifting of roof etc. Almost 70% of the population in the rural sector and 50% of the population in the urban sector are living below the poverty level with earnings too little to pay for all needs. It is this group of people most impoverished that is to be provided with good housing. About 75% of the dwelling in rural areas is of kutcha construction (Mud, Bamboo, Woven Bamboo etc.) and that 23% of urban and more than 40% of rural dwellings are of a temporary nature. They can rarely survive against even a moderate intensity storm. Evidence from the field in strong wind-prone areas indicates that there is a socially perceived need of more engineering knowledge and improved construction of domestic dwelling.

Bangladesh is a land hungry country. The urban population of this country is increasing at a very fast rate making the housing problem worse every day. One possible solution of the

housing problem is to construct multistoried buildings. The knowledge of wind loading on a single tall building or on a group of tall buildings is essential for their economic design. The flow around a combination of pentagonal and hexagonal model cylinder can be ideally considered analogous to that of the flow around a combination of tall pentagonal and hexagonal -shaped building. Therefore, a study of wind flow around groups of pentagonal and hexagonal cylinders would be helpful in this respect. For designing groups of tall buildings, knowledge of the effect of wind loading on a single tall building is not sufficient because the effects of nearby buildings on the loads imposed on a structure would be quite different. In the areas with high-rise buildings, other problems like unpleasant wind conditions may be developed near ground level in passages between and through buildings and many instances of such conditions, causing discomfort for the pedestrians and damage to doors and windows in and near the passage, have been reported. In order to eliminate these nuisances, architects and town-planners of Bangladesh should have a better knowledge of the wind flow around the buildings, which can save the nation from making both loss of lives and properties. In the present study, it has been tried to give an understanding about the variation of wind load pattern imposed on building due to the influence of the nearby buildings. To find the complete solutions of the above-mentioned problems a more detailed study in this regard is needed.

There are many examples of failures of buildings and structures in different parts of the world, which has made the enthusiastic investigators puzzled to find the exact causes, and research works are being carried out to find the proper remedial measures for eliminating these failures. The investigators of this country may contribute a lot to the nation by conducting appropriate research work in this field.

Though the problem regarding the wind loadings on buildings and structures is common to all parts of the world and it is expected that the solution will not be significantly different from country to country, yet research work should be carried out in this field considering the climatic conditions and problem of this country so that a clear picture about the nature of wind loading can be obtained. The data from these research works should enable to the architects, engineers and town planners of Bangladesh to design buildings and structures more efficiently.

1.5 Importance of Model Study

Differences between wind tunnel and full-scale result can occur due to Reynolds number inequality, incorrect simulation of the atmospheric boundary layer and small-scale difference between wind tunnel and prototype model. In most wind tunnels tests the full scale Reynolds number is rarely achieved. Boundary layer separation depends on Reynolds number. For sharp edged structures, separation point does not depend on Reynolds number. On the other hand, the flow field around curved surfaces is very much Reynolds number dependent, so tests on these configurations must be treated with care the crosswind scales in wind tunnels are often less than reality. This can cause underestimation of cross wind effects. The scale difference between wind tunnel model and prototype is found in the high frequency fluctuation. High peaks found on the cladding in full-scale are not found in the wind tunnel. Those effects may be caused by structural details that are not simulated in the wind tunnel model.

Now-a-days, both the studies with models and full-scale buildings are being performed to compare the result for varying the validity of the former. But full-scale experiments are both costly and difficult to perform. For the present study with staggered buildings full- scale experiments will not only be complex and costly but it would be difficult to record reliable pressure distribution simultaneously on the group of buildings as there will be variation of speeds and direction of wind with time. The flow around buildings in actual environment is very complex and formulation of a mathematical model to predict the flow is almost impossible. Thus model study is a must and the results obtained under simulated condition in the laboratory are found to be quite satisfactory for practical purposes.

1.6 Aim of the Study

In the present experimental investigation, pentagonal and hexagonal cylinders with a combination will be taken into consideration. The objectives of the study are as follows:

a) To measure the pressure distribution around single pentagonal and hexagonal cylinders at different angle of attack
b) To measure the pressure distribution around staggered pentagonal and hexagonal cylinders at zero angle of attack only.
c) To determine the wind load for the static pressure distributions and observe the effect of different longitudinal and transverse spacing of the cylinders.

d) To make comparisons of wind loads for staggered combinations, spacing and side dimensions of the pentagonal and hexagonal cylinders.

It is expected that the wind load on the pentagonal and hexagonal combination will be comparable to that with the same type of cylinders. The result will be enable the engineers and architects to design buildings more efficiently. Since the results will be expressed in the non-dimensional form, they may be applied for the prototype buildings.

1.7 Scope of the Study

This section contains the brief description of the different themes which has been presented in the various chapters.

The brief description of the wind characteristics and its effect on buildings and structures has been incorporated in **chapter 1.** The importance of the study and the aim of the study have also been included in this chapter.

In **chapter 2** the brief survey of the various related literatures has been provided. Usually, the research works which are directly related to the present study has been included in this chapter. Some works which are in line with the present study have also been included.

The description of the experimental set-up and the measuring equipments has been given in **chapter 3** in a nutshell. The detail feature of the cylinder used for the study has also been shown in this chapter.

The mathematical model to calculate the pressure coefficient, drag coefficient and lift coefficient has been given in **chapter 4.** The sample calculation of finding various coefficients has also been included here.

The most important part of the thesis is the results and discussion, which have been provided in **chapter 5.** The pressure coefficient, drag coefficient and lift coefficient have been discussed elaborately in this chapter.

Finally, in **chapter 6** the conclusions and the recommendations for future researchers have been given.

CHAPTER-2
REVIEW OF LITERATURE

2.1 General

During the last half century much emphasis has been given to the study of wind loading on buildings and structures. In the past, there were some occurrences of disastrous collapse of suspension bridges and damages to buildings and structures, which stimulated the relevant researchers to pay attention for performing researches in this field. Many researchers carried out work mainly on isolated bluff bodies primarily. Later, they started conducting work on group of buildings and structures. They also carried out the research work about the effect of environment on the buildings in parallel. Information concerning the flow over staggered pentagonal and hexagonal cylinders is not probably available in detail, although this is a problem of practical significance. In this chapter, a brief description of some of the papers related to the present state of the problem will be mentioned.

2.2 Existing Research Work

Baines, W. D. [1] presented in his paper the effects of velocity distribution on wind loads and flow patterns around buildings. He measured pressure distributions on models of walls and rectangular block structures in a wind tunnel. Tall buildings with square sections have also been included in his study. The tests were conducted both in an artificially produced velocity gradient used to simulate natural conditions and in a constant velocity field for comparison with standard procedures.

Barriga, A. R. [2] studied the effects of angle of attack, turbulence intensity and scale on the pressure distribution of a single square cylinder placed in a turbulent cross flow. They found that when the square cylinder was positioned in a cross flow with one face normal to the flow direction, only drag force was produced, but in the same flow a negative lift force was developed at small positive angle of attack, the magnitude of which was depended on the turbulence characteristics of the cross flow. It was suggested that the negative lateral forces on the square cylinder oriented at a small positive angle of attack was due to the relatively large negative pressure co-efficient in the separated zone on the windward side wall. It was also concluded that the effect of turbulence intensity was to decrease the pressure near the

front corner of the windward side wall and promote flow reattachment near the rear, giving rise to a very significant increase in aerodynamic moment.

Bearman, P. W. and Wadcock, A. J. [4] presented in their paper how the flow around two circular cylinders, displaced in a plane normal to the free stream, interacts as the two bodies are brought close together. Surface pressure measurements at a Reynolds number of 25000 based on the diameter of a single cylinder (d), showed the presence of a mean repulsive force between the cylinders. At gaps between 0.1d and 1d a marked asymmetry in the flow was observed with the two cylinders experiencing different drags and base pressures. The base pressure was found to change from one steady value to another or simply fluctuated between the two extremes. They also showed how mutual interference influenced the formation of vortex streets from the two cylinders.

Biswas, N. [5] performed an experimental investigation of wind load on tall buildings with square cross section having rounded facet in a uniform flow. Five different facet dimensions were considered in the study. The study included both the single cylinder and the group consisting of two cylinders. The inter spacing between the cylinders in the group were also varied. The test was conducted in an open circuit wind tunnel at a Reynolds number of 54000 based on the face width length across the flow. He found that there is remarkable effect of rounded facet on the drag coefficient.

Bostock, B. R. and Mair, W. A. [6] studied the pressure distributions and forces on rectangular and D-shaped cylinders placed in two-dimensional flow with a Reynolds number of 190000. It was found that for rectangular cylinders a maximum drag coefficient was obtained when the height (normal to the stream) of the section was about 1.5 times the width. Reattachments on the sides of the cylinders occurred only for height diameter ratio less than 0.35.

Castro, I. P. and Robins, A. G. [8] described in their paper the flow around surface mounted cubes in uniform, irrigation and sheared turbulent flows. The shear flow was simulated atmospheric boundary layer with a height ten times of the body dimensions. They presented measurements of body surface pressure and mean and fluctuating velocities within the wake region. These measurements reflected the effects of upstream turbulence and shear on the wake flow. It was found that in the reversed flow region directly behind the body the addition of upstream turbulence and shear considerably reduced the size of cavity zone. Unlike the

case of uniform flow the separating shear layers reattached to the body surface. Measurements for a variety of cube size boundary layer height ratio further revealed that reattachments occurred even for cube heights larger than the boundary layer height. They found that in the case of uniform flow approaching the cube at 45 degrees, the near wake and pressure fields were dominated by strong vortex shed from the top edge of the body.

Islam, A. T. M. and Mandal, A. C. [11] conducted an experimental investigation of static pressure distributions on a group of rectangular cylinders in a uniform cross flow. They determined the effects of longitudinal spacing and side dimension of the rectangular cylinders. Finally, they calculated the lift and drag coefficients from the measured data of surface static pressure.

Farok, G. M. G. [12] carried out an experimental investigation of wind effect on rectangular cylinders with rounded corners. They considered both the single cylinder and group of cylinders in their study. They observed that with the rounded corners the drag on the cylinders reduces remarkably in comparison to that on the sharp-edged cylinders. The effect of inter-spacing is also considered in their study.

Hua, C. K. [13] conducted the measurements of fluctuating lift and the oscillating amplitudes on a square cylinder in a wind tunnel test.

Davis, R. W. and Moore, E. F. [15] carried out a numerical study of vortex, shedding from rectangular cylinders. They attempted to present numerical solutions for two-dimensional time dependent flow about rectangles in infinite domains. They investigated the initiations and subsequent development of the vortex shedding phenomena for Reynolds number varying from 100 to 2800. It is found that the properties of these vortices were strongly dependent on the Reynolds number. Lift, drag and Strouhal number were also found to be influenced by Reynolds number.

Lee, B. E. [16] conducted the study of the effect of turbulence on the surface pressure field of a square prism. He presented measurements of the mean and fluctuating pressures on a square cylinder placed in a two-dimensional uniform and turbulent flow. It was observed that the addition of turbulence to the flow raised the base pressure and reduced the drag of the cylinder. He suggested that this phenomenon was attributable to the manner in which the increased turbulence intensity thickened the shear layers, which caused them to be deflected by the downstream corners of the body and resulted in the downstream movement of the

vortex formation region. The strength of the vortex shedding was shown to be reduced as the intensity of the incident turbulence was increased. Measurements of drag at various angles of attack (0° to 45°) showed that with increase in turbulence level the minimum drag occurred at smaller values of angle of attack.

Mandal, A. C. and Farok, G. M. G. [19] presented a paper on static pressure distributions on the cylinder with either square or rectangular cross-section having rounded corners. The experiment was performed for different corner radii and side dimensions of the cylinders at zero angle of attack. The wind load decreased appreciably for the cylinder with rounded corner compared to that with sharp corner. The experimental results reveal that the corner radius of the cylinder has significant effect while the side dimension has small effect on the drag coefficient.

Hussain, H. S. and Islam, O. [22] measured coefficient of pressure and coefficient of lift on circular, parabolic and elliptic shell roof in a uniform velocity. The investigation was performed in a small wind tunnel. As the experiment was carried out in a uniform velocity, the estimated results would be higher than that in reality.

Hossain et al [23] made an experimental investigation of wind effect on staggered cylinders of square and rectangular sections with variable longitudinal spacing. In their paper they found that there is significant effect of inter-spacing on the wind load of cylinders.

Islam, A. M. T. and Mandal, A. C. [24] performed an experimental investigation of surface static pressure distributions on rectangular cylinders for a uniform cross-flow. They measured the surface static pressure distribution and they obtained the drag and lift coefficients. For all side ratios of the rectangular cylinders it was observed that the minimum drag occurred within 8^0 and 12^0 angle of attack.

Islam, A. M. T. and Mandal, A. C. [25] presented a paper on surface static pressure distributions on a group of rectangular cylinders for a uniform cross flow. They considered the effect of side ratios and longitudinal spacing on pressure distribution. They obtained the drag and lift coefficients from the measured surface pressure distribution. It is observed that with the increase of the side ratio the drag coefficients increased in general.

Koeing, K. and Roshiko, A. [26] described in their paper an experimental investigation of the shielding effects of various disks placed co-axially upstream of an axisymmetric flat faced

cylinder. For certain combinations of the diameter and gap ratios they observed a considerable decrease in the drag of such a system. By flow visualization technique they showed that for such optimum shielding the upstream surface, which separated from the disk reattached smoothly onto the front edge on the downstream cylinder.

Leutheusser, J. [29] made wind tunnel tests on scale models of typical building configurations. The experiment was conducted on four models each with different height and cross-section. He found out the static wind loading on each of the buildings in free standing condition and as a member of a group of buildings. He concluded that the wind loading of a building was less severe when is formed a part of a group than when it was free standing.

Mandal, A. C. and Farok, G. M. G. [30] measured the static pressure distributions on a group of cylinders with either square or rectangular cross-section having rounded corners. The experiment was performed for a group consisting of two cylinders one behind the other along the flow direction with different side dimensions at zero angle of attack for various inter-spacing between the cylinders. It is observed from the experimental results that there is appreciable effect of the side dimension and interspacing on the drag coefficient of the cylinders. The results are applicable to a group consisting of two tall buildings one behind the other along the wind velocity direction and each building of either square or rectangular cross-section having rounded corners.

Mandal, A. C. and Islam, O. [31] made a study of wind effects on a group of square cylinders with variable longitudinal spacing. The test was conducted in an open circuit wind tunnel at a Reynolds number of 27800 based on the side dimension of the square model. The maximum blockage area was 6.96 percent. Three cylinders were arranged in the staggered form (one in upstream and two in downstream side) varying the longitudinal and transverse spacing and measurements of pressure coefficients were taken for the upstream and downstream cylinders. Experiments were also carried out for drag coefficients, lift coefficients, total force coefficients and moment coefficients. After all, it was concluded from the results that wind loading on a building is generally less severe when the building forms part of a group than when it is free-standing.

Mandal, A. C. and Islam, O. [32] performed an experimental investigation of wind effect on staggered square cylinders with variable transverse and longitudinal spacing. They measured the surface static pressure distributions of each of the cylinders and then they calculated the

drag and total force coefficients from the static pressure. They observed that the net wind load on the individual cylinder of the group decreased in general; however, there appeared high local pressure coefficient in some cases.

Matsumoto, M. [34] made an investigation on the aerodynamic forces acting on an oscillating square prism in a steady flow both experimentally and theoretically. First, a few experiments were performed to examine the aerodynamic forces in the direction of the wind stream and in a plane normal to it, acting on an oscillating square prism. Karman's theory about a thin plate was extended to the case of a square prism and the aerodynamic forces in a plane of the direction of the wind stream were obtained. Good correlation was found between the theoretical and experimental results.

Nakamura, Y. and Matskawa, T. [36] made experimental investigation on the vortex excitation of rectangular cylinders with the long side normal to the flow in a mode of lateral translation using free and oscillation methods.

Nakamura, Y. and Ohya, Y. [37] studied the effects of turbulences on the mean flow past square rods. Measurements were made on square rods with different lengths with their square face normal to the flow to investigate the effects of turbulence intensity and scale on the mean flow characteristics. The turbulence intensity varied from 3.5% to 13% and the length to size ratio of the rods ranged from 0.1 to 2.0. It was found out that there were two main effects of turbulence on the mean flow past a three-dimensional sharp edged bluff body. Small-scale turbulence increased the growth rate of the shear layer, while the large-scale turbulence enhanced the roll up of the shear layer. For a square plate, both small and large-scale turbulence reduced the size of the base cavity. As the length of the square rod was increased beyond the critical (0.6 times the heights), the shear-layer-edge direct interaction controlled the near wake eventually leading to flow reattachment. The effect of small scale turbulence was to promote the shear layer direct interaction.

Nakamura, Y. and Yujiohya [38] attempted to study vortex shedding from square prisms placed to smooth and turbulent approaching flows. They made flow visualization and measured the velocity and pressure for the flow past prism of variable length with square section. They found that square prisms shed vortices in one of the two-fixed wake planes, which were parallel with the plate sides. The plane of shedding was switched irregularly from one to the other.

Roberson, J. A. [41] carried out experiments on circular cylinders, spool shaped bodies, cup-shaped bodies, square rods and rectangular rods to observe the effect of turbulence on the drag of these bodies. For square rods with their axes parallel to the flow direction it was found the C_d decreased approximately 25% when the turbulence intensity increased from 1% to 10%. Two rectangular rods used; one had a square cross-section and the other had a length (in the free stream direction) to breadth ratio of two. The drag was measured with the axes of the rectangular rods oriented normal to the free stream direction. It was noted that on the sides of the square rod the pressure change with a change in turbulent intensity was about the same as for the face; while for the rectangular rod, the change in pressure on the sides was large, and it was small on the rear face. They concluded that bodies, which have shapes such that reattachment of the flow is not a factor, experience an increase in C_d with the increased turbulence intensity. On the other hand, bodies for which reattachment or near reattachment of flow occur with increased turbulence may experience either a decrease or increase in C_d with increased turbulence intensity depending upon the shape of the body.

Roberson, J. A. [42] measured pressure distribution on rectangular rods placed in a cross flow with the rods oriented at small angle of attack with respect to the direction. The Reynolds number based on the minimum dimension of the rod was 40000 and the turbulence intensity of the cross flow ranged between 1% and 10%. They concluded that the free stream turbulence had a significant effect on the pressure distribution about bodies of rectangular cross-section. With small angle of attack these bodies had a significantly lower pressure on their windward side wall than did the same bodies with zero angle of attack. To study the pressure distributions on bodies that more nearly represents building configurations, tests were made on bodies of square cross-section placed on the floor of the wind tunnel. It was found that decreasing relative height of the body had an attenuating effect on the negative pressure on the windward side wall and it also increased the critical angle of attack.

Sakamoto, H. and Arie, M. [44] collected experimental data on the vortex shedding frequency behind a vertical rectangular prism and a vertical circular cylinder attached to a plane wall and immersed in a turbulent boundary layer. They tried to investigate the effects of the aspect ratio (height/width) of these bodies and the boundary layer characteristics on the vortex shedding frequency. Measurements revealed that two types of vortex were formed behind the body, depending on the aspect ratio; they were the arch-type vortex and the Karman-type vortex. The arch-type vortex appeared at an aspect ratio less than 2.0 and 2.5

for rectangular and circular cylinders respectively. The Karman type vortex appeared for the aspect ratio greater than the above values. The whole experiment was conducted at a turbulence level of 0.2% and free stream velocity of 20 m/s. The aspect ratio was varied from 0.5 to 0.8.

Vickery, B. J. [46] presented in his paper the results of the measurements of fluctuating lift and drag on a long square cylinder. He attempted to establish a correlation of lift along the cylinder and the distribution of fluctuating pressure on the cross-section. The magnitude of the fluctuating lift was found to be considerably greater than that for a circular cross-section and the span wise correlation much stronger. It was also reported that the presence of large-scale turbulence in the stream had a remarkable influence on both the steady and the fluctuating forces. At small angle of attack (less than 10°) turbulence caused a reduction in base suction and a decrease in fluctuating lift of about 50%.

Besides these, many authors have performed study on flow patterns, wind loads and their effects on buildings and structures, which have been mentioned in the references.

Besides the above research works, many other works have also been done by many researchers in the different places, but probably no where they have taken the combination of pentagonal and hexagonal cylinders for study. Especially the pentagonal and hexagonal cylinders in staggered condition have not been included for finding the wind load. Thus this study would definitely add to the new idea in regard to the wind loading for tall buildings.

CHAPTER-3
EXPERIMENTAL SET-UP

3.1 General

The experimental investigation to find wind load on the pentagonal and hexagonal cylinders was conducted at the exit end of a subsonic open circuit wind tunnel. The test was done on a single pentagonal cylinder and a single hexagonal cylinder and on a group consisting of one pentagonal cylinder in the upstream side and another two identical hexagonal cylinders in the downstream side in a uniform cross flow. The surface static pressures at the different locations of the cylinder were measured with the help of an inclined multi-manometer. In this chapter a brief description regarding the construction of the pentagonal and hexagonal cylinders, the wind tunnel, the testing procedure etc. has been provided systematically.

3.2 Wind tunnel

The test was done in an open circuit subsonic wind tunnel as shown in Figure 3.1. It was the low speed wind tunnel having the maximum wind velocity of 14 m/s in the test section. The tunnel consists of various components such as, fan, valve, silencer, honey comb etc. It is 5.93 meter long with a test section of 460-mm x 460 mm cross-section. In order to make the flow uniform a honeycomb is fixed near the end of the wind tunnel. There is a converging bell mouth shaped entry. To generate the wind velocity, two axial flow fans are used. Each of the fans is connected with the motor of 2.25 kilowatt and 2900 rpm. There is a butterfly valve to control the wind speed. There is a silencer just after the butterfly valve as shown in the figure.

The central longitudinal axis of the wind tunnel is maintained at a constant height of 990 mm from the floor. The axis of the model coincides with that of the wind tunnel. The converging mouth entry is incorporated in the wind tunnel for smooth entry of air into the tunnel and to maintain uniform flow into the duct free from outside disturbances. The induced flow through the wind tunnel is produced by two-stage rotating axial flow fan of capacity 18.16 m^3/s at the head of 152.4 mm of water and 1475 rpm.

A butterfly valve, actuated by a screw thread mechanism, is placed behind the fan and used to control the flow. A silencer is fitted at the end of the flow controlling section in order to

reduce the noise of the system. This section is incorporated with a honeycomb. The diverging and converging section of the wind tunnel is 1550mm long and made of 16 SWG black sheets. The angle of divergence and convergence is 7°, which has been done with a view to minimizing expansion and contraction loss and reducing the possibility of flow separation.

In each case of the tests, wind velocity is measured directly with the help of a digital anemometer. The flow velocity in the test section was maintained at 13.5m/s approximately. The measured velocity distribution was almost uniform across the tunnel test section in the upstream side of the test models. The pattern of the flow velocity is shown in Figure 3.2 in the non-dimensional form.

3.3 Test Section

In reality the test was done at the exit end of the wind tunnel in the open air as shown in Figure 3.1. In order to fix the cylinder a steel frame was fabricated, the top floor of which was at the same level of the wind tunnel at the exit end. Two side walls were attached to the steel frame at the two sides by the help of nut and bolt. The distance between the extended side walls was equal to the distance of the side walls of the wind tunnel exit end. This distance of between the side walls was 460 mm. The length of the test section was 400 mm. There was no cover plate at the top and bottom of the extended test section.

The cylinders were fixed with the extended sidewalls. The sidewalls were made of plywood. In one side, the model cylinder was fastened with the side wall using nut and bolt. The bolt was fixed with one end of the cylinder. Through the other end of the cylinder, the plastic tubes were taken out in order to connect them with the inclined multi-manometer. This end was supported in the groove of the sidewall of the extended portion, compatible with the pentagonal and hexagonal end of the cylinder. The capillary tube made of copper was used to make the tapping on the sides of the pentagonal and hexagonal model cylinders. These copper tubes were connected with the plastic tubes. The cylinder was leveled and then fixed very carefully so that its top side was parallel to the flow direction.

There was a provision for rotation of the test cylinder at various angles to obtain the wind load at different angles of attack. The Reynolds number was 4.22×10^4 based on the projected width of the cylinder across the flow direction. Since the top and bottom of the extended part of the wind tunnel was open; as such no correction for blockage was done in the analysis. The test cylinders were placed very close to the end of the wind tunnel so that the approach

velocity on the test cylinders was approximately identical as that in the exit end of the wind tunnel. The provision was also kept in the extended wall to fix the two hexagonal cylinders and one pentagonal cylinder along the flow direction. There was also a scope to change the inter-spacing between the cylinders.

The inter-spacing between the two hexagonal cylinders was varied at L_2=2D, 3D, 5D and between pentagonal and hexagonal cylinders was varied at L_1=1D, 2D, 4D, 6D and 8D, where D is the width of the cylinder across the flow direction. With a view to achieving this, several groups were made on the side walls of the test section. When the test was conducted, the unnecessary groves were sealed. The cylinders were fixed at one end by the help of bolt and nut and the other ends were fixed in groove. Through the grooves the plastic tubes were taken out and connected with the inclined multi-manometer as in the single cylinder. During fixing the cylinders, it was carefully checked whether the top side of the cylinders were parallel to the free stream velocity direction. Leveling of the test cylinder was always checked by a standard spirit level.

3.4 Constructional Details of Cylinders

For the study, two hexagonal cylinders and one pentagonal cylinder of identical size were constructed. Each of the cylinders was made of seasoned teak wood in order to avoid the bucking and expansion due to the change of temperature and humidity. The tapping positions on the cross-section of the cylinder are shown in Figure 3.3. The width of the hexagonal and pentagonal cylinder was 50mm as shown in the figure. Each face of the cylinder contained five tappings. In Figure 3.4 the tapping positions on the longitudinal section of the cylinder is shown. There were five tappings on each face of the cylinder. The distance between the consecutive tapping points was equal (Δd) as shown in the figure. However, the location of the corner tapping was at a distance of $\frac{1}{2}(\Delta d)$.

Each tapping was identified by a numerical number from 1 to 30 for hexagonal cylinder and from 1 to 25 for pentagonal cylinder as can be seen from the figure. It can be seen from the longitudinal section that the tappings were not made along the cross-section of the cylinder. They were located within some span of the cylinder as shown in Figure 3.4. To avoid manufacturing problem this technique was followed. Since the velocity was two-dimensional flow, this would not make any effect on the experimental result.

On one side of the cylinder a steel plate was attached through which there was a bolt for fixing the cylinder with the side wall of the extended tunnel as shown in Figure 3.4. The other side of the cylinder was hollow through which the plastic tubes were allowed to pass. The plastic tubes were connected with the copper capillary tubes at one side and at the other side with the inclined multi-manometer. The manometer liquid was water. The tappings were made of copper tubes of 1.71 mm outside diameter. Each tapping was of 10mm length approximately. From the end of the copper tube flexible plastic tube of 1.70 mm inner diameter was press fitted.

3.5 Single Cylinder

In the first phase of the experimental investigation, the single cylinder was taken into consideration. The velocity at the upstream side of the cylinder was maintained at 13.5 m/s. The upstream velocity was assumed to be uniform and the flow occurred across the cylinder. In Figure 3.5 the position of the single cylinder at zero angle of attack is shown in the wind tunnel test section. In this position the top and bottom faces of the hexagonal cylinder and top face of the pentagonal cylinder were parallel to the flow direction. In this position the width of the cylinder was 50 mm in a direction perpendicular to the flow. Based on this width the Reynolds number was calculated. The surface static pressure distributions on faces of the cylinder were measured in this position. Then the cylinder was rotated at an angle of 10° for hexagonal cylinder and 9^0 for pentagonal cylinder and the static pressure distributions on each face of the cylinder were measured again. The same test procedure was repeated to measure the surface static pressure distributions of the cylinders with angles of attack of 0^0, 10^0, 20°, 30°, 40° and 50° for hexagonal cylinder and with angles of attack of 0^0, 9^0, 18°, 27°, 36°, 45^0 ,54^0 ,63^0 and 72^0 for pentagonal cylinder.

3.6 Cylinders in Group

In the second phase of the experimental investigation, two hexagonal cylinders and one pentagonal cylinder were used, one pentagonal cylinder in the upstream side and another two identical hexagonal cylinders in the downstream side in a uniform cross flow. One pentagonal cylinder was placed centrally along the flow direction. In Figure 3.6 the position of the group of cylinders at zero angle of attack is shown in the wind tunnel test section. The inter-spacing between pentagonal and hexagonal cylinders was taken as L_1=1D i.e. 50mm and between the two hexagonal cylinders was taken as L_2=2D. Then static surface pressure distributions were measured on the six faces of the hexagonal cylinder and on the five faces of the pentagonal

cylinder. Keeping everything identical the inter-spacing between the two hexagonal cylinders was changed to L_2=3D, 5D and the experiment was repeated. Next, the inter-spacing between pentagonal and hexagonal cylinders was varied to L_1=2D, 4D, 6D and 8D and in each case inter-spacing between the two hexagonal cylinders was varied to L_2=2D, 3D and 5D, the static pressure distributions on both the pentagonal and hexagonal cylinders were taken. All the measurements were taken at zero angle of attack only.

3.7 Measuring Equipment

The wind velocity across the test section of the wind tunnel was measured with the help of digital anemometer. A pitot tube was also used to measure the velocity in order to cross check. The pitot tube was connected to an inclined manometer the limb of which contained water. The surface static pressures were measured with the help of inclined manometer. The manometer liquid was water. The inclination of the manometer was sufficient to record the pressure with reasonable accuracy. Where there was a little fluctuation in the manometer limb the mean of the value was recorded. During the manometer reading it was done very carefully, so that no air bubble was deposited anywhere in the limb.

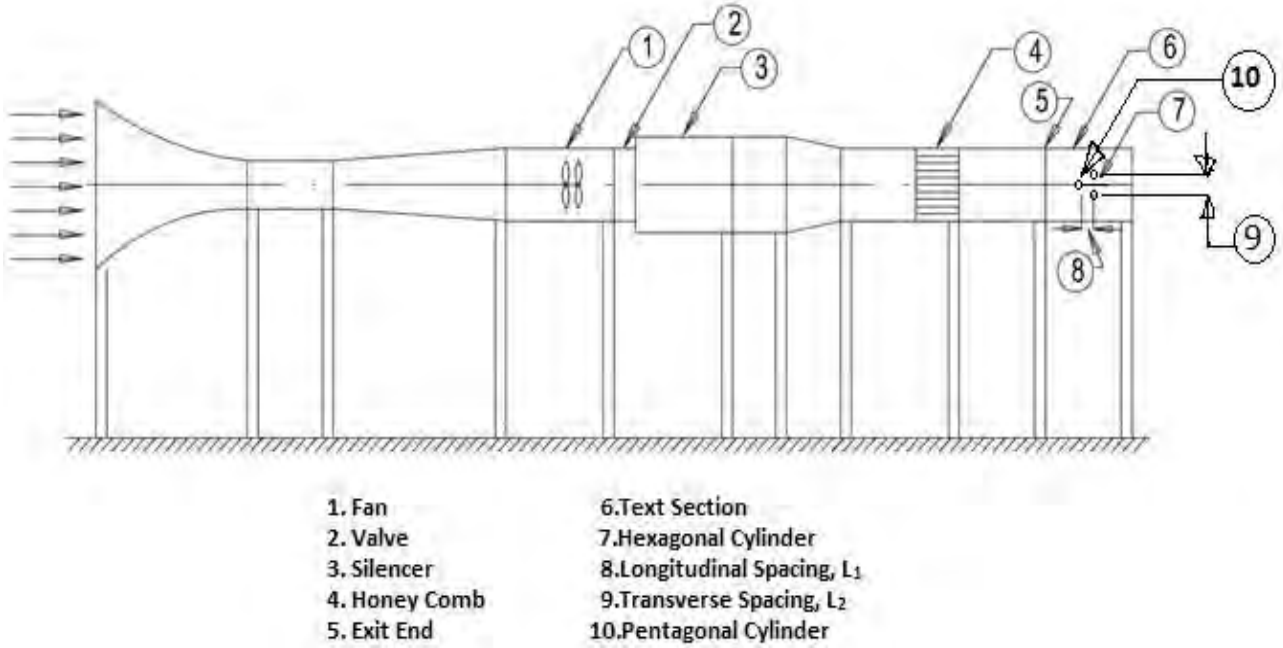

Figure 3.1: Schematic Diagram of Wind Tunnel

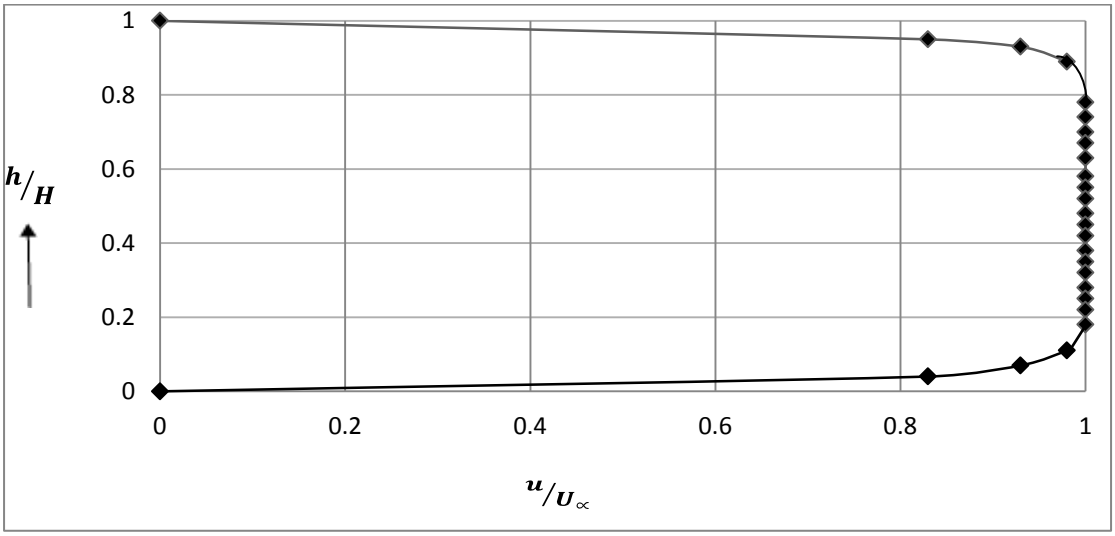

Figure 3.2: Velocity Distribution at Upstream Side of Model

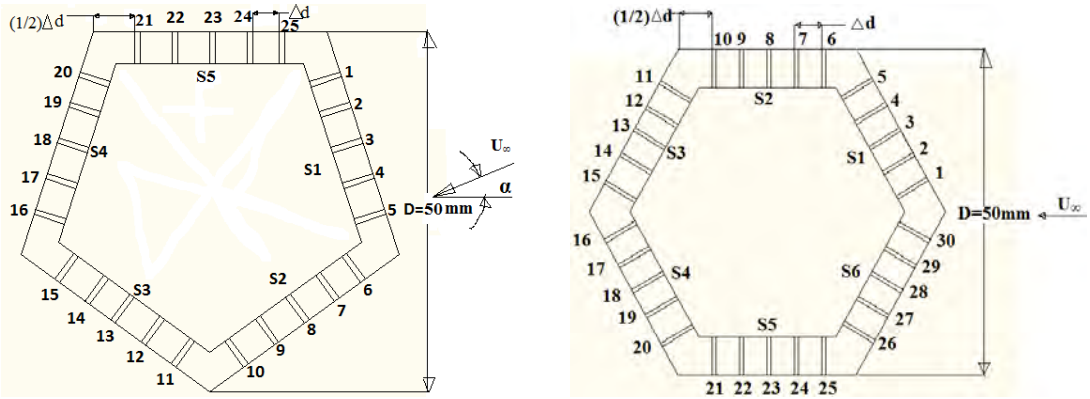

Pentagonal Cylinder **Hexagonal Cylinder**

Figure 3.3: Tapping Positions Shown on Cross-Section of Cylinder

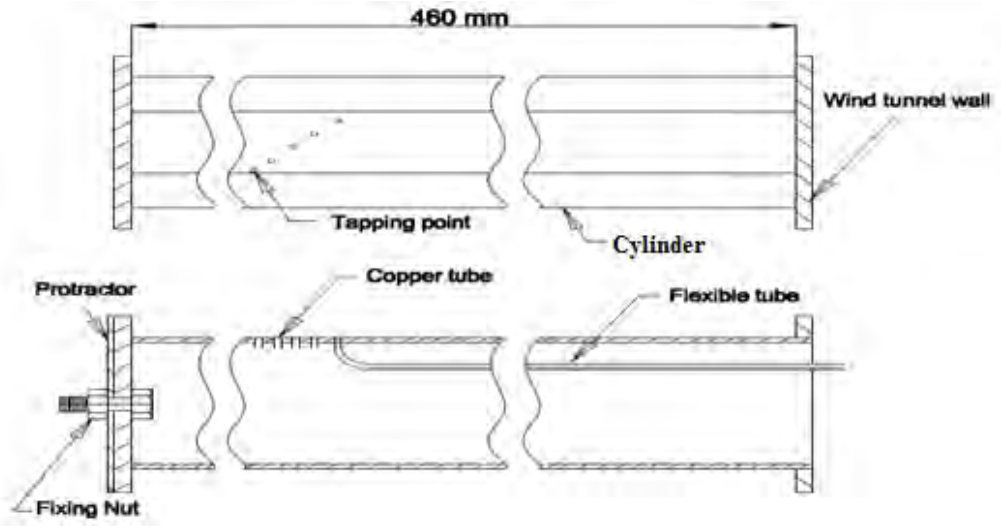

Figure 3.4: Tapping positions shown on longitudinal section of cylinder

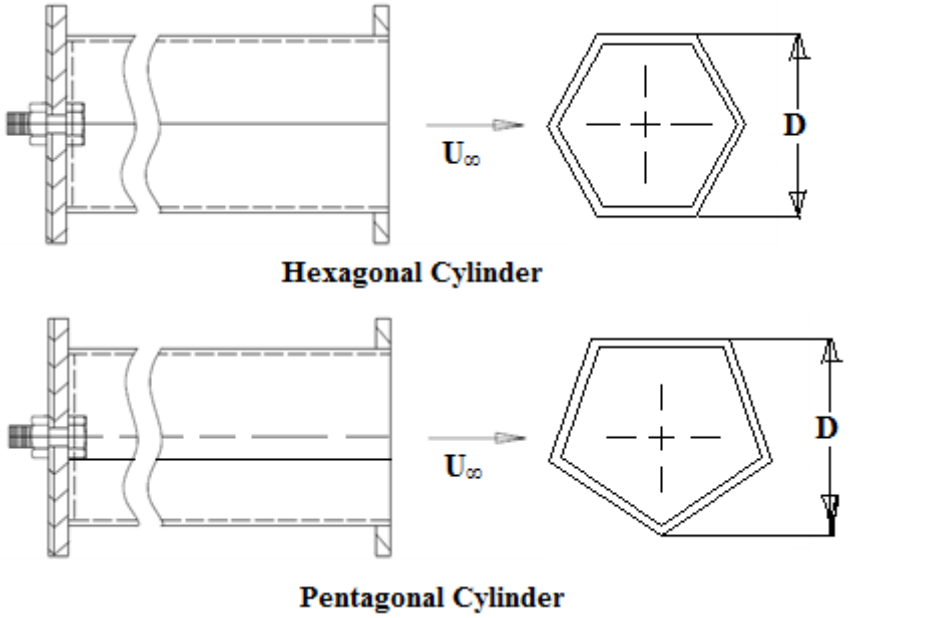

Figure 3.5: Tunnel test section showing position of single cylinder

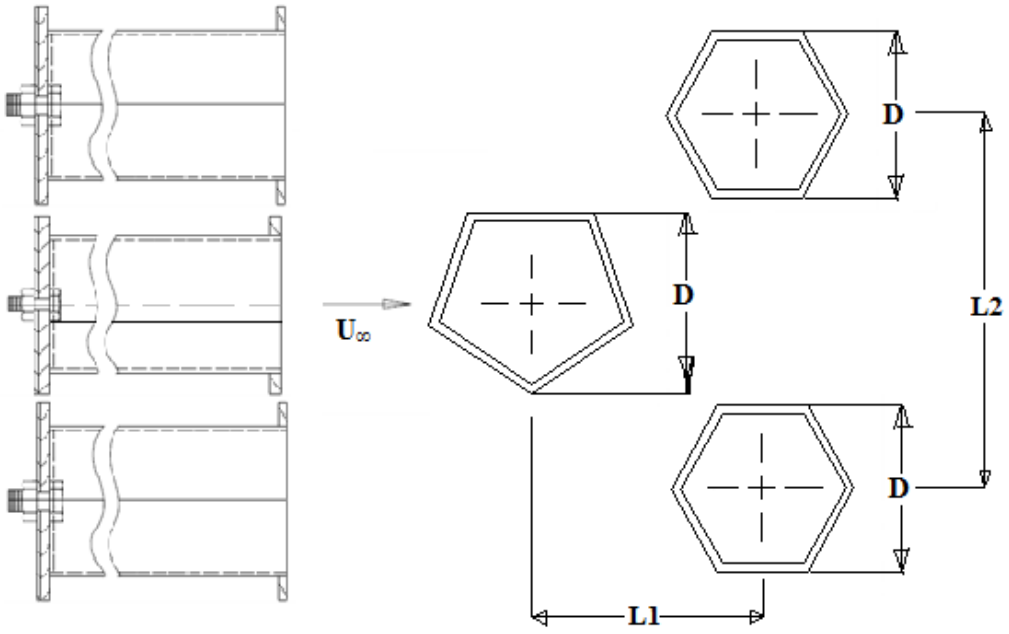

Figure 3.6: Tunnel test section showing position of group cylinders

CHAPTER-4
MATHEMATICAL MODEL

4.1 General

The calculation procedure of finding pressure coefficients, drag and lift coefficients has been described in a nutshell in this chapter. From the measured surface static pressure on the pentagonal and hexagonal cylinders the pressure coefficients are obtained. Then the drag and lift coefficients are found from the pressure coefficients. With the help of numerical integration method drag and lift coefficients are determined.

4.2 Determination of pressure coefficient

The pressure coefficient is defined as

$$C_p = \frac{\Delta P}{\frac{1}{2}\rho U_\infty^2} \tag{4.1}$$

Where, $\Delta P = P - P_0$

P is the static pressure on the surface of the cylinder

P_0 is the ambient pressure

ρ is the density of the air

U_∞ is the free stream velocity

ΔP is obtained from

$$\Delta P = -\Delta h_w \times \gamma_w \tag{4.2}$$

Where, Δh_w is the manometer reading

γ_w is the specific weight of manometer liquid, that is water

Figure 4.1 shows the section of the model pentagonal and hexagonal cylinders with the pressure tapping points, at each of them the static pressure was recorded with the help of inclined multi-manometer. The cylinder was rotated at various angles of 0^0,10^0, 20^0, 30^0, 40^0 and 50^0 for hexagonal cylinder and at various angles of 0^0, 9^0, 18°, 27°, 36°, 45^0 ,54^0 , 63^0 and

72^0 for pentagonal cylinder and at each angle surface static pressures were recorded. Next two hexagonal cylinders and one pentagonal cylinder were placed at various inter-spacing along the flow direction at zero angle of attack only. Then the surface static pressures were measured for pentagonal and hexagonal cylinder with the help of multi-manometer.

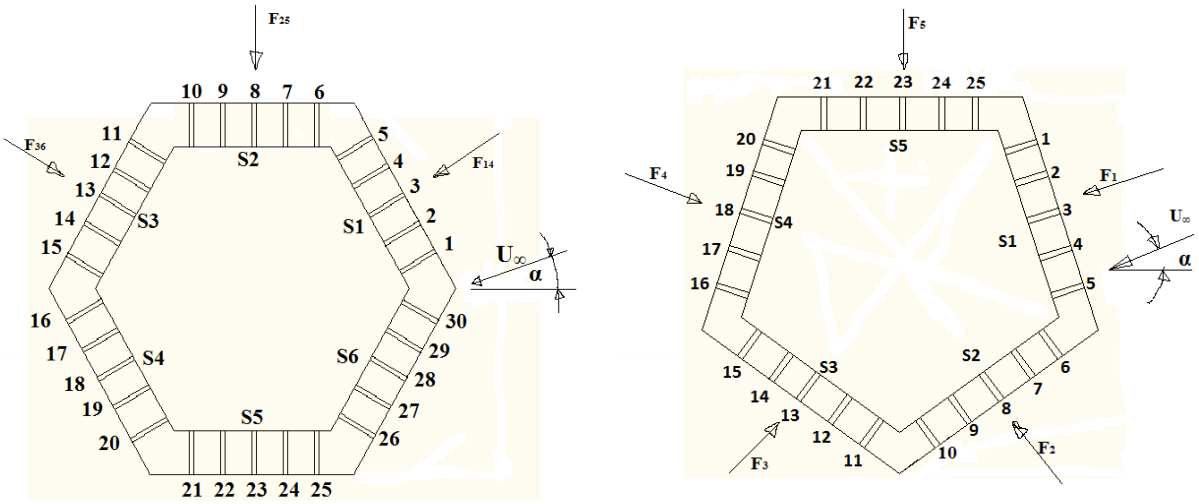

Hexagonal Cylinder **Pentagonal Cylinder**

Figure 4.1: Cross-section of Cylinders Showing Forces

4.3 Determination of Drag and Lift Coefficients

4.3.1 Hexagonal Cylinder

As shown in Figure 4.1 that the cylinder has six faces S_1, S_2, S_3, S_4, S_5 and S_6. The pressure differences between the various tapping points along the face S_1 and S_4 can be obtained from

$\Delta P_{1-20} = P_1 - P_{20}$ is the pressure difference between tapping points 1 and 20

$\Delta P_{2-19} = P_2 - P_{19}$ is the pressure difference between tapping points 2 and 19

$\Delta P_{3-18} = P_3 - P_{18}$ is the pressure difference between tapping points 3 and 18

$\Delta P_{4-17} = P_4 - P_{17}$ is the pressure difference between tapping points 4 and 17

$\Delta P_{5-16} = P_5 - P_{16}$ is the pressure difference between tapping points 5 and 16

If F_{14} indicates the net force along the faces S_1 and S_4, then using Simpson's rule, one can find

$$F_{14} = \frac{\Delta A}{3}[\Delta P_{1\text{-}20} + 4\Delta P_{2\text{-}19} + 2\Delta P_{3\text{-}18} + 4\Delta P_{4\text{-}17} + \Delta P_{5\text{-}16}] \quad (4.3)$$

If the length of the cylinder is chosen as unity, then the above expression becomes

$$F_{14} = \frac{\Delta d \times 1}{3}[\Delta P_{1\text{-}20} + 4\Delta P_{2\text{-}19} + 2\Delta P_{3\text{-}18} + 4\Delta P_{4\text{-}17} + \Delta P_{5\text{-}16}]$$

$$= \frac{\Delta d}{3}[(P_1 - P_{20}) + 4(P_2 - P_{19}) + 2(P_3 - P_{18}) + 4(P_4 - P_{17}) + (P_5 - P_{16})]$$

$$= \frac{\Delta d}{3}[(P_1 - P_0) - (P_{20} - P_0) + 4(P_2 - P_0) - 4(P_{19} - P_0) + 2(P_3 - P_0) - 2(P_{18} - P_0)$$

$$+4(P_4 - P_0) - 4(P_{17} - P_0) + (P_5 - P_0) - (P_{16} - P_0)] \quad (4.4)$$

If the component of the force $F_{d_{14}}$ occurs along the flow direction, then one can find the expression of F as $F_{d_{14}}$

$$F_{d_{14}} = F_{14}\cos(30^0 - \alpha) \quad (4.5)$$

Similarly the force component $F_{L_{14}}$ in a direction perpendicular to the flow may be written as

$$F_{L_{14}} = -F_{14}\sin(30^0 - \alpha) \quad (4.6)$$

The net force F_{25} along the faces S_2 and S_5 can be obtained in the same way as above and that is

$$F_{25} = \frac{\Delta d}{3}[(P_6 - P_0) - (P_{25} - P_0) + 4(P_7 - P_0) - 4(P_{24} - P_0) + 2(P_8 - P_0) - 2(P_{23} - P_0)$$

$$+4(P_9 - P_0) - 4(P_{22} - P_0) + (P_{10} - P_0) - (P_{21} - P_0)] \quad (4.7)$$

Therefore the components of the drag and lift forces along the faces S_2 and S_5 are respectively

$$F_{d_{25}} = F_{25}\cos(90^0 - \alpha) \quad (4.8)$$

$$F_{L_{25}} = -F_{25}\sin(90^0 - \alpha) \quad (4.9)$$

The net force F_{36} along the faces S_3 and S_6 can be obtained in the same way as above and that is

$$F_{36} = \frac{\Delta d}{3}[(P_{11} - P_0) - (P_{30} - P_0) + 4(P_{12} - P_0) - 4(P_{29} - P_0) + 2(P_{13} - P_0) - 2(P_{28} - P_0)$$

$$+4(P_{14} - P_0) - 4(P_{27} - P_0) + (P_{15} - P_0) - (P_{26} - P_0)] \quad (4.10)$$

Therefore the components of the drag and lift forces along the faces S_3 and S_6 are respectively

$$F_{d_{36}} = F_{36}\cos(150^0 - \alpha) \quad (4.11)$$

$$F_{L_{36}} = -F_{36}\sin(150^0 - \alpha) \quad (4.12)$$

Drag and lift coefficients are defined as follows

$$C_D = \frac{F_d}{\frac{1}{2}\rho A U_\infty^2} \tag{4.13}$$

$$\text{and } C_L = \frac{F_L}{\frac{1}{2}\rho A U_\infty^2} \tag{4.14}$$

Where, A is the frontal area of the cylinder

The total drag force along the flow direction is

$$F_d = F_{d_{14}} + F_{d_{25}} + F_{d_{36}} \tag{4.15}$$

and total lift force in a direction perpendicular to flow is

$$F_L = F_{L_{14}} + F_{L_{25}} + F_{L_{36}} \tag{4.16}$$

Now from equations (4.13) and (4.15), the expression of drag coefficient becomes

$$C_D = \frac{F_{d_{14}} + F_{d_{25}} + F_{d_{36}}}{\frac{1}{2}\rho A U_\infty^2}$$

Now substituting the values of $F_{d_{14}}$,$F_{d_{25}}$ and $F_{d_{36}}$ from equations (4.5), (4.8) and (4.11) respectively, the expression of drag coefficient becomes

$$C_D = \frac{F_{14}\cos(30^0 - \alpha) + F_{25}\cos(90^0 - \alpha) + F_{36}\cos(150^0 - \alpha)}{\frac{1}{2}\rho A U_\infty^2}$$

$$= \frac{\cos(30^0 - \alpha)}{A} \cdot \frac{F_{14}}{\frac{1}{2}\rho U_\infty^2} + \frac{\cos(90^0 - \alpha)}{A} \cdot \frac{F_{25}}{\frac{1}{2}\rho U_\infty^2}$$

$$+ \frac{\cos(150^0 - \alpha)}{A} \frac{F_{36}}{\frac{1}{2}\rho U_\infty^2} \tag{4.17}$$

Now inserting the values of F_{14}, F_{25} and F_{36} from equations (4.4), (4.7) and (4.10) respectively, one finds

$$C_D = \frac{\cos(30^0 - \alpha)\times\Delta d}{3A} \cdot \frac{1}{\frac{1}{2}\rho U_\infty^2} \cdot [(P_1 - P_0) - (P_{20} - P_0) + 4(P_2 - P_0) - 4(P_{19} - P_0) + 2(P_3 - P_0) - 2(P_{18} - P_0) + 4(P_4 - P_0) - 4(P_{17} - P_0) + (P_5 - P_0) - (P_{16} - P_0)] + \frac{\cos(90^0 - \alpha)\times\Delta d}{3A} \cdot \frac{1}{\frac{1}{2}\rho U_\infty^2} \cdot [(P_6 - P_0) - (P_{25} - P_0) + 4(P_7 - P_0) - 4(P_{24} - P_0) + 2(P_8 - P_0) - 2(P_{23} - P_0) + 4(P_9 - P_0) - 4(P_{22} - P_0) + (P_{10} - P_0) - (P_{21} - P_0)] + \frac{\cos(150^0 - \alpha)\times\Delta d}{3A} \cdot \frac{1}{\frac{1}{2}\rho U_\infty^2} \cdot [(P_{11} - P_0) - (P_{30} - P_0) + 4(P_{12} - P_0) - 4(P_{29} - P_0) + 2(P_{13} - P_0) - 2(P_{28} - P_0) + 4(P_{14} - P_0) - 4(P_{27} - P_0) + (P_{15} - P_0) - (P_{26} - P_0)]$$

Now writing in terms of pressure coefficients the above equation is transformed into

$$C_D = \frac{\cos(30^0-\alpha)\times\Delta d}{3A}\cdot[C_{p_1} - C_{p_{20}} + 4C_{p_2} - 4C_{p_{19}} + 2C_{p_3} - 2C_{p_{18}} + 4C_{p_4} - 4C_{p_{17}} + C_{p_5} - C_{p_{16}}] + \frac{\cos(90^0-\alpha)\times\Delta d}{3A}\cdot[C_{p_6} - C_{p_{25}} + 4C_{p_7} - 4C_{p_{24}} + 2C_{p_8} - 2C_{p_{23}} + 4C_{p_9} - 4C_{p_{22}} + C_{p_{10}} - C_{p_{26}}] + \frac{\cos(135^0-\alpha)\times\Delta d}{3A}\cdot[C_{p_{11}} - C_{p_{30}} + 4C_{p_{12}} - 4C_{p_{29}} + 2C_{p_{13}} - 2C_{p_{28}} + 4C_{p_{14}} - 4C_{p_{27}} + C_{p_{15}} - C_{p_{26}}]$$

Now rearranging the expression of C_D becomes of the following form

$$C_D = \frac{\cos(30^0-\alpha)\times\Delta d}{3A}\cdot[(C_{p_1} + 4C_{p_2} + 2C_{p_3} + 4C_{p_4} + C_{p_5}) - (C_{p_{16}} + 4C_{p_{17}} + 2C_{p_{18}} + 4C_{p_{19}} + C_{p_{20}})] + \frac{\cos(90^0-\alpha)\times\Delta d}{3A}\cdot[(C_{p_6} + 4C_{p_7} + 2C_{p_8} + 4C_{p_9} + C_{p_{10}}) - (C_{p_{21}} + 4C_{p_{22}} + 2C_{p_{23}} + 4C_{p_{24}} + C_{p_{25}}) + \frac{\cos(150^0-\alpha)\times\Delta d}{3A}\cdot[(C_{p_{11}} + 4C_{p_{12}} + 2C_{p_{13}} + 4C_{p_{14}} + C_{p_{15}}) - (C_{p_{26}} + 4C_{p_{27}} + 2C_{p_{28}} + 4C_{p_{29}} + C_{p_{30}})] \quad (4.18)$$

Similarly the expression of lift coefficient C_L can be obtained as,

$$C_L = -\frac{\sin(30^0-\alpha)\times\Delta d}{3A}\cdot[(C_{p_1} + 4C_{p_2} + 2C_{p_3} + 4C_{p_4} + C_{p_5}) - (C_{p_{16}} + 4C_{p_{17}} + 2C_{p_{18}} + 4C_{p_{19}} + C_{p_{20}})] - \frac{\sin(90^0-\alpha)\times\Delta d}{3A}\cdot[(C_{p_6} + 4C_{p_7} + 2C_{p_8} + 4C_{p_9} + C_{p_{10}}) - (C_{p_{21}} + 4C_{p_{22}} + 2C_{p_{23}} + 4C_{p_{24}} + C_{p_{25}})] - \frac{\sin(150^0-\alpha)\times\Delta d}{3A}\cdot[(C_{p_{11}} + 4C_{p_{12}} + 2C_{p_{13}} + 4C_{p_{14}} + C_{p_{15}}) - (C_{p_{26}} + 4C_{p_{27}} + 2C_{p_{28}} + 4C_{p_{29}} + C_{p_{30}})] \quad (4.19)$$

4.3.2 Pentagonal Cylinder

As shown in Figure 4.1 that the cylinder has five faces S_1, S_2, S_3, S_4 and S_5. The pressure at the various tapping points along the face S_1 can be written as

P_1 = Pressure at tapping point 1

P_2 = Pressure at tapping point 2

P_3 = Pressure at tapping point 3

P_4 = Pressure at tapping point 4

P_5 = Pressure at tapping point 5

If F_1 indicates the force along the faces S_1, then using Simpson's rule, one can find

$$F_1 = \frac{\Delta A}{3}[P_1 + 4P_2 + 2P_3 + 4P_4 + P_5]$$

If the length of the cylinder is chosen as unity, then the above expression becomes

$$F_1 = \frac{\Delta d \times 1}{3}[P_1 + 4P_2 + 2P_3 + 4P_4 + P_5]$$

$$= \frac{\Delta d}{3}[(P_1 - P_0) + 4(P_2 - P_0) + 2(P_3 - P_0) + 4(P_4 - P_0) + (P_5 - P_0) + 12P_0] \quad (4.20)$$

If the component of the force F_{d_1} occurs along the flow direction, then one can find the expression of F as F_{d_1}

$$F_{d_1} = F_1 \cos(18^0 - \alpha) \quad (4.21)$$

Similarly the force component F_{L_1} in a direction perpendicular to the flow may be written as

$$F_{L_1} = -F_1 \sin(18^0 - \alpha) \quad (4.22)$$

The net force F_2 along the face S_2 can be obtained in the same way as above and that is

$$F_2 = \frac{\Delta d}{3}[(P_6 - P_0) + 4(P_7 - P_0) + 2(P_8 - P_0) + 4(P_9 - P_0) + (P_{10} - P_0) + 12P_0] \quad (4.23)$$

Therefore the components of the drag and lift forces along the face S_2 are respectively

$$F_{d_2} = -F_2 \cos(126^0 - \alpha) \quad (4.24)$$

$$F_{L_2} = F_2 \sin(126^0 - \alpha) \quad (4.25)$$

The net force F_3 along the face S_3 can be obtained in the same way as above and that is

$$F_3 = \frac{\Delta d}{3}[(P_{11} - P_0) + 4(P_{12} - P_0) + 2(P_{13} - P_0) + 4(P_{14} - P_0) + (P_{15} - P_0) + 12P_0] \quad (4.26)$$

Therefore the components of the drag and lift forces along the face S_3 are respectively

$$F_{d_3} = -F_3 \cos(54^0 - \alpha) \quad (4.27)$$

$$F_{L_3} = F_3 \sin(54^0 - \alpha) \quad (4.28)$$

The net force F_4 along the face S_4 can be obtained in the same way as above and that is

$$F_4 = \frac{\Delta d}{3}[(P_{16} - P_0) + 4(P_{17} - P_0) + 2(P_{18} - P_0) + 4(P_{19} - P_0) + (P_{20} - P_0) + 12P_0] \quad (4.29)$$

Therefore the components of the drag and lift forces along the face S_4 are respectively

$$F_{d_4} = F_4 \cos(162^0 - \alpha) \quad (4.30)$$

$$F_{L_4} = -F_4 \sin(162^0 - \alpha) \quad (4.31)$$

The net force F_5 along the face S_5 can be obtained in the same way as above and that is

$$F_5 = \frac{\Delta d}{3}[(P_{21} - P_0) + 4(P_{22} - P_0) + 2(P_{23} - P_0) + 4(P_{24} - P_0) + (P_{25} - P_0) + 12P_0] \quad (4.32)$$

Therefore the components of the drag and lift forces along the face S_5 are respectively

$$F_{d_5} = F_5 \cos(90^0 - \alpha) \tag{4.33}$$

$$F_{L_5} = -F_5 \sin(90^0 - \alpha) \tag{4.34}$$

Drag and lift coefficients are defined as follows

$$C_D = \frac{F_d}{\frac{1}{2}\rho A U_\infty^2} \tag{4.35}$$

$$\text{and} \quad C_L = \frac{F_L}{\frac{1}{2}\rho A U_\infty^2} \tag{4.36}$$

Where, A is the frontal area of the cylinder

The total drag force along the flow direction is

$$F_d = F_{d_1} + F_{d_2} + F_{d_3} + F_{d_4} + F_{d_5} \tag{4.37}$$

and total lift force in a direction perpendicular to flow is

$$F_L = F_{L_1} + F_{L_2} + F_{L_3} + F_{L_4} + F_{L_5} \tag{4.38}$$

Now from equations (4.35) and (4.37), the expression of drag coefficient becomes

$$C_D = \frac{F_{d_1} + F_{d_2} + F_{d_3} + F_{d_4} + F_{d_5}}{\frac{1}{2}\rho A U_\infty^2}$$

Now substituting the values of $F_{d_1}, F_{d_2}, F_{d_3}, F_{d_4}$ and F_{d_5} from equations (4.21), (4.24), (4.27), (4.30) and (4.33) respectively, the expression of drag coefficient becomes

$$C_D = \frac{F_1 \cos(18^0 - \alpha) - F_2 \cos(126^0 - \alpha) - F_3 \cos(54^0 - \alpha) + F_4 \cos(162^0 - \alpha) + F_5 \cos(90^0 - \alpha)}{\frac{1}{2}\rho A U_\infty^2}$$

$$= \frac{\cos(18^0 - \alpha)}{A} \cdot \frac{F_1}{\frac{1}{2}\rho U_\infty^2} - \frac{\cos(126^0 - \alpha)}{A} \cdot \frac{F_2}{\frac{1}{2}\rho U_\infty^2} - \frac{\cos(54^0 - \alpha)}{A} \cdot \frac{F_3}{\frac{1}{2}\rho U_\infty^2} + \frac{\cos(162^0 - \alpha)}{A} \cdot \frac{F_4}{\frac{1}{2}\rho U_\infty^2} + \frac{\cos(90^0 - \alpha)}{A} \cdot \frac{F_5}{\frac{1}{2}\rho U_\infty^2} \tag{4.39}$$

Now inserting the values of F_1, F_2, F_3, F_4 and F_5 from equations (4.20), (4.23), (4.26), (4.29) and (4.32) respectively, one finds

$$C_D = \frac{\cos(18^0-\alpha)\times\Delta d}{3A}\cdot\frac{1}{\frac{1}{2}\rho U_\infty^2}\cdot[(P_1-P_0)+4(P_2-P_0)+2(P_3-P_0)+4(P_4-P_0)+(P_5-P_0)+12P_0] - \frac{\cos(126^0-\alpha)\times\Delta d}{3A}\cdot\frac{1}{\frac{1}{2}\rho U_\infty^2}\cdot[(P_6-P_0)+4(P_7-P_0)+2(P_8-P_0)+4(P_9-P_0)+(P_{10}-P_0)+12P_0] - \frac{\cos(54^0-\alpha)\times\Delta d}{3A}\cdot\frac{1}{\frac{1}{2}\rho U_\infty^2}\cdot[(P_{11}-P_0)+4(P_{12}-P_0)+2(P_{13}-P_0)+4(P_{14}-P_0)+(P_{15}-P_0)+12P_0] + \frac{\cos(162^0-\alpha)\times\Delta d}{3A}\cdot\frac{1}{\frac{1}{2}\rho U_\infty^2}\cdot[(P_{16}-P_0)+4(P_{17}-P_0)+2(P_{18}-P_0)+4(P_{19}-P_0)+(P_{20}-P_0)+12P_0] + \frac{\cos(90^0-\alpha)\times\Delta d}{3A}\cdot\frac{1}{\frac{1}{2}\rho U_\infty^2}\cdot[(P_{21}-P_0)+4(P_{22}-P_0)+2(P_{23}-P_0)+4(P_{24}-P_0)+(P_{25}-P_0)+12P_0]$$

Now writing in terms of pressure coefficients and using $12P_0 = 0$ [P_0 is the ambient gauge pressure=0] the above equation is transformed into

$$C_D = \frac{\cos(18^0-\alpha)\times\Delta d}{3A}\cdot[C_{p_1}+4C_{p_2}+2C_{p_3}+4C_{p_4}+C_{p_5}] - \frac{\cos(126^0-\alpha)\times\Delta d}{3A}\cdot[C_{p_6}+4C_{p_7}+2C_{p_8}+4C_{P_9}+C_{p_{10}}] - \frac{\cos(54^0-\alpha)\times\Delta d}{3A}\cdot[C_{p_{11}}+4C_{p_{12}}+2C_{p_{13}}+4C_{p_{14}}+C_{p_{15}}] + \frac{\cos(162^0-\alpha)\times\Delta d}{3A}\cdot[C_{p_{16}}+4C_{p_{17}}+2C_{p_{18}}+4C_{p_{19}}+C_{p_{20}}] + \frac{\cos(90^0-\alpha)\times\Delta d}{3A}\cdot[C_{p_{21}}+4C_{p_{22}}+2C_{p_{23}}+4C_{p_{24}}+C_{p_{25}}] \quad (4.40)$$

Similarly the expression of lift coefficient C_L can be obtained as,

$$C_L = -\frac{\sin(18^0-\ )\times\Delta d}{3A}\cdot[C_{p_1}+4C_{p_2}+2C_{p_3}+4C_{p_4}+C_{p_5}] + \frac{\sin(126^0-\ )\times\Delta d}{3A}\cdot[C_{p_6}+4C_{p_7}+2C_{p_8}+4C_{P_9}+C_{p_{10}}] + \frac{\sin(54^0-\ )\times\Delta d}{3A}\cdot[C_{p_{11}}+4C_{p_{12}}+2C_{p_{13}}+4C_{p_{14}}+C_{p_{15}}] - \frac{\sin(162^0-\ )\times\Delta d}{3A}\cdot[C_{p_{16}}+4C_{p_{17}}+2C_{p_{18}}+4C_{p_{19}}+C_{p_{20}}] - \frac{\sin(90^0-\ )\times\Delta d}{3A}\cdot[C_{p_{21}}+4C_{p_{22}}+2C_{p_{23}}+4C_{p_{24}}+C_{p_{25}}] \quad (4.41)$$

4.4 Sample Calculation

Calculation procedure to obtain the numerical values of the coefficient of pressure, coefficients of drag and lift has been provided here as an example.

4.4.1 Coefficient of pressure

Pressure coefficient will be calculated from the following equation

$$C_p = \frac{\Delta P}{\frac{1}{2}U_\infty^2}$$

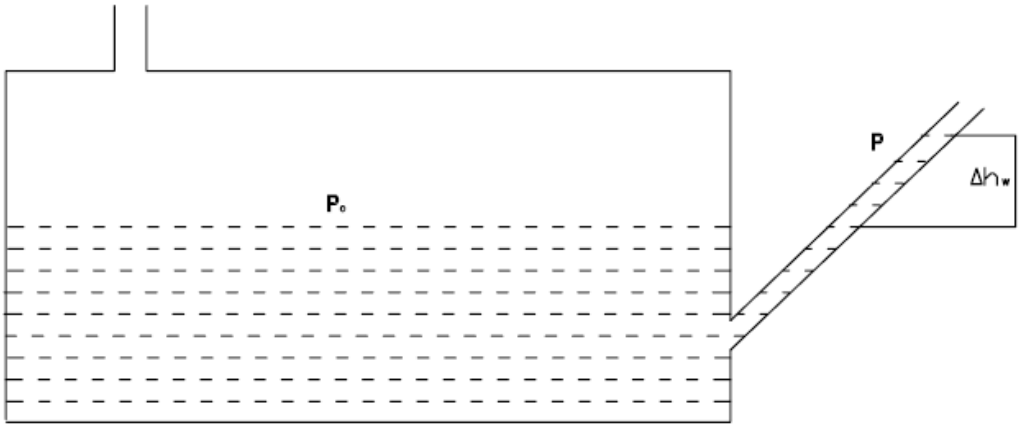

Figure 4.2: Inclined Manometer Showing Suction Head

Δh_w is the suction head in the manometer limb. The manometer liquid is water. Now making the pressure balance one can find

$$P_0 = P + \Delta h_w \times \gamma_w \tag{4.42}$$

Where, γ_w is the specific weight of manometer liquid. From equation (4.42), Δp can be obtained as

$$\Delta P = P - P_0 = -\Delta h_w \times \gamma_w$$

Therefore inserting the value of ΔP, pressure coefficient may be written as

$$C_p = -\frac{\Delta h_w \times \gamma_w}{\frac{1}{2} U_\infty^2}$$

Now writing $\gamma_w = \rho_w \times g$, the above equation becomes

$$C_p = -\frac{\Delta h_w \times \rho_w \times g}{\frac{1}{2} U_\infty^2}$$

Where, density of water ρ_w=1000kg/m^3 and density of air ρ=1.22kg/m^3, Therefore, one obtains

$$C_p = -\frac{\Delta h_w \times 1000 \times 9.81}{\frac{1}{2} \times 1.22 \times U_\infty^2}$$

Where, Δh_w is in meter of water height. Now one can write the above expression as

$$C_p = \frac{-1000 \times 9.81 \times \frac{\Delta h_w}{1000}}{\frac{1}{2} \times 1.22 \times U_\infty^2}$$

$$= 16.082 \times \frac{\Delta h_w}{U_\infty^2} \tag{4.43}$$

Where,Δh_w is in mm of water height and U_∞ is in m/s. The velocity of air in the wind tunnel may be written as

$$U_\infty = \sqrt{2gh_a} = \sqrt{2 \times 9.81 \times h_a} = 4.43\sqrt{h_a} \quad (4.44)$$

Where, h_a is the air head. If $_a$ is the specific weight of air, then a relation is obtained as

$$_a h_a = \ _w h_w$$

Therefore, the air head can be written as

$$h_a = \frac{_w h_w}{_a}$$

Now inserting $_w = 1000 kg/m^3$ and $_a = 1.22 kg/m^3$, the above equation becomes

$$h_a = \frac{1000}{1.22} h_w = 819.672 h_w \quad (4.45)$$

Now from equations (4.44) and (4.45), the expression of velocity is written as

$$U_\infty = 123.83\sqrt{h_w}$$

Where, h_w is in meter of water head. Changing h_w in mm of water head, air velocity in the wind tunnel is

$$U_\infty = 4.0107\sqrt{h_w} \quad (4.46)$$

Using equation (4.46) the free stream velocity in the wind tunnel was obtained and that was cross- checked with the help of a digital anemometer. For h_w = 10.85 mm of water head, the free stream velocity was calculated from equation (4.46), which was $U_\infty = 13.21 m/s$

For a suction head of $\Delta h_w = 8.1$ mm of water and $U_\infty = 13.21$ m/s, the pressure coefficient C_p is found from the equation (4.43), which was $C_p = 0.75$.

4.4.2 Coefficient of Drag

4.4.2.1 Hexagonal Cylinder

The value of drag coefficient was calculated from the following relation

$$C_D = \frac{\cos(30^0 - \ ) \times \Delta d}{3A} \cdot [(C_{p_1} + 4C_{p_2} + 2C_{p_3} + 4C_{p_4} + C_{p_5}) - (C_{p_{16}} + 4C_{p_{17}} + 2C_{p_{18}} + 4C_{p_{19}} + C_{p_{20}})] + \frac{\cos(90^0 - \ ) \times \Delta d}{3A} \cdot [(C_{p_6} + 4C_{p_7} + 2C_{p_8} + 4C_{p_9} + C_{p_{10}}) - (C_{p_{21}} + 4C_{p_{22}} + 2C_{p_{23}} + 4C_{p_{24}} + C_{p_{25}}) + \frac{\cos(150^0 - \alpha) \times \Delta d}{3A} \cdot [(C_{p_{11}} + 4C_{p_{12}} + 2C_{p_{13}} + 4C_{p_{14}} + C_{p_{15}}) - (C_{p_{26}} + 4C_{p_{27}} + 2C_{p_{28}} + 4C_{p_{29}} + C_{p_{30}})]$$

Writing $= 0^0$, $\frac{\Delta d}{A} = \frac{1}{10\cos 30^0}$ and inserting the values of surface static pressure coefficient in equation (4.18), the drag coefficient becomes

$C_D = \frac{1}{30\cos 30^0}.[\cos 30^0\{(0.75 + 4 \times 0.722 + 2 \times 0.65 + 4 \times 0.41 + 0) - (-0.675 - 4 \times 0.671 - 2 \times 0.636 - 4 \times 0.635 - 0.6612)\} + 0 + \cos 150^0 \{(-0.6612 - 4 \times 0.635 - 2 \times 0.636 - 4 \times 0.671 - 0.675) - (0.0261 + 4 \times 0.41 + 2 \times 0.644 + 4 \times 0.722 + 0.75)\}] = 0.96$

4.4.2.2 Pentagonal Cylinder

The value of drag coefficient was calculated from the following relation

$C_D = \frac{\cos(18^0 - \alpha) \times \Delta d}{3A} \cdot [C_{p_1} + 4C_{p_2} + 2C_{p_3} + 4C_{p_4} + C_{p_5}] - \frac{\cos(126^0 - \alpha) \times \Delta d}{3A} \cdot [C_{p_6} + 4C_{p_7} + 2C_{p_8} + 4C_{P_9} + C_{p_{10}}] - \frac{\cos(54^0 - \alpha) \times \Delta d}{3A} \cdot [C_{p_{11}} + 4C_{p_{12}} + 2C_{p_{13}} + 4C_{p_{14}} + C_{p_{15}}] + \frac{\cos(162^0 - \alpha) \times \Delta d}{3A} \cdot [C_{p_{16}} + 4C_{p_{17}} + 2C_{p_{18}} + 4C_{p_{19}} + C_{p_{20}}] + \frac{\cos(90^0 - \alpha) \times \Delta d}{3A} \cdot [C_{p_{21}} + 4C_{p_{22}} + 2C_{p_{23}} + 4C_{p_{24}} + C_{p_{25}}]$

Writing $= 0^0$, $\frac{\Delta d}{A} = \frac{1}{10\cos 18^0}$ and inserting the values of surface static pressure coefficient in equation (4.40), the drag coefficient becomes

$C_D = \frac{1}{30\cos 18^0}.[\cos 18^0(1.547 + 4 \times 4.034 + 2 \times 3.362 + 4 \times 2.914 + 2.734) - \cos 126^0 (0.964 + 4 \times 1.031 + 2 \times 1.703 + 4 \times 1.703 + 0.874) - \cos 54^0 (0.112 + 4 \times 0.202 + 2 \times 0.090 + 4 \times 0.045 + 0.336) + \cos 162^0 (0.179 + 4 \times 0.179 + 2 \times 0.314 + 4 \times 0.403 + 0.157) + \cos 90^0 (0.179 + 4 \times 0.291 + 2 \times 0.628 + 4 \times 0.157 + 1.345)] = 1.48$

4.4.3 Coefficient of Lift

4.4.3.1 Hexagonal Cylinder

The value of lift coefficient was calculated from the following relation

$C_L = -\frac{\sin(30^0 - \alpha) \times \Delta d}{3A} \cdot [(C_{p_1} + 4C_{p_2} + 2C_{p_3} + 4C_{p_4} + C_{p_5}) - (C_{p_{16}} + 4C_{p_{17}} + 2C_{p_{18}} + 4C_{p_{19}} + C_{p_{20}})] - \frac{\sin(90^0 - \alpha) \times \Delta d}{3A} \cdot [(C_{p_6} + 4C_{p_7} + 2C_{p_8} + 4C_{P_9} + C_{p_{10}}) - (C_{p_{21}} + 4C_{p_{22}} + 2C_{p_{23}} + 4C_{p_{24}} + C_{p_{25}}) - \frac{\sin(150^0 - \alpha) \times \Delta d}{3A} \cdot [(C_{p_{11}} + 4C_{p_{12}} + 2C_{p_{13}} + 4C_{p_{14}} + C_{p_{15}}) - (C_{p_{26}} + 4C_{p_{27}} + 2C_{p_{28}} + 4C_{p_{29}} + C_{p_{30}})]$

Writing $= 0^0$, $\frac{\Delta d}{A} = \frac{1}{10\cos 30^0}$ and inserting the values of surface static pressure coefficient in equation (4.19), the lift coefficient becomes

$C_L = \frac{1}{30\cos 30^0}.[-\sin 30^0\{(0.75 + 4 \times 0.722 + 2 \times 0.65 + 4 \times 0.41 + 0) - (-0.675 - 4 \times 0.671 - 2 \times 0.636 - 4 \times 0.635 - 0.6612)\} - \text{Sin } 90^0 \{(-0.6003 - 4 \times 0.64 - 2 \times 0.678 - 4 \times 0.6438 - 0.609) - (-0.609 - 4 \times 0.64 - 2 \times 0.669 - 4 \times 0.64 - 0.609)\}$

$-\sin 150^0\ \{(-0.6612-4\times0.635-2\times0.636-4\times0.671-0.675)-(0.0261+4\times0.41+2\times0.644+4\times0.722+0.75\ )\}]=0.0$

4.4.3.2 Pentagonal Cylinder

The value of lift coefficient was calculated from the following relation

$C_L = -\frac{\sin(18^0-\alpha)\times\Delta d}{3A}\cdot[C_{p_1}+4C_{p_2}+2C_{p_3}+4C_{p_4}+C_{p_5}] + \frac{\sin(126^0-\alpha)\times\Delta d}{3A}\cdot[C_{p_6}+4C_{p_7}+2C_{p_8}+4C_{P_9}+C_{p_{10}}]+\frac{\sin(54^0-\alpha)\times\Delta d}{3A}\cdot[C_{p_{11}}+4C_{p_{12}}+2C_{p_{13}}+4C_{p_{14}}+C_{p_{15}}]-\frac{\sin(162^0-\alpha)\times\Delta d}{3A}\cdot[C_{p_{16}}+4C_{p_{17}}+2C_{p_{18}}+4C_{p_{19}}+C_{p_{20}}]-\frac{\sin(90^0-\alpha)\times\Delta d}{3A}\cdot[C_{p_{21}}+4C_{p_{22}}+2C_{p_{23}}+4C_{p_{24}}+C_{p_{25}}]$

Writing $=0^0$, $\frac{\Delta d}{A}=\frac{1}{10\cos 18^0}$ and inserting the values of surface static pressure coefficient in equation (4.41), the lift coefficient becomes

$C_L=\frac{1}{30\cos 18^0}.[-\sin 18^0\ (1.547+4\times4.034+2\times3.362+4\times2.914+2.734)+\sin 126^0\ (0.964+4\times1.031+2\times1.703+4\times1.703+0.874)\ +\sin 54^0\ (0.112+4\times0.202+2\times0.090+4\times0.045+0.336)-\sin 162^0\ (0.179+4\times0.179+2\times0.314+4\times0.403+0.157\ )-\sin 90^0\ (0.179+4\times0.291+2\times0.628+4\times0.157+1.345\ )]=-0.11$

CHAPTER-5
RESULTS AND DISCUSSIONS

5.1 General

In this chapter the results of the experimental investigation regarding the surface static pressure coefficients, drag and lift coefficients have been discussed. First of all, the static pressure coefficients on the surface of a single hexagonal cylinder and a single pentagonal cylinder at various angles of attack are taken into consideration. Then the distributions of the static pressure coefficients-on the surface of the cylinders in group for various inter-spacing are considered. The calculated drag and lift coefficients for the single cylinder and for the group of cylinder are also discussed. The results of the present research work have been compared with those of the existing research works in some cases.

5.2 Single Cylinder

In this section the distributions of the pressure coefficients, drag and lift coefficients have been taken into consideration for discussion for a single hexagonal cylinder and pentagonal cylinder at different angles of attack. Pressure coefficients have been calculated from the measured values of the surface static pressures. Then the drag and lift coefficients have been obtained from the pressure coefficients by the numerical integration method. All the coefficients are determined for the uniform cross flow on the cylinder at Reynolds of 4.22 x 10^4 based on the width of the cylinder across the flow direction at zero angle of attack.

Before going to discuss the results of the experimental investigation, it will be relevant here to present the typical flow pattern over a single square cylinder at zero, small and moderate angles of attack as shown in Figure 5.1. Although the hexagonal and pentagonal cylinder will give a bit different flow pattern, formation of the vortex pair will be similar. Therefore, the typical flow over the single square cylinder has been discussed. As the angle of attack increases, the path of the shear layers is altered from their point of origin at the front corners of the square cylinder to the vortex formation region as shown in Figure 5.1, In the absence of turbulence in the incident flow, the shear layers which originate at the front corners of the square cylinder curve outward and form the familiar vortex street in the wake close behind the body. The pressure developed on the back surface depends on the distance of the vortices. The longer is the distance of the vortices from the body, higher is the back pressure and vice

versa. For the above reasons, pressures increase at the rear surface of the model cylinder around the angle of attack of 15°, while in the higher range of angle of attack, decrease.

5.2.1 Distribution of Pressure Coefficients

5.2.1.1 Hexagonal Cylinder

The cross-section of the single hexagonal model cylinder with 30 numbers of tappings, five numbers on each surface of the cylinder at an angle of attack has been shown in Figure 5.2. The six surfaces have been identified with S_1, S_2, S_3, S_4, S_5 and S_6. Pressure coefficient for each taping point has been determined from the measured surface static pressure. In Figures 5.3 to 5.8, the distributions of static pressure coefficients for angles of attack of 0° to 50° with a step of 10° have been presented respectively. While in Figure 5.9, the distributions of pressure coefficients for all angles of attack have been shown for relative comparison.

From Figure 5.3 one can observe that the distribution of the pressure coefficients is symmetric at zero angle of attack. It can be further noticed from this figure that there is no stagnation point. It is due to the fact that the location at the stagnation point has not been selected for the tapping. The pressure coefficient values are positive on the surfaces S_1 and S_6, while on the surfaces S_2 to S_5 there are negative pressure coefficients. However, one interesting point can be seen from this figure that almost uniform pressure coefficient distributions are found on surfaces S_2 to S_5. Baines, W. D. [1] has stated that, velocities in the wake region are much smaller than the mean flow, and hence, almost uniform pressures exist on the body surfaces.

In Figure 5.4 at angle of attack of 10^o, the value of the pressure coefficient has increased slightly on surface S_1, while it has dropped slightly on surface S_6. However, on the other four surfaces S_2 to S_5, the distributions of pressure coefficient are almost uniform. At = 10°, the Cp-distribution is close to that at = 0°.

In Figure 5.5 at angle of attack of 20°, there is further rise of C_p values on surface S_1 and further drop of C_p values on surface S_6. However, on surfaces S_3 to S_5 almost uniform C_p-distribution occurs. While on surface S_2 there is high suction near the tapping point 6. Probably, the shear layer deviates much in the outward direction near this point.

At = 30°, an interesting point can be observed from Figure 5.6, where on surface S_1, there is stagnation point on tapping point 3. The distributions of C_p on surfaces S_2 and S_6 are symmetric, which is expected at this angle of attack. On surfaces S_2 and S_6 near the tapping

points 6 and 30 respectively, there are high suction, which indicates the high deviation of the shear layer in the outward direction from the body, while reattachment is seen to occur at the downstream side of the surfaces S_2 and S_6. However, there is almost uniform Cp-distribution on the surfaces S_3 to S_5.

It is observed from Figure 5.7 that, there is still stagnation point on surface S_1, but it occurs at tapping point 4. Due to further rotation the surface S_2 shows positive values of C_p. However, on the surfaces S_3 to S_5, there is more or less uniform distribution of C_p. While on surface S_6 the C_p values become less negative. There appears reattachment near the tapping point 27 on the surface S_6.

Finally, from Figure 5.8 at $\alpha = 50°$, it is seen that the stagnation point still occurs at tapping point 4 and there is further rise of positive C_p values on the surface S_2 and all values are positive on this surface. On the surfaces S_3 to S_5, the C_p values are more or less uniform. While on the surface S_6, there is very high suction. Further rotation of the cylinder has not been made because at $\alpha = 0°$ and $\alpha = 60°$, they are identical.

In Figure 5.9 the Cp-distribution at all angles of attack has been presented to show the relative comparison of them.

5.2.1.2 Pentagonal Cylinder

The cross-section of the single pentagonal model cylinder with 25 numbers of tappings, five numbers on each surface of the cylinder at an angle of attack has been shown in Figure 5.2. The five surfaces have been identified with S_1, S_2, S_3, S_4 and S_5. Pressure coefficient for each taping point has been determined from the measured surface static pressure. In Figures 5.12 to 5.20, the distributions of static pressure coefficients for angles of attack of 0° to 72° with a step of 9° have been presented respectively. While in Figure 5.21, the distributions of pressure coefficients for all angles of attack have been shown for relative comparison.

From Figure 5.12 one can observe that on surface S_2, there is stagnation point on tapping point 7 at zero angle of attack. It can be further noticed from this figure that the pressure coefficient values are positive on the all surfaces. However, one interesting point can be seen from this figure that almost uniform pressure coefficient distributions are found on surfaces S_3 to S_5.

In Figure 5.13 at angle of attack of 9^o, there is no stagnation point and the value of the pressure coefficient has increased slightly on surface S_1, while it has dropped slightly on surface S_2 and S_5. However, on the other surfaces S_3 and S_4, the distributions of pressure coefficient are almost uniform. It can be further noticed from this figure that the pressure coefficient values are positive on the all surfaces except surface S_5.

In Figure 5.14 at angle of attack of 18°, there is no stagnation point and there is further rise of C_p values on surface S_1 and S_5 and further drop of C_p values on surface S_2. However, on surfaces S_3 to S_4 almost uniform C_p-distribution occurs.

At = 27°, one can be observed from Figure 5.15, there is no stagnation point. However, there is almost uniform Cp-distribution on the surfaces S_2 to S_4.

In Figure 5.16 at angle of attack of 36^o, there is no stagnation point. On the surfaces S_2 and S_4, the distributions of pressure coefficient are almost uniform. It can be further noticed from this figure that the pressure coefficient values are positive on the all surfaces.

From Figure 5.17 one can observe that the distribution of the pressure coefficients is symmetric at = 45°. It can be further noticed from this figure that nowhere there is stagnation point. It is due to the fact that the location at the stagnation point has not been selected for the tapping. The pressure coefficient values are positive on the all surfaces. However, one interesting point can be seen from this figure that almost uniform pressure coefficient distributions are found on surfaces S_2 to S_4.

In Figure 5.18 at angle of attack of 54^o, the value of the pressure coefficient has decreased slightly on surface S_1, while it has increase slightly on surface S_5. However, on the other three surfaces S_2 to S_4, the distributions of pressure coefficient are almost uniform. At = 54°, the Cp-distribution is close to that at = 45°.

In Figure 5.19 at angle of attack of 63^o, the value of the pressure coefficient has decreased further on surface S_1, while it has increase slightly on surface S_5. However, on the other three surfaces S_2 to S_4, the distributions of pressure coefficient are almost uniform. It can be further noticed from this figure that nowhere there is stagnation point. The pressure coefficient values are positive on the all surfaces. Further rotation of the cylinder has not been made because at α = 0° and α = 72°, they are identical.

In Figure 5.21 the Cp-distribution at all angles of attack has been presented to show the relative comparison of them.

5.2.2 Variation of Drag Coefficient

5.2.2.1 Hexagonal Cylinder

Variation of drag coefficient at various angles of attack on single hexagonal cylinder is shown in Figure 5.10. The drag coefficient at different angles of attack on a single square cylinder at uniform flow obtained by Mandal, A. C. [18] is also presented in this figure for comparison. It can be noticed from this figure that there is significant drop in the drag coefficient values for the hexagonal cylinder in comparison to that of the square cylinder and the values approach to that of the circular cylinder. It is seen from this figure that at zero angle of attack, the drag coefficient is about 0.95 and at all other angles of attack, the values are close to 0.80 except at angle of attack of 10°, where the value is about 0.50. The values of the drag coefficient at various angles of attack for the hexagonal cylinder can be explained from the Cp-distribution curves.

5.2.2.2 Pentagonal Cylinder

Variation of drag coefficient at various angles of attack on single pentagonal cylinder is shown in Figure 5.22. The drag coefficient at different angles of attack on a single square cylinder at uniform flow obtained by Mandal, A. C. [18] is also presented in this figure for comparison. It can be noticed from this figure that there is significant drop in the drag coefficient values for the pentagonal cylinder in comparison to that of the square cylinder and the values is higher than the hexagonal cylinder. It is seen from this figure that at zero angle of attack, the drag coefficient is about 1.48 and at all other angles of attack, the values are close to 1.55 except at angle of attack of 9° and 18^0, where the value is about 1.30 and 1.22 respectively. The values of the drag coefficient at various angles of attack for the pentagonal cylinder can be explained from the Cp-distribution curves.

5.2.3 Variation of Lift Coefficient

5.2.3.1 Hexagonal Cylinder

In Figure 5.11 the variation of lift coefficient at various angles of attack on single hexagonal cylinder is shown. The lift coefficient at different angles of attack on a square cylinder at uniform flow obtained by Mandal, A. C. [18] is also presented in this figure for comparison. It can be noticed from this figure that the variation of the lift coefficient on the single hexagonal cylinder is not appreciable; they are close to zero value except at angles of attack

of 10° and 50°, where some insignificant values are observed. For the single square cylinder the variation of lift coefficient with angle of attack is remarkable. The values of the lift coefficients for the single hexagonal cylinder can be explained from the Cp-distribution curves.

5.2.3.2 Pentagonal Cylinder

In Figure 5.23 the variation of lift coefficient at various angles of attack on single pentagonal cylinder is shown. The lift coefficient at different angles of attack on a square cylinder at uniform flow obtained by Mandal, A. C. [18] is also presented in this figure for comparison. It can be noticed from this figure that the variation of the lift coefficient on the single pentagonal cylinder is shifted 9^0 and pattern is more or less similar with the variation of lift coefficient for the single square cylinder except at angle of attack of 0°. The values of the lift coefficients for the single pentagonal cylinder can be explained from the Cp-distribution curves.

5.3 Group of Cylinders

In this section discussion in regard to the results of the group consisting of two hexagonal cylinders and one pentagonal cylinder will be done. In Figure 5.24, the group of cylinders is shown at zero angle of attack. One pentagonal cylinder is positioned in the upstream side designated as the front cylinder and another two hexagonal cylinders is positioned in the downstream side designated as the rear cylinders. All of them are placed along the flow direction. The inter-spacing between the two hexagonal cylinders was varied at L_2=2D, 3D, 5D and between pentagonal and hexagonal cylinders was varied at L_1=1D, 2D, 4D, 6D and 8D, where D is the width of the cylinder across the flow direction keeping the angle of attack constant. Tapping points are shown along the cross-section on the six surfaces S_1, S_2, S_3, S_4, S_5 and S_6 of the hexagonal cylinder and on the five surfaces S_1, S_2, S_3, S_4 and S_5 of the pentagonal cylinder, where the surface static pressures are measured.

5.3.1 Distribution of Pressure Coefficients on Hexagonal Cylinder

The Cp-distribution on the hexagonal cylinder of the group at L_1=8D, L_2=2D is shown in Figure 5.25. It can be seen from this figure that the C_p-distribution is symmetric. There is little effect on the Cp-distribution of the hexagonal cylinder due the presence of the pentagonal cylinder.

In Figure 5.27, the C_p-distribution on the hexagonal cylinder at L_1=6D, L_2=2D has been presented. It can be observed from this figure that there has been appreciable increase in the back pressure due to presence of the pentagonal cylinder. The average C_p values on the surfaces S_2 to S_5 is approximately -1 compared that of-1.50 in case of the inter-spacing L_1=8D, L_2=2D. However, C_p-distribution on the surfaces S_2 to S_5 is of uniform nature approximately. About same pattern of C_p-distribution is seen in Figure 5.29 at L_1=4D, L_2=2D on the hexagonal cylinder. There is remarkable effect on the Cp-distribution at both the inter-spacing L_1 of 4D and 6D due to the presence of the pentagonal cylinder.

As shown in Figure 5.31, the Cp-distribution on the hexagonal cylinder at L_1=2D, L_2=2D is slight rise of C_p values on the surfaces S_1. The surfaces S_2 and S_4 show uniform Cp-distribution approximately. The C_p-distribution at L_1=1D, L_2=2D is almost close to that at L_1=2D, L_2=2D**,** as shown in Figure 5.33. The Cp-distribution on the hexagonal cylinder of the group at inter-spacing L_2 of 3D and 5D with in each case of inter-spacing L_1 of 1D**,**2D, 4D, 6D and 8D is shown in figure 5.35,5.37,5.39,5.41,5.43,5.45,5.47,5.49,5.51,5.53 and this are more or similar to inter-spacing L_2 of 2D.

5.3.2 Distribution of Pressure Coefficient on Pentagonal Cylinder

The Cp-distribution on the pentagonal Cylinder of the group at L_1=8D, L_2=2D is shown in Figure 5.26. It can be observed from this figure that there is remarkable effect on C_p-distribution due the presence of the hexagonal cylinder. The pattern of the C_p-distribution is similar as that of the angle of attack zero degree but the values decreases. From S_2 to S_5, the C_p-distribution is symmetric and the C_p-distribution is more uniform on the surfaces S_3 to S_4.

It is observed from Figure 5.28 that on the pentagonal Cylinder of the group at L_1=6D, L_2=2D, the pattern of the C_p-distribution is similar as that of the L_1=8D, L_2=2D but the values increases. The C_p-distribution is more uniform on the surfaces S_3 to S_5.

However, a picture is seen in Figure 5.30 for the C_p-distribution on the pentagonal Cylinder of the group at L_1=4D, L_2=2D, the pattern of the C_p-distribution is similar as that of the L_1=6D, L_2=2D but the values increases for the surfaces S_3 to S_5 and C_p-distribution is more uniform.

At L_1=2D, L_2=2D on the pentagonal Cylinder of the group, there is further rise of the pressure on the surfaces S_2 to S_5 compared to that for the pentagonal cylinder at L_1=4D, L_2=2D, which is shown in Figure 5.32. The pattern of the C_p-distribution is similar as that of

the L_1=2D, L_2=2D for the pentagonal cylinder at L_1=1D, L_2=2D, which is shown in Figure 5.34. The Cp-distribution on the pentagonal cylinder of the group at inter-spacing L_2 of 3D and 5D with in each case of inter-spacing L_1 of 1D, 2D, 4D, 6D and 8D is shown in figure 5.36,5.38,5.40,5.42,5.44,5.46,5.48,5.50,5.52,5.54 and this are more or similar to inter-spacing L_2 of 2D.

5.3.3 Variation of Drag and Lift Coefficient on Pentagonal and Hexagonal Cylinder

The variation of drag coefficients on the hexagonal and pentagonal cylinders of the group with L_1 for different values of L_2 at zero degree angle of attack has been presented in Figure 5.55 and 5.57 respectively. It can be seen from figure 5.55 that, as the inter-spacing L_2 increase drag coefficient also increase for the all values of inter-spacing L_1 except L_1=2D,where drug coefficient is near to 1 for L_2 for hexagonal cylinder. It can be seen from figure 5.57 that, pentagonal cylinder in group has lower drag coefficient than single pentagonal cylinder. For L_2= 2D, at L_1=4D drag coefficient is equal to 1 and for higher L_1 drag coefficient is more than 1 and for lower L_1 drag coefficient is less than 1. For L_2= 5D, drag coefficient is higher than L_2= 2D for the all values of inter-spacing L_1. For L_2= 3D, drag coefficient is lower than L_2= 2D for the all values of inter-spacing L_1 except L_1=1D and 8D.

The variation of lift coefficients on the hexagonal and pentagonal cylinders of the group with L_1 for different values of L_2 at zero degree angle of attack has been presented in Figure 5.56 and 5.58 respectively. It can be seen from figure 5.56 that, for L_2=3D and 5D, the pattern of lift coefficient for hexagonal cylinder is similar. For L_2=2D, lift coefficient is negative for the all values of inter-spacing L_1 except L_1=4D and 8D. It can be seen from figure 5.58 that, for L_2=2D and 3D, lift coefficient is decrease with increase of L_1 and for L_2=5D, firstly lift coefficient is decrease with increase of L_1 up to 4D then increase for pentagonal cylinder.

5.4 Error in Measurements

During measurement of the surface static pressures on the cylinders for several days, the room temperature is assumed to be constant. As such the density of the air is taken as constant in the calculation. In reality there is minor variation of the temperature during taking all the readings, which has been neglected in the calculation. The fluctuation of the manometer reading was observed especially on the suction side of the cylinders. But that fluctuation was not significant. While taking the reading, always the mean value of the manometer was recorded. Since fluctuation was insignificant the error in the measured values was negligible.

5.5 Validation

Variation of drag coefficient at various angles of attack on single hexagonal cylinder is shown in Figure 5.59. The drag coefficient at different angles of attack on a single hexagonal cylinder at uniform flow obtained by Sultana, K. R. [52] is also presented in this figure for validation. It can be noticed from this figure that the drag coefficient distributions for single hexagonal cylinder at uniform flow for both experiment are almost similar.

In Figure 5.60 the variation of lift coefficient at various angles of attack on single hexagonal cylinder is shown. The lift coefficient at different angles of attack on a single hexagonal cylinder at uniform flow obtained by Sultana, K. R. [52] is also presented in this figure for validation. It can be noticed from this figure that the lift coefficient distributions for single hexagonal cylinder at uniform flow for both experiment are almost similar.

5.6 Synthesize Results

Variation of drag coefficient at Various Angles of Attack on different shapes of cylinder is shown in Figure 5.61. It can be noticed from this figure that the drag coefficient distributions for single circular cylinder at uniform flow is lowest and for rectangular cylinder is highest. For all other cylinder like octagonal, hexagonal, pentagonal, square cylinder the drag coefficient distributions are between circular and rectangular cylinder. Again in Figure 5.62 variation of lift coefficient at Various Angles of Attack on different shapes of cylinder like octagonal, hexagonal, pentagonal, square, rectangular cylinder is shown for comparison.

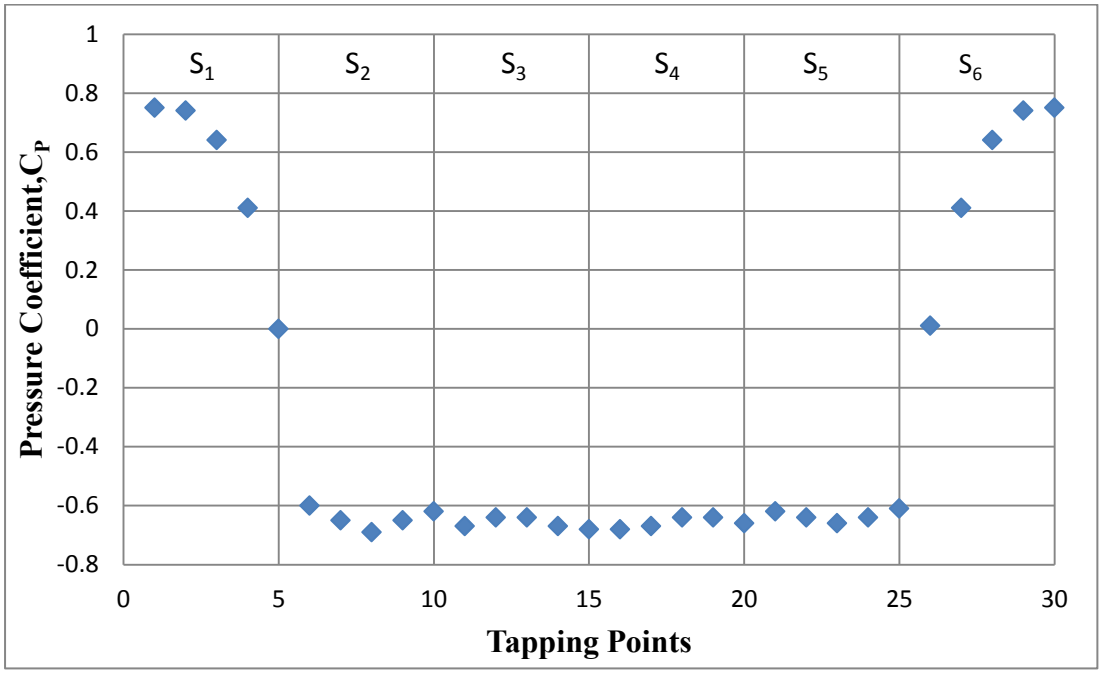

Figure 5.3: Distribution of Pressure Coefficient on Hexagonal Cylinder at Angle of Attack of 0^0

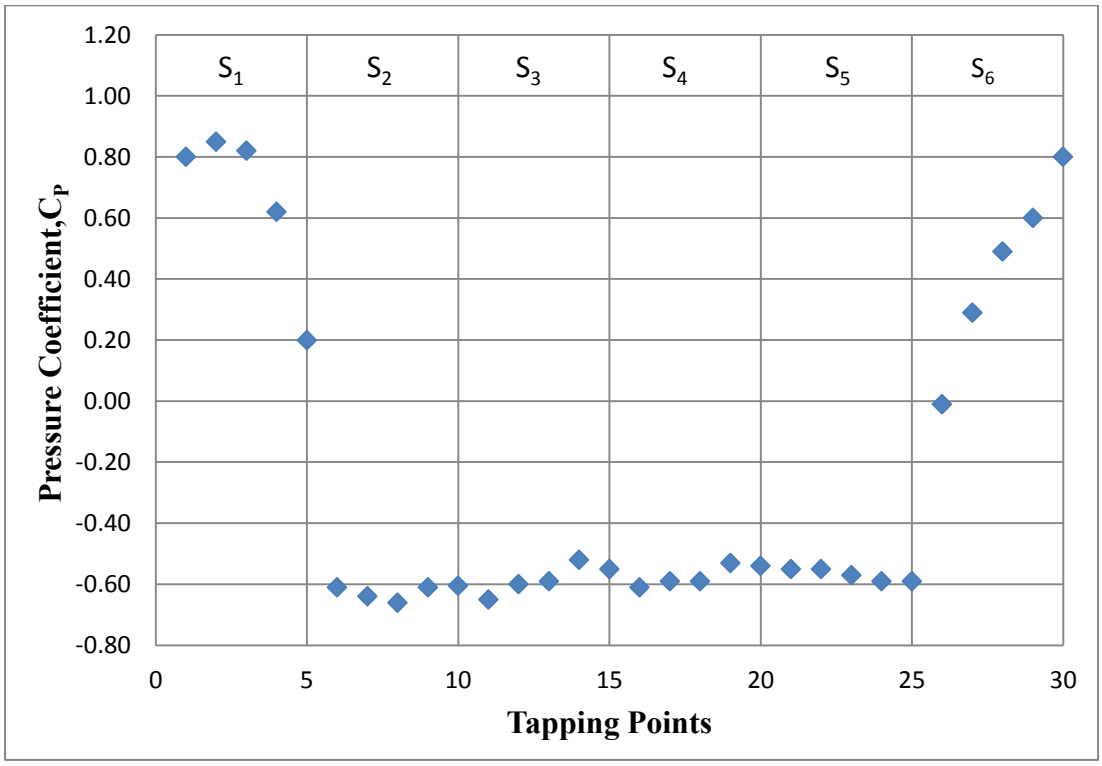

Figure 5.4: Distribution of Pressure Coefficient on Hexagonal Cylinder at Angle of Attack of 10^0

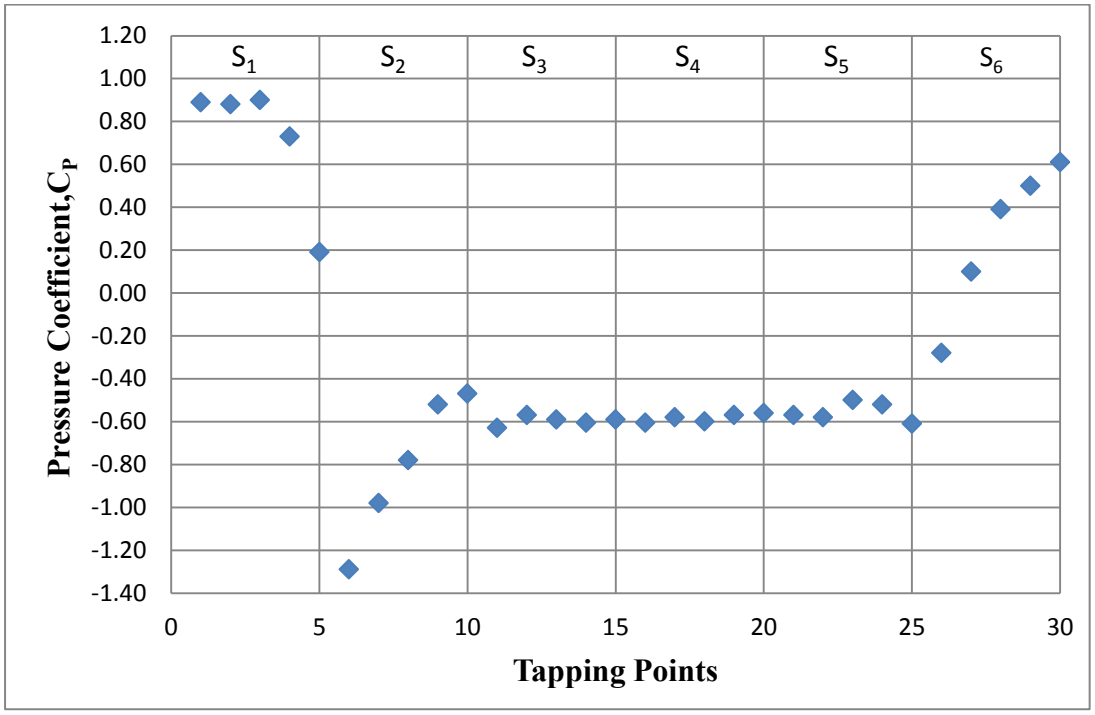

Figure 5.5: Distribution of Pressure Coefficient on Hexagonal Cylinder at Angle of Attack of 20^0

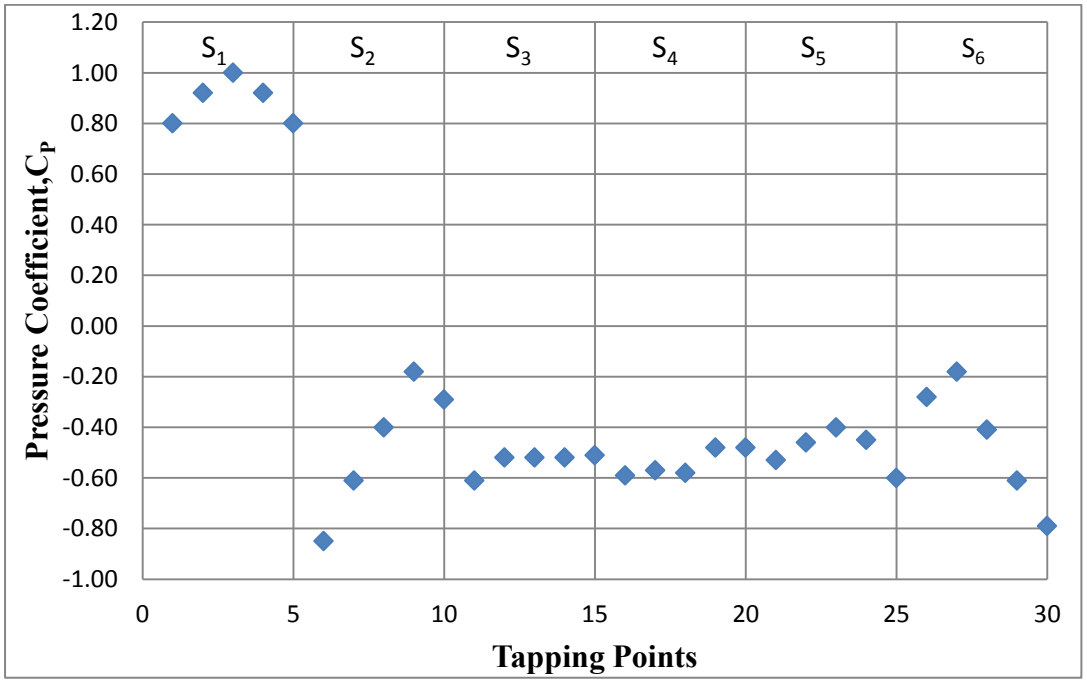

Figure 5.6: Distribution of Pressure Coefficient on Hexagonal Cylinder at Angle of Attack of 30^0

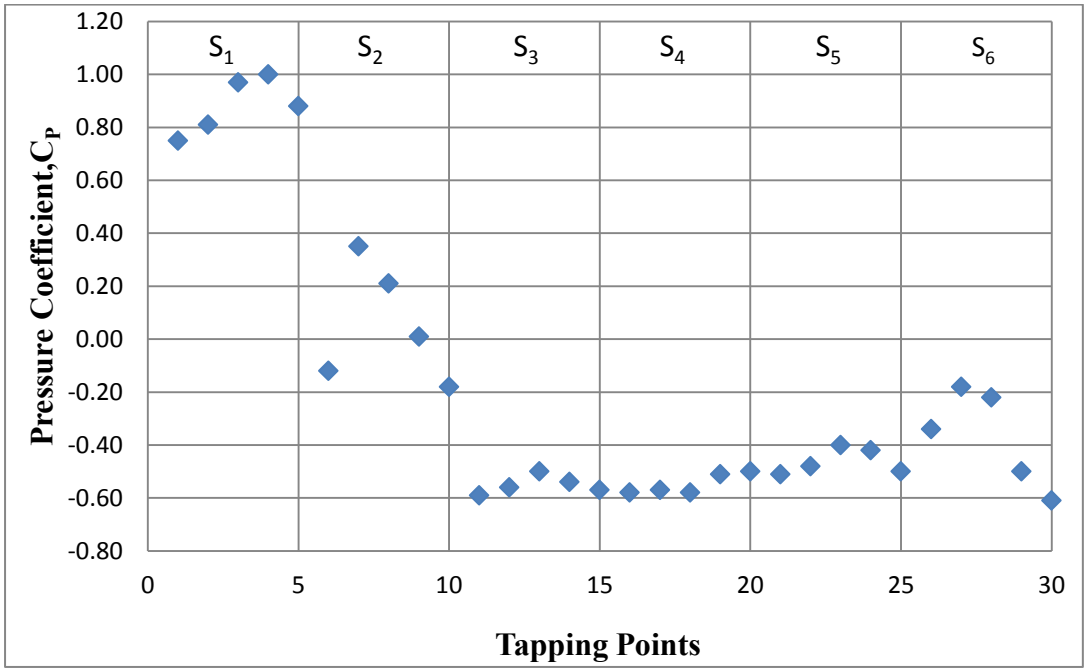

Figure 5.7: Distribution of Pressure Coefficient on Hexagonal Cylinder at Angle of Attack of 40^0

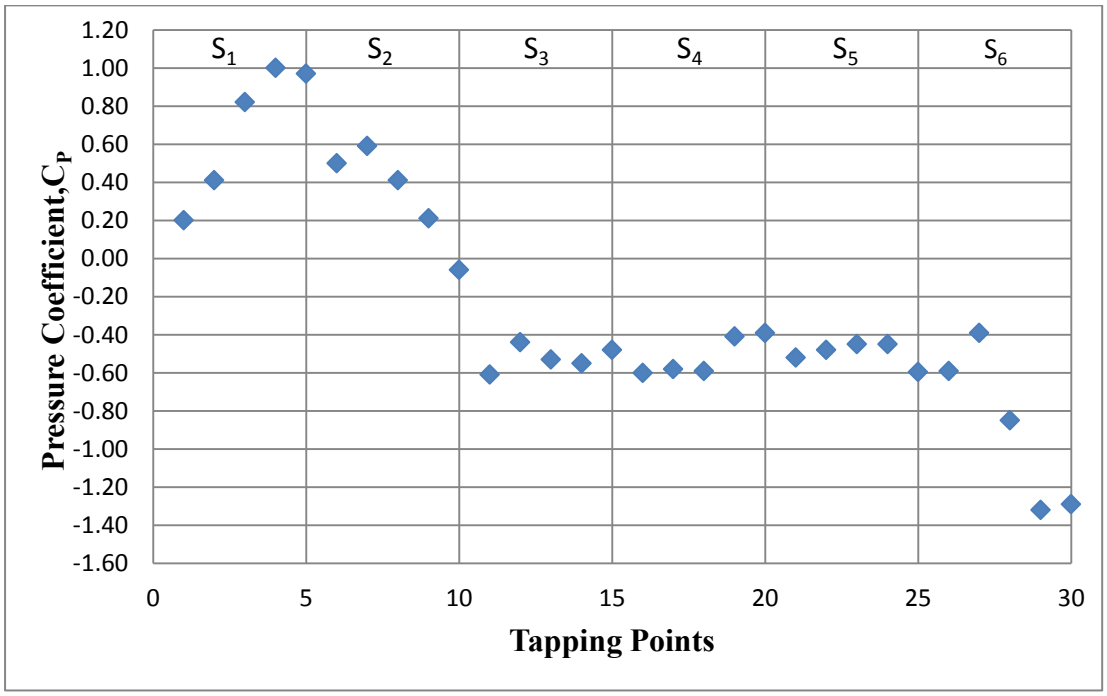

Figure 5.8: Distribution of Pressure Coefficient on Hexagonal Cylinder at Angle of Attack of 50^0

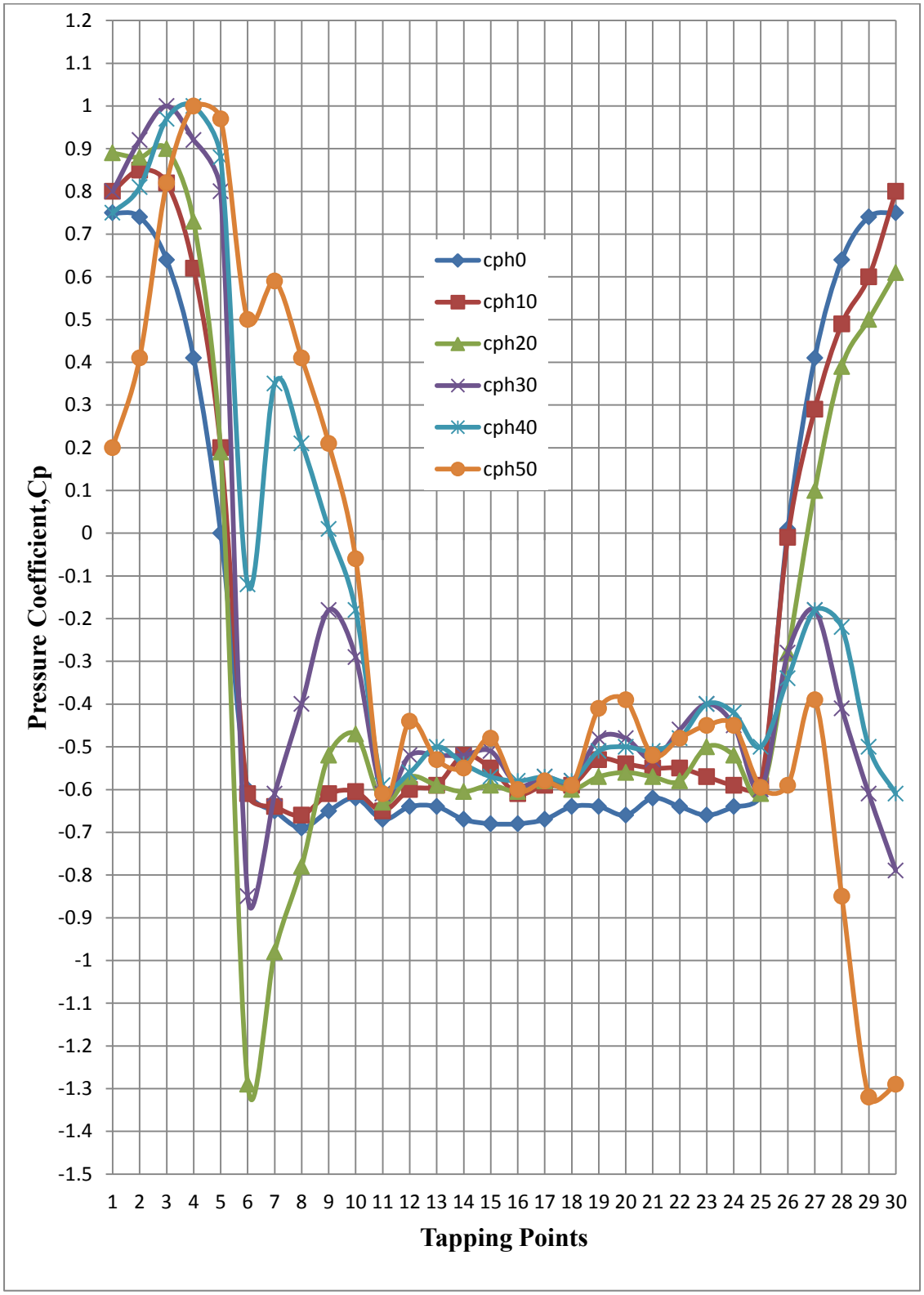

Figure 5.9: Distribution of Pressure Coefficients at Different Angles of Attack on Hexagonal Cylinder

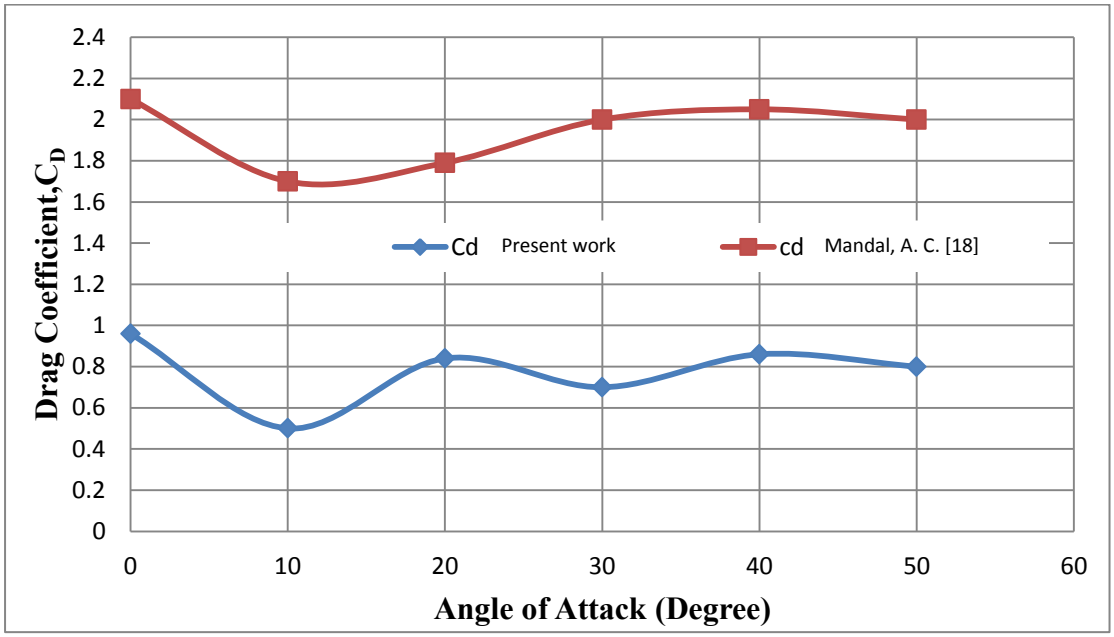

Figure 5.10: Variation of Drag Coefficient at Various Angles of Attack on Single Hexagonal Cylinder

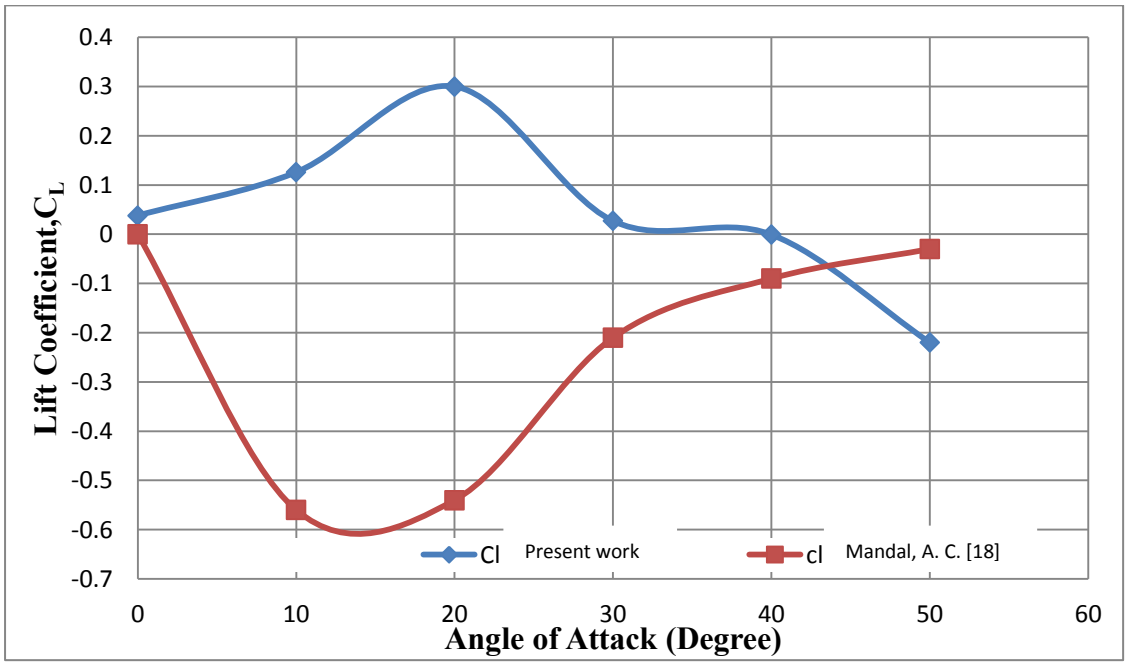

Figure 5.11: Variation of Lift Coefficient at Various Angles of Attack on Single Hexagonal Cylinder

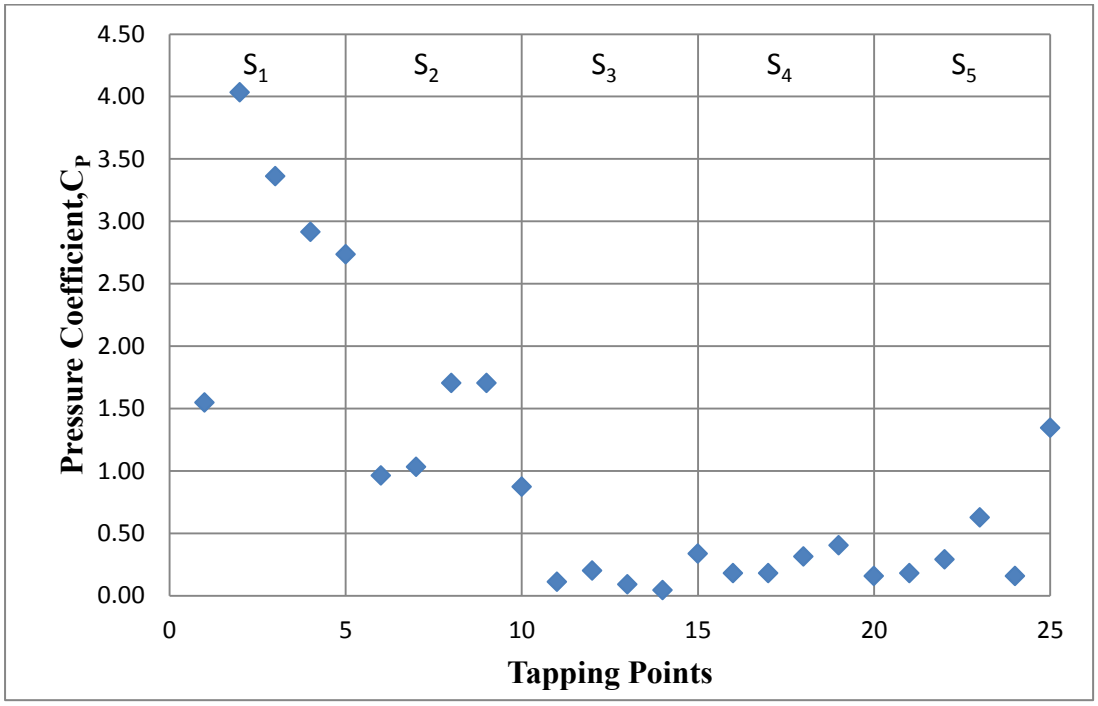

Figure 5.12: Distribution of Pressure Coefficient on Pentagonal Cylinder at Angle of Attack of 0^0

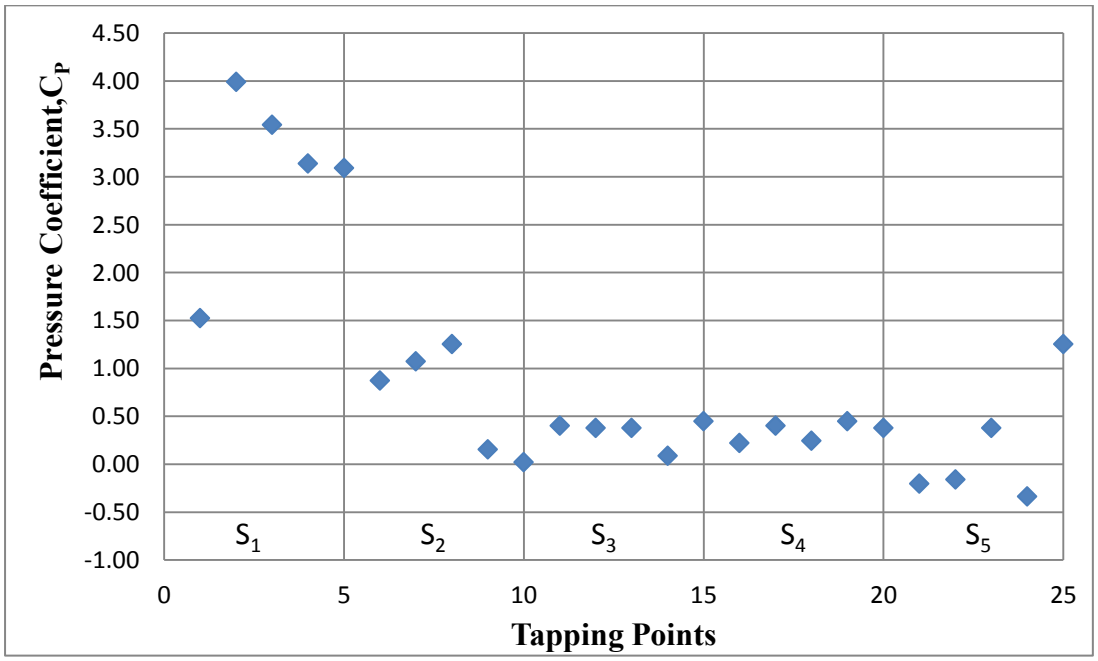

Figure 5.13: Distribution of Pressure Coefficient on Pentagonal Cylinder at Angle of Attack of 9^0

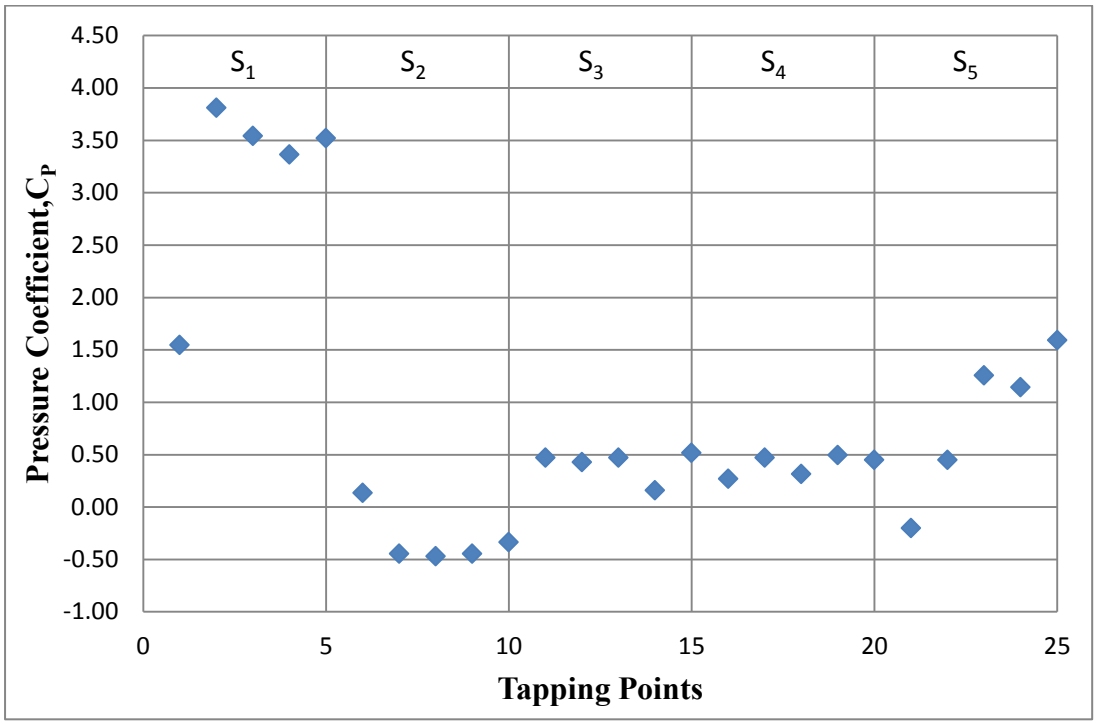

Figure 5.14: Distribution of Pressure Coefficient on Pentagonal Cylinder at Angle of Attack of 18^0

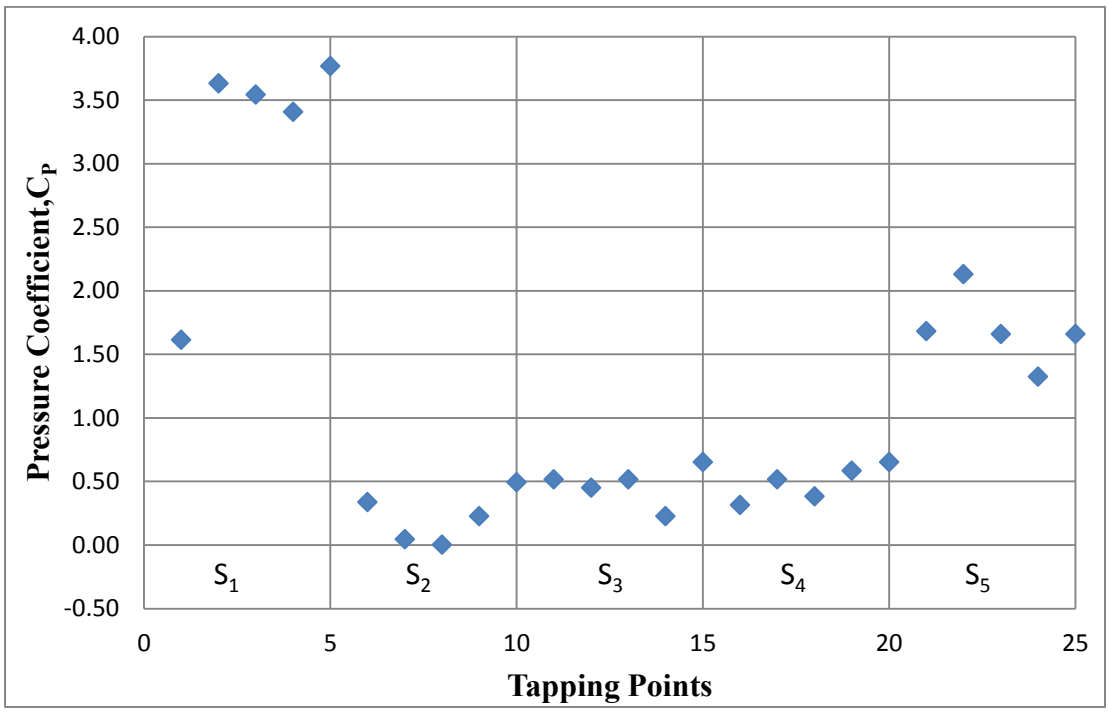

Figure 5.15: Distribution of Pressure Coefficient on Pentagonal Cylinder at Angle of Attack of 27^0

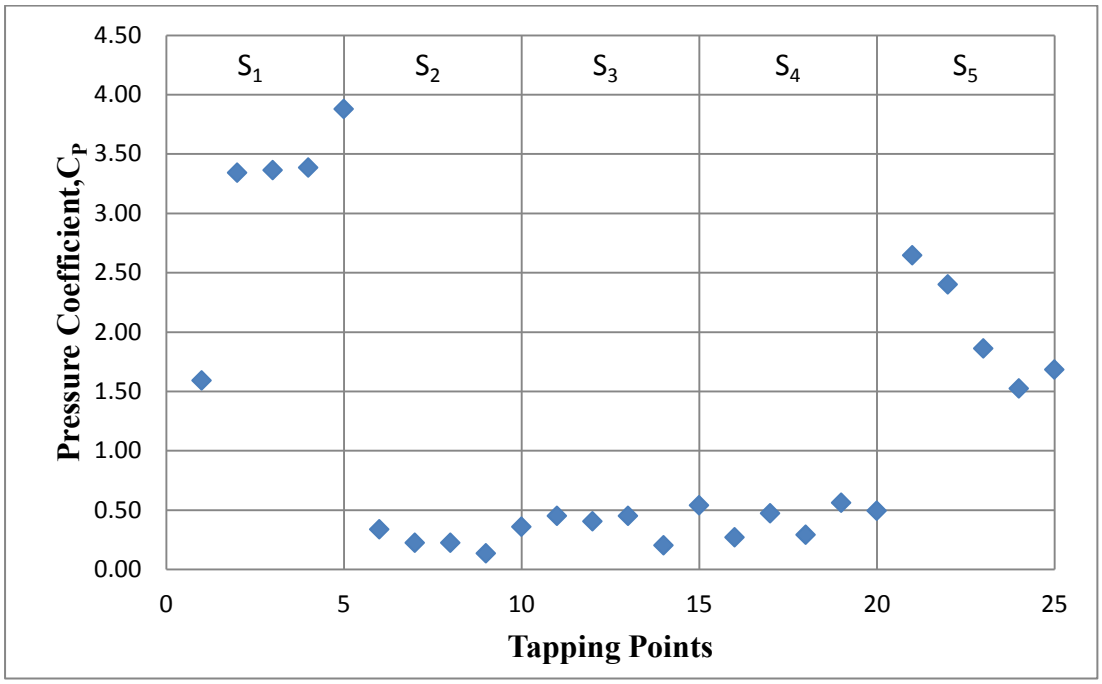

Figure 5.16: Distribution of Pressure Coefficient on Pentagonal Cylinder at Angle of Attack of 36^0

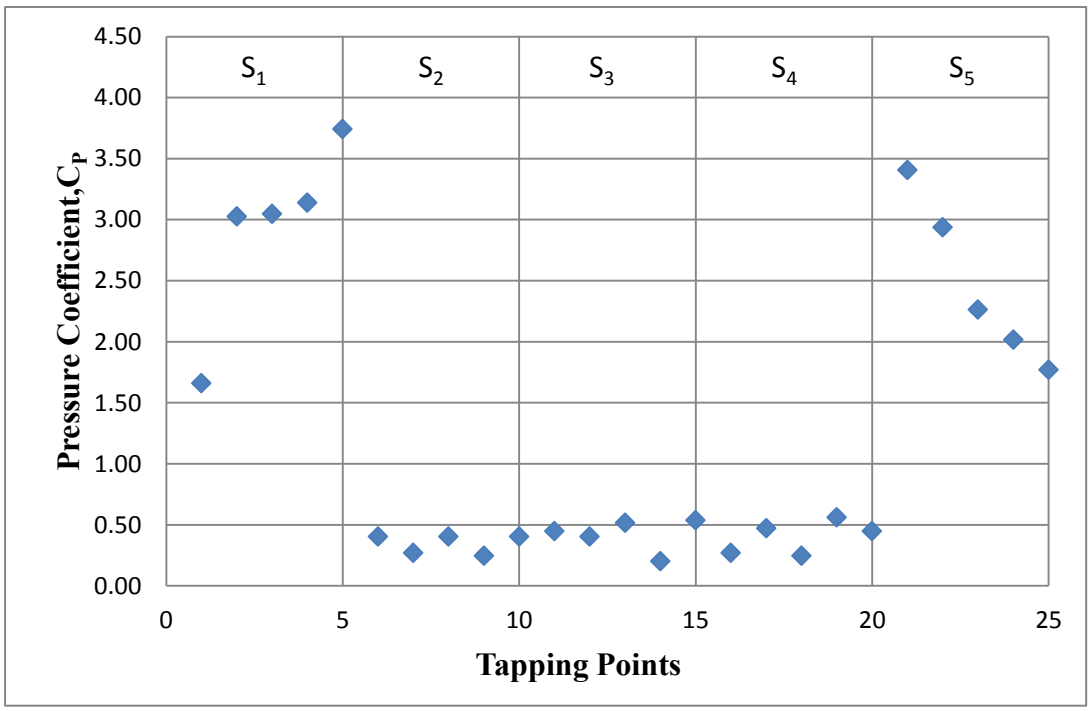

Figure 5.17: Distribution of Pressure Coefficient on Pentagonal Cylinder at Angle of Attack of 45^0

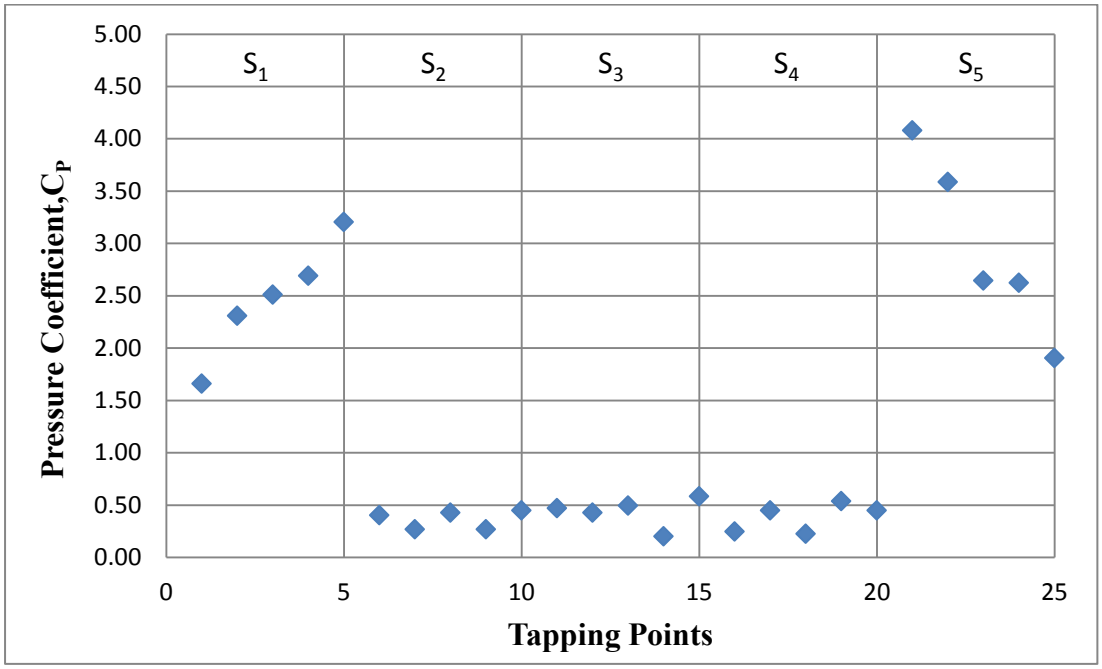

Figure 5.18: Distribution of Pressure Coefficient on Pentagonal Cylinder at Angle of Attack of 54^0

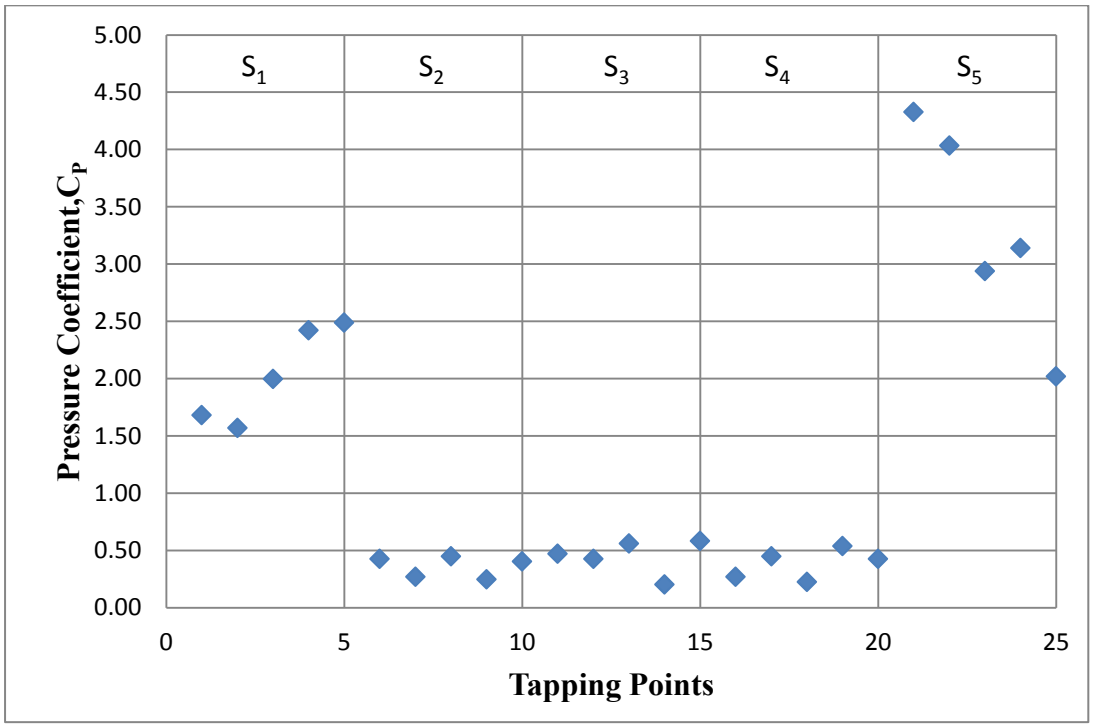

Figure 5.19: Distribution of Pressure Coefficient on Pentagonal Cylinder at Angle of Attack of 63^0

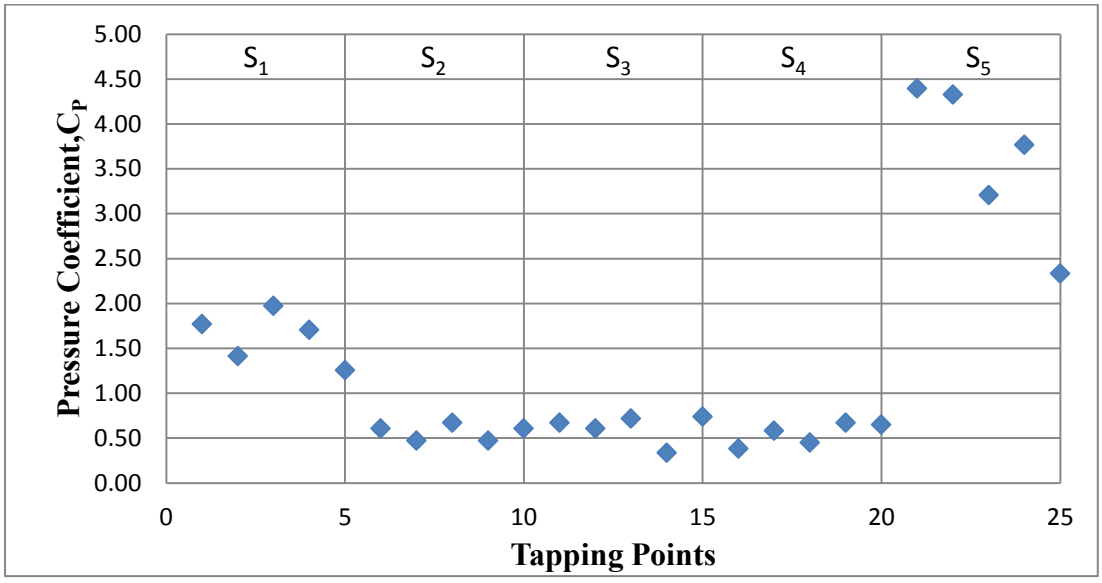

Figure 5.20: Distribution of Pressure Coefficient on Pentagonal Cylinder at Angle of Attack of 72^0

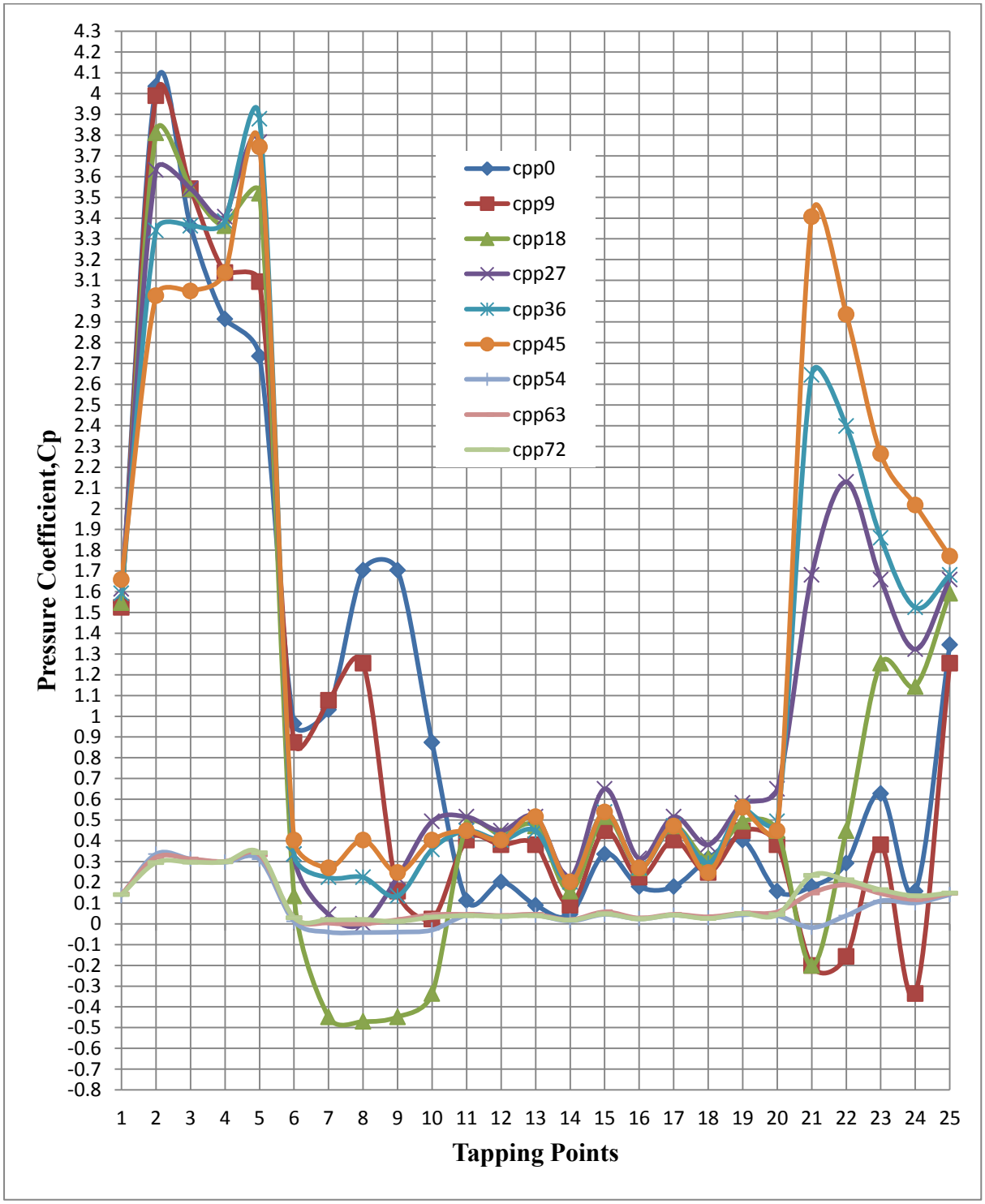

Figure 5.21: Distribution of Pressure Coefficients at Different Angles of Attack on Pentagonal Cylinder

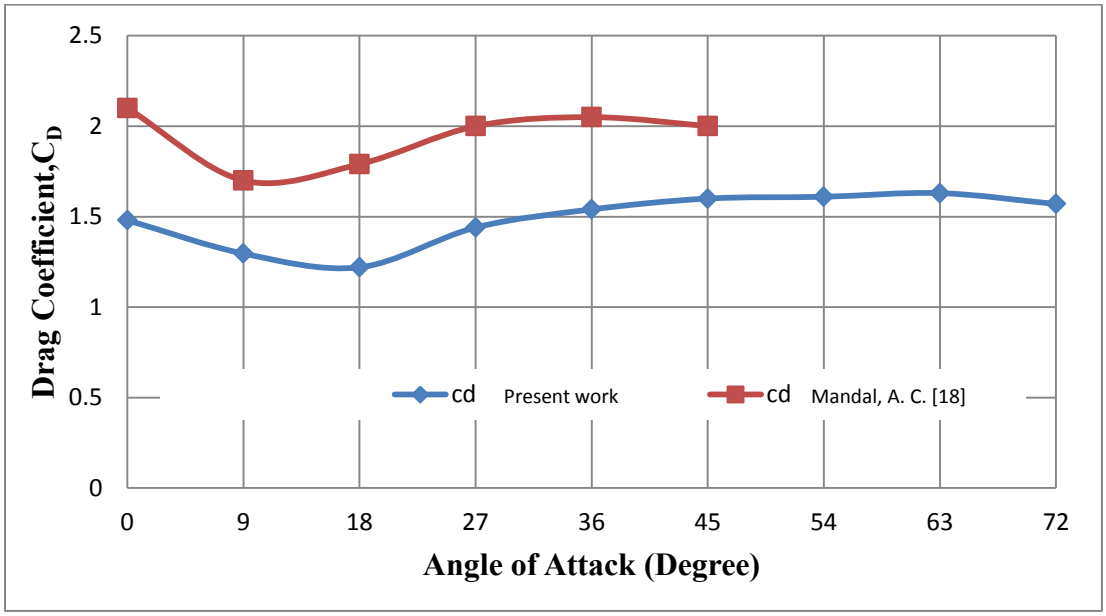

Figure 5.22: Variation of Drag Coefficient at Various Angles of Attack on Single Pentagonal Cylinder

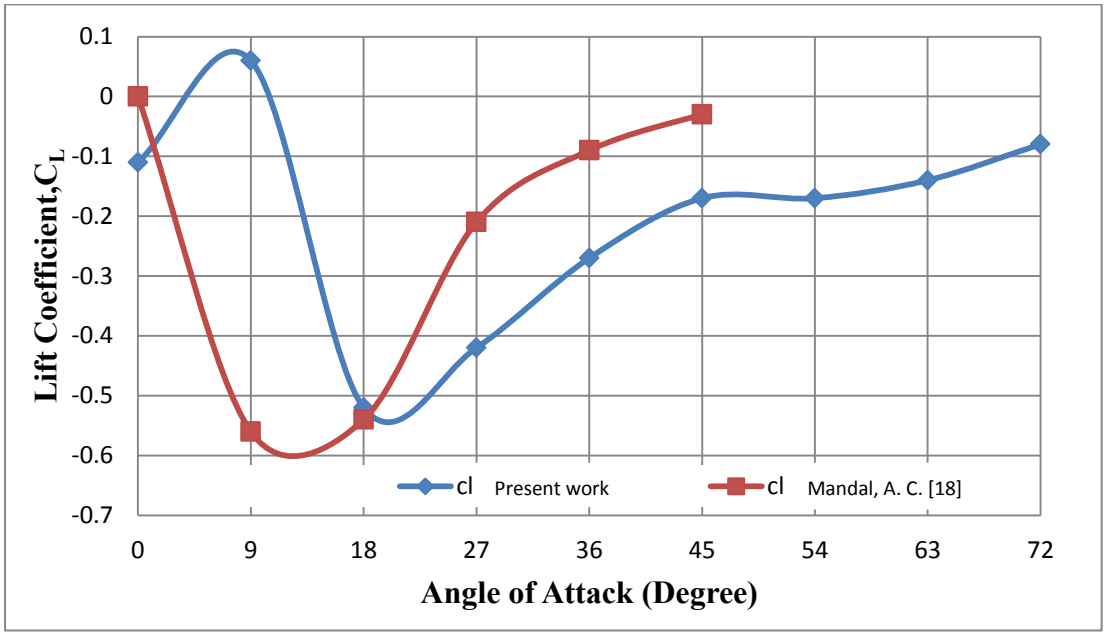

Figure 5.23: Variation of Lift Coefficient at Various Angles of Attack on Single Pentagonal Cylinder

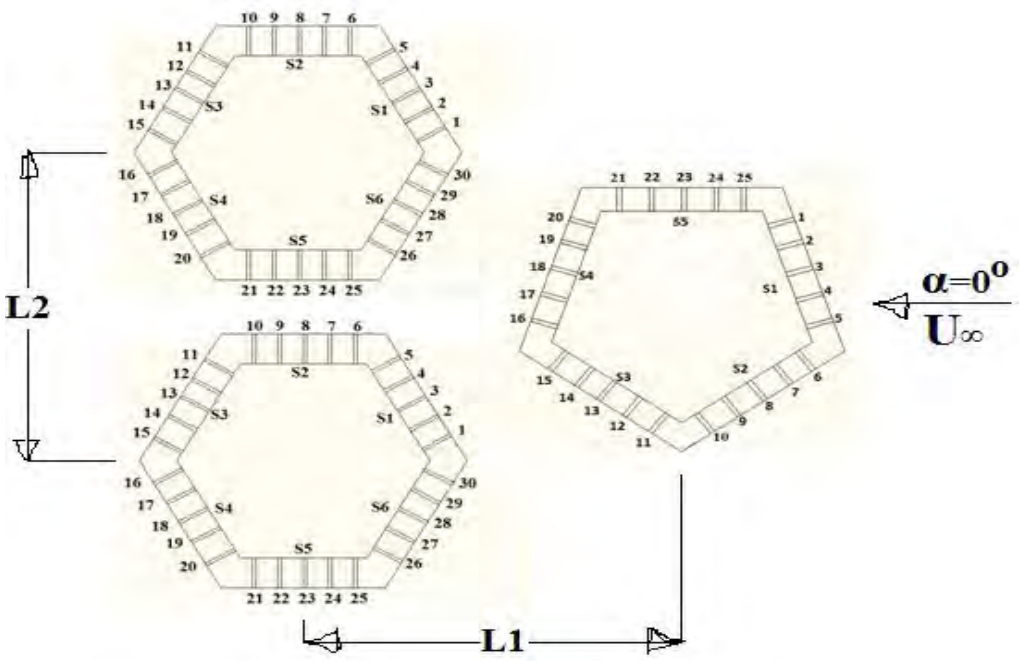

Figure 5.24: Flow over Cylinder in Group at Zero Angle of Attack

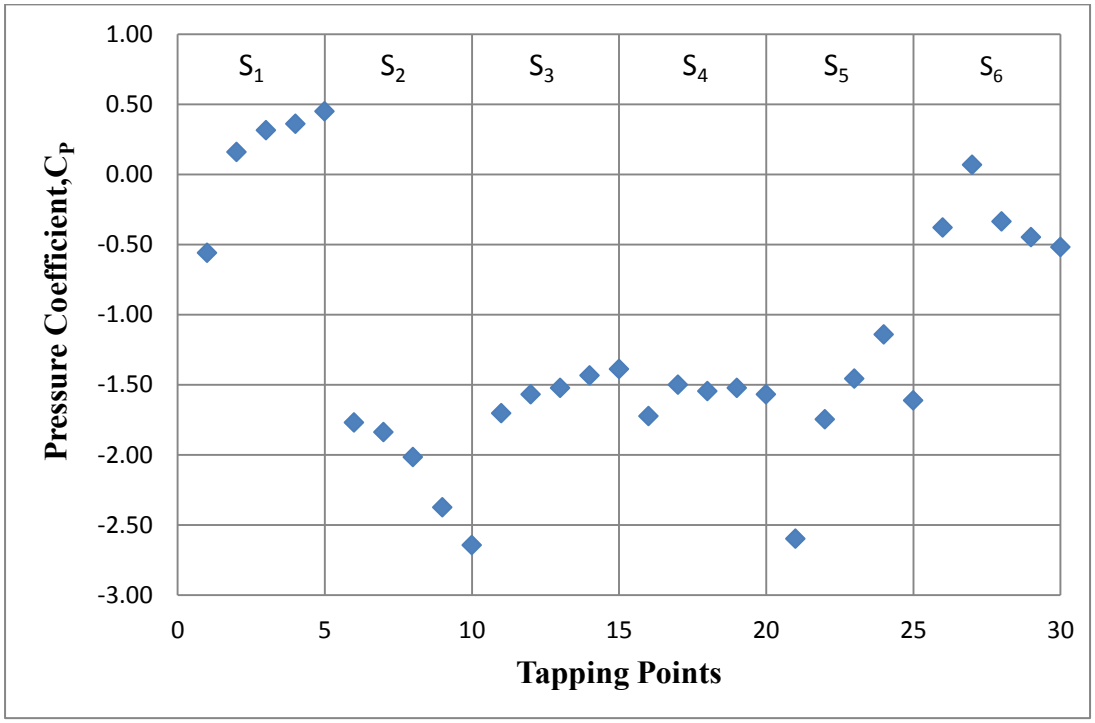

Figure 5.25: Distribution of Pressure Coefficient on Hexagonal Cylinder at L_1=8D, L_2=2D

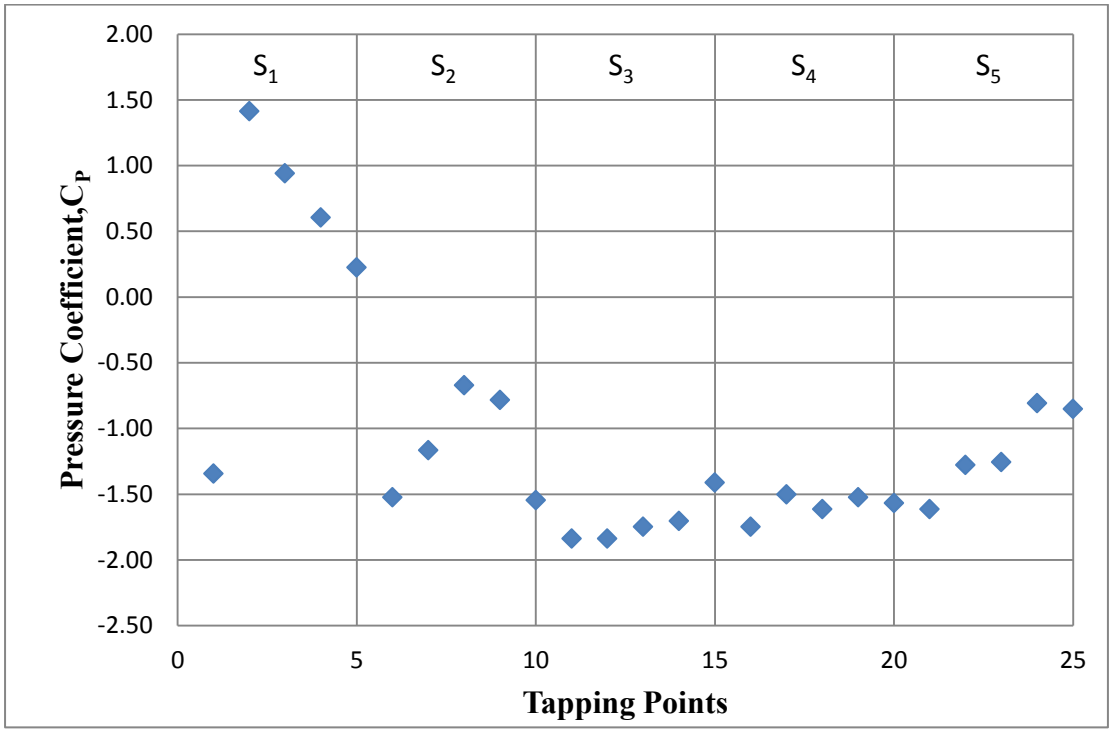

Figure 5.26: Distribution of Pressure Coefficient on Pentagonal Cylinder at L_1=8D, L_2=2D

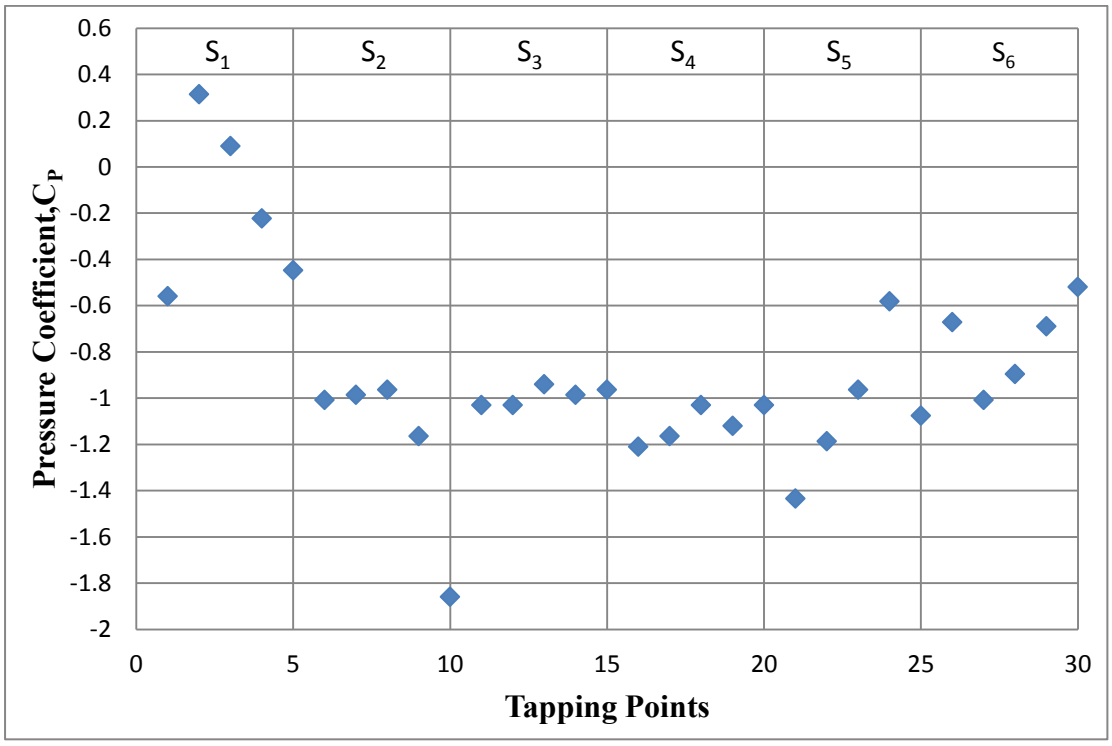

Figure 5.27: Distribution of Pressure Coefficient on Hexagonal Cylinder at L_1=6D, L_2=2D

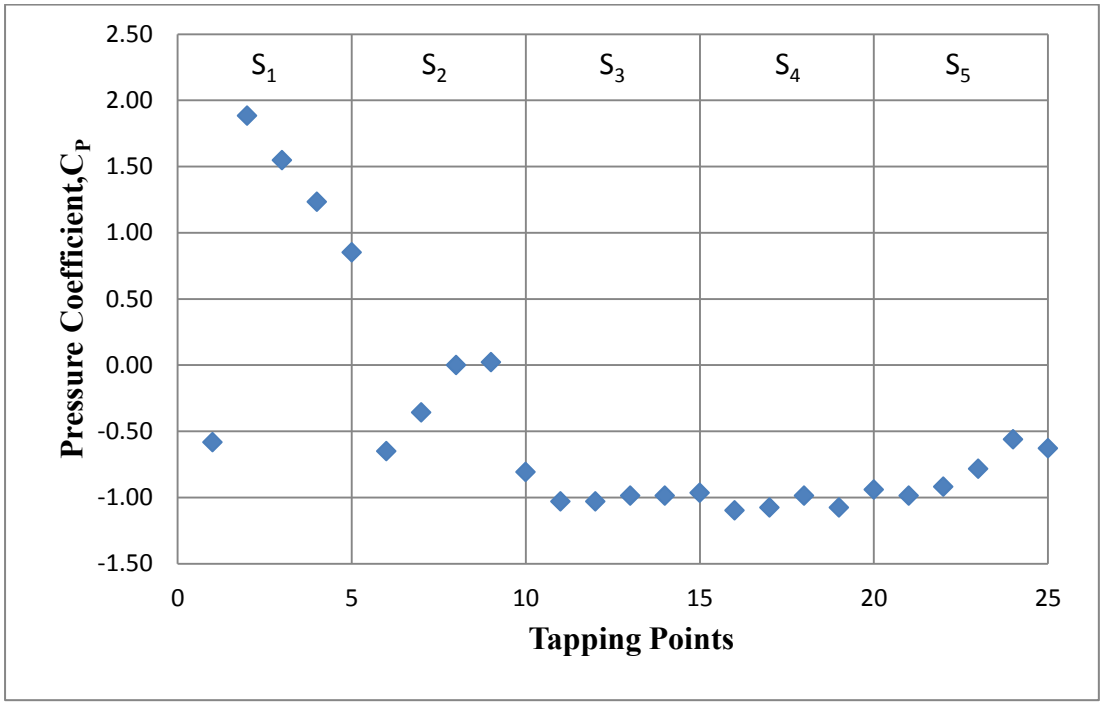

Figure 5.28: Distribution of Pressure Coefficient on Pentagonal Cylinder at L_1=6D, L_2=2D

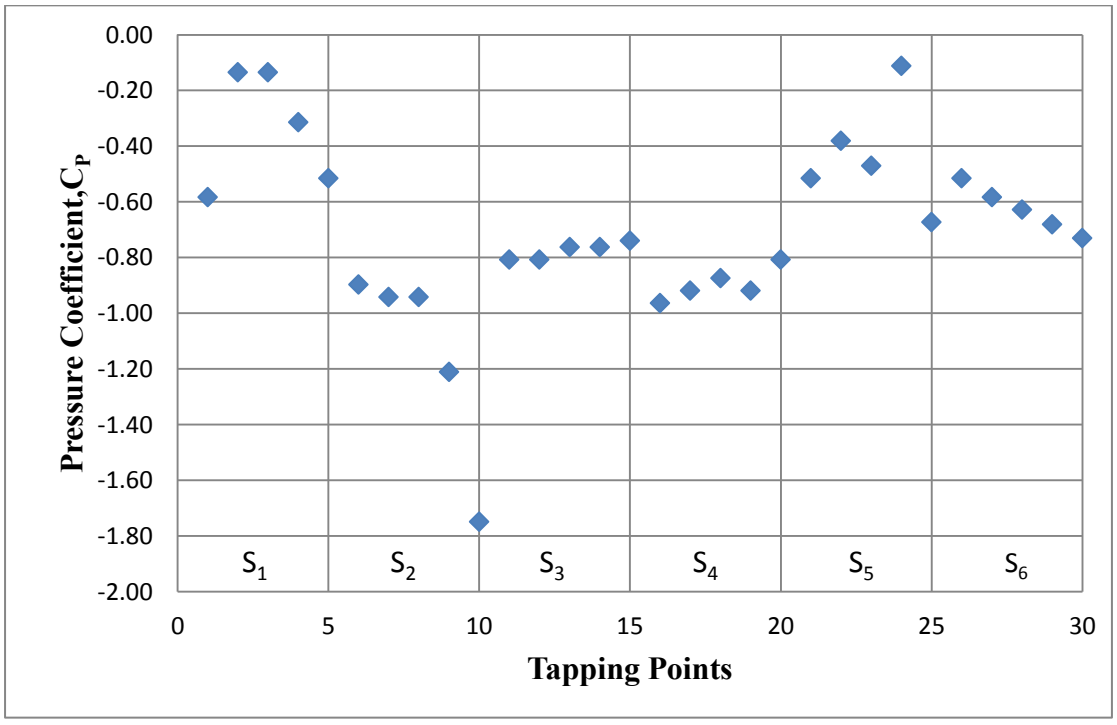

Figure 5.29: Distribution of Pressure Coefficient on Hexagonal Cylinder at L_1=4D, L_2=2D

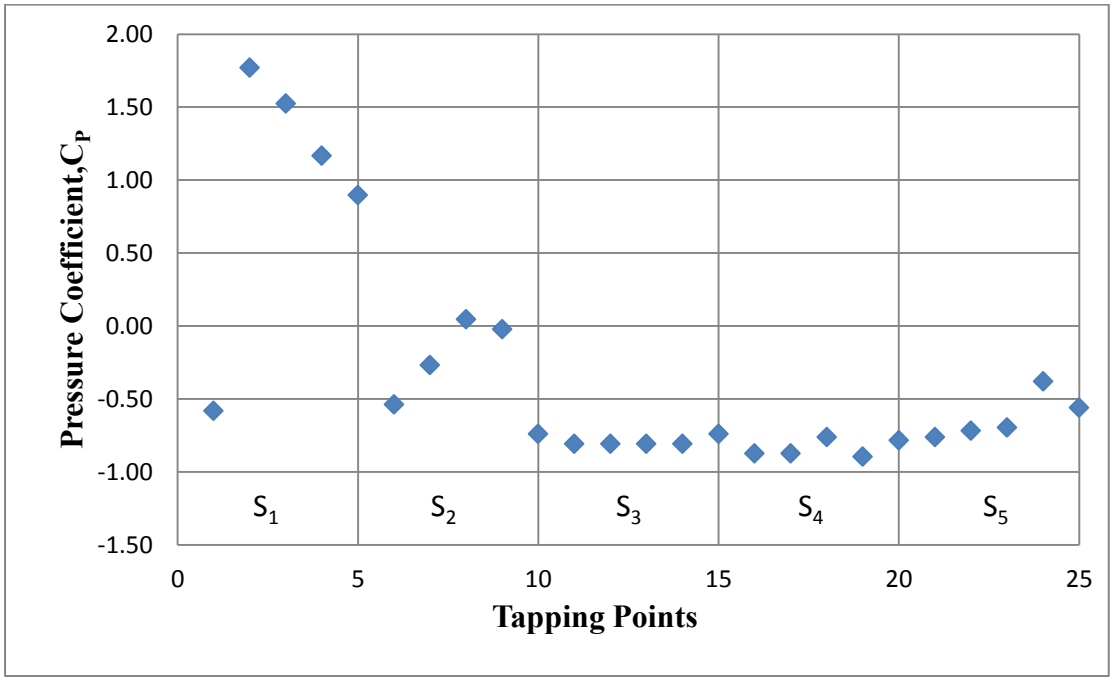

Figure 5.30: Distribution of Pressure Coefficient on Pentagonal Cylinder at L_1=4D, L_2=2D

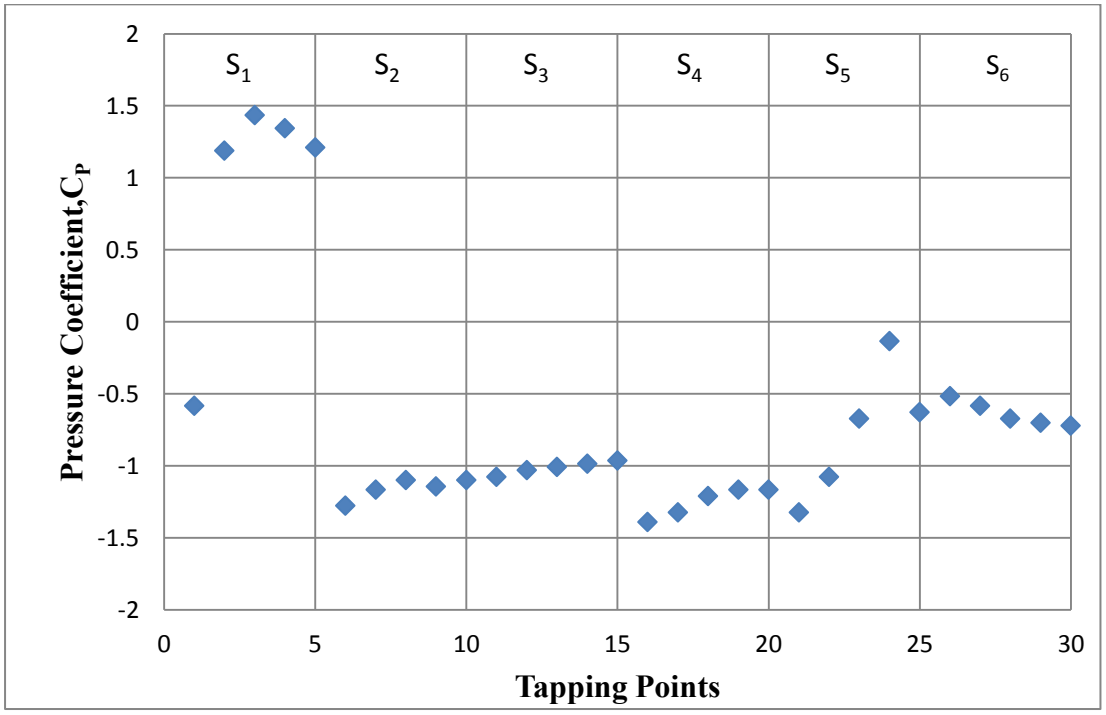

Figure 5.31: Distribution of Pressure Coefficient on Hexagonal Cylinder at L_1=2D, L_2=2D

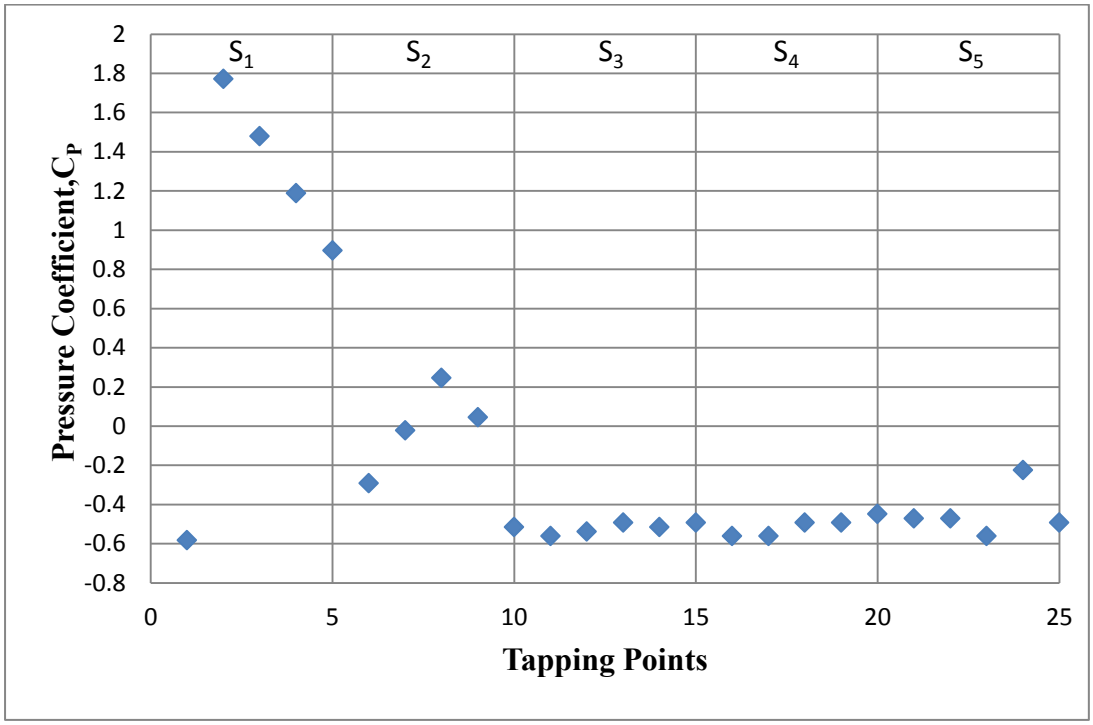

Figure 5.32: Distribution of Pressure Coefficient on Pentagonal Cylinder at L_1=2D, L_2=2D

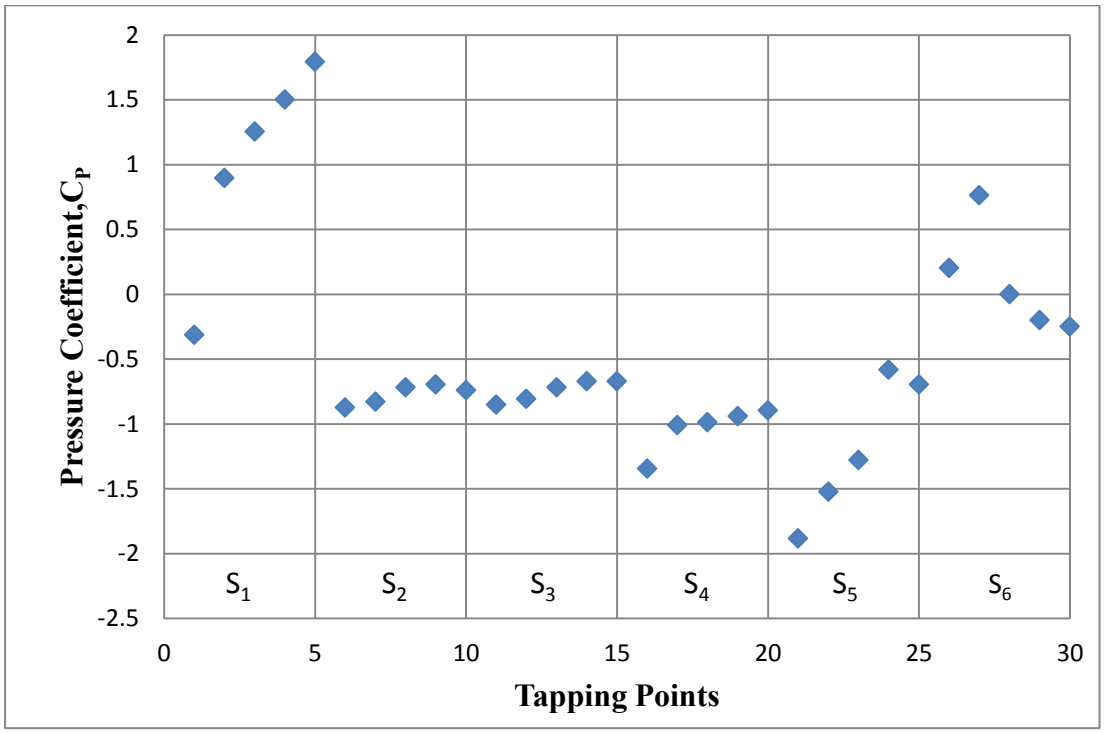

Figure 5.33: Distribution of Pressure Coefficient on Hexagonal Cylinder at L_1=1D, L_2=2D

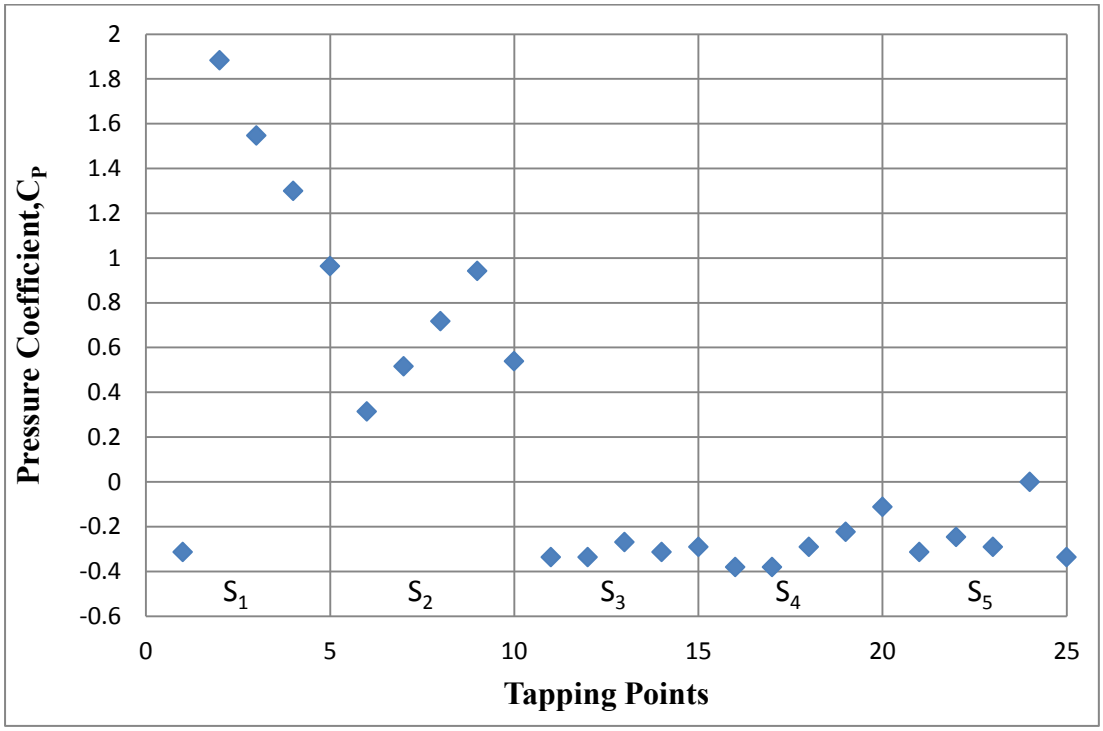

Figure 5.34: Distribution of Pressure Coefficient on Pentagonal Cylinder at L_1=1D, L_2=2D

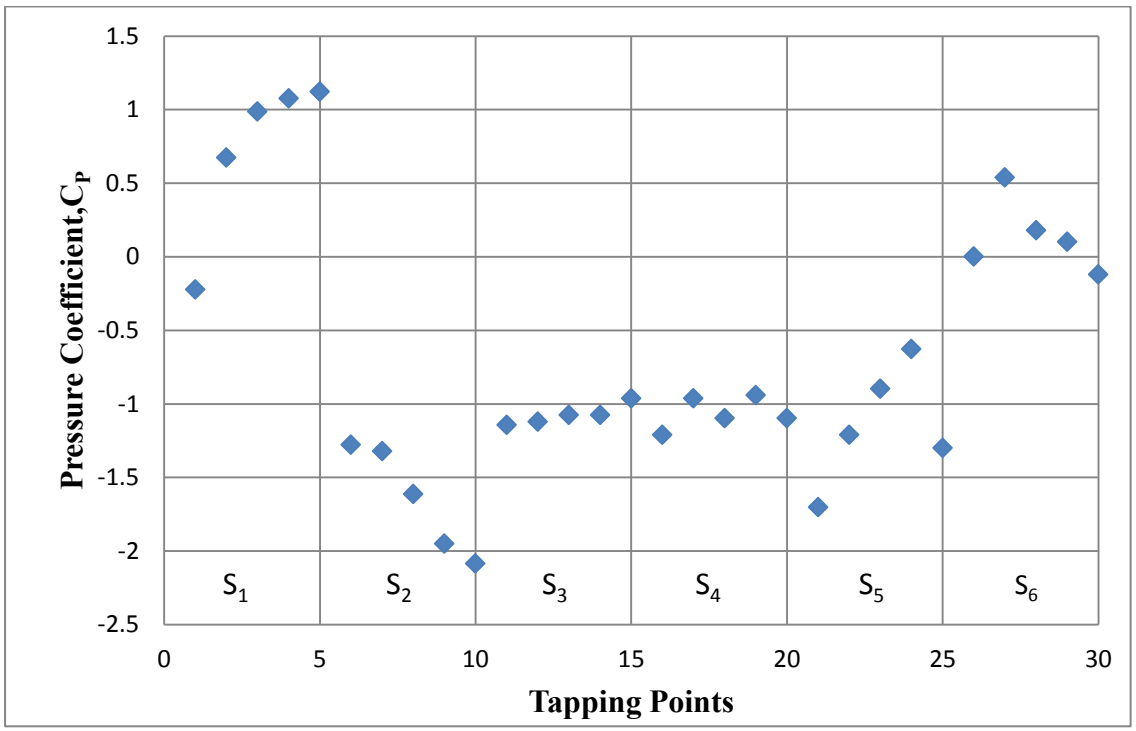

Figure 5.35: Distribution of Pressure Coefficient on Hexagonal Cylinder at L_1=8D, L_2=3D

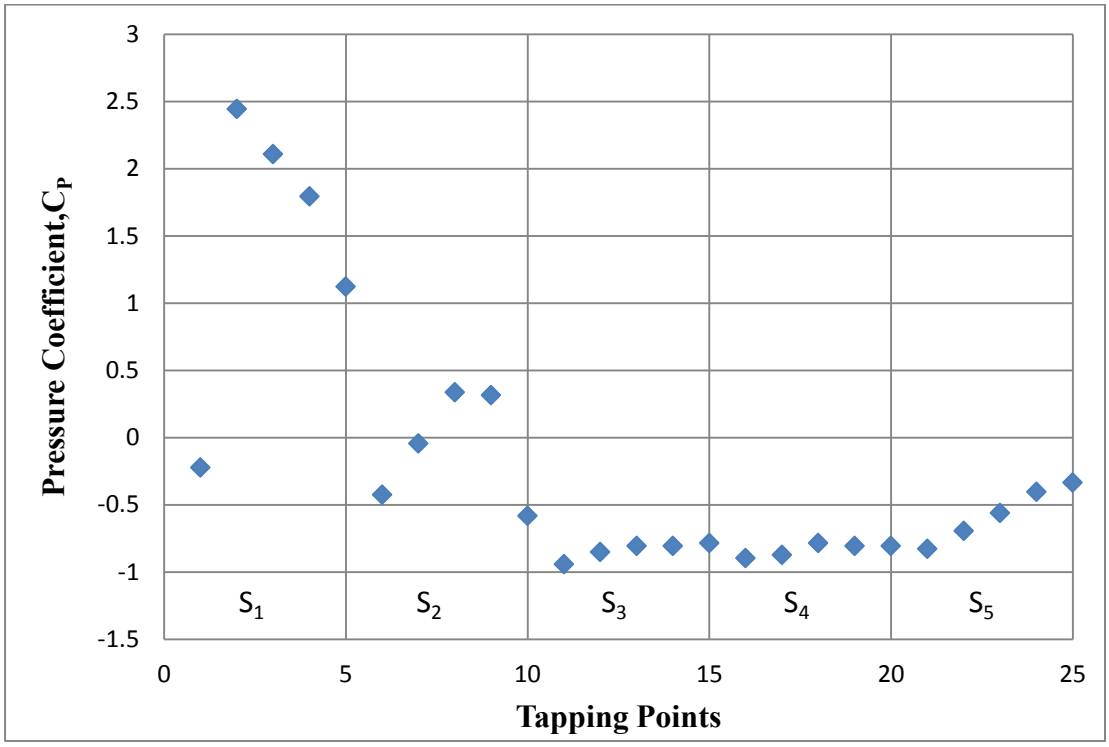

Figure 5.36: Distribution of Pressure Coefficient on Pentagonal Cylinder at L_1=8D, L_2=3D

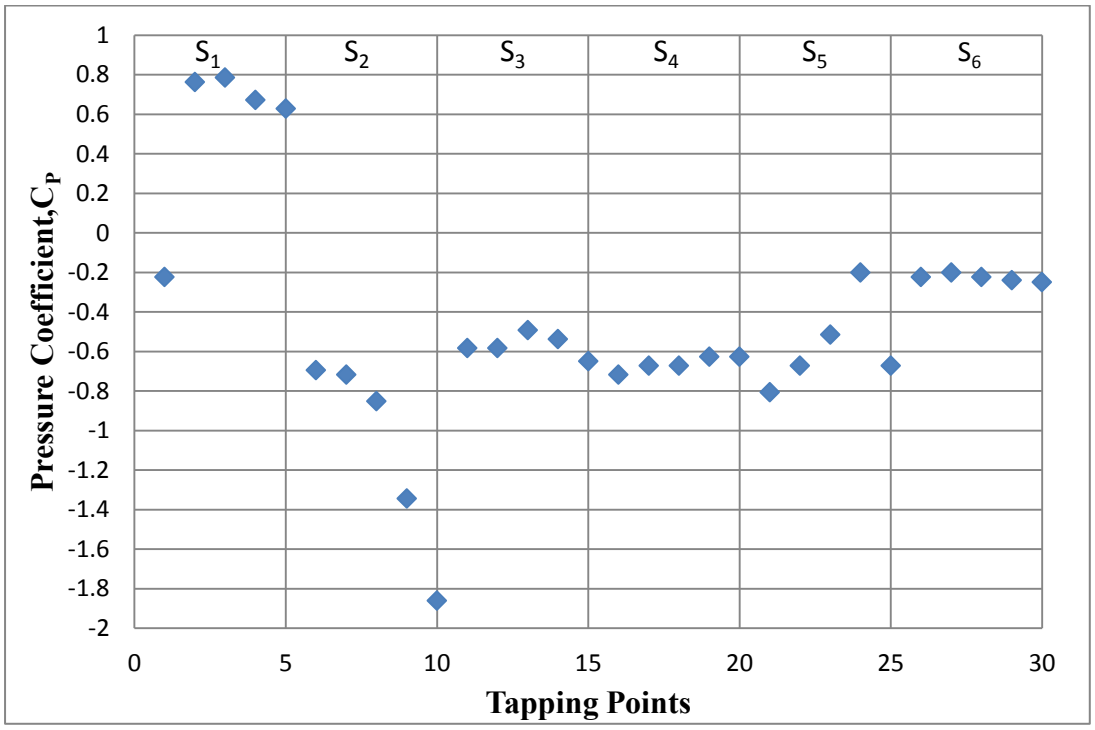

Figure 5.37: Distribution of Pressure Coefficient on Hexagonal Cylinder at L_1=6D, L_2=3D

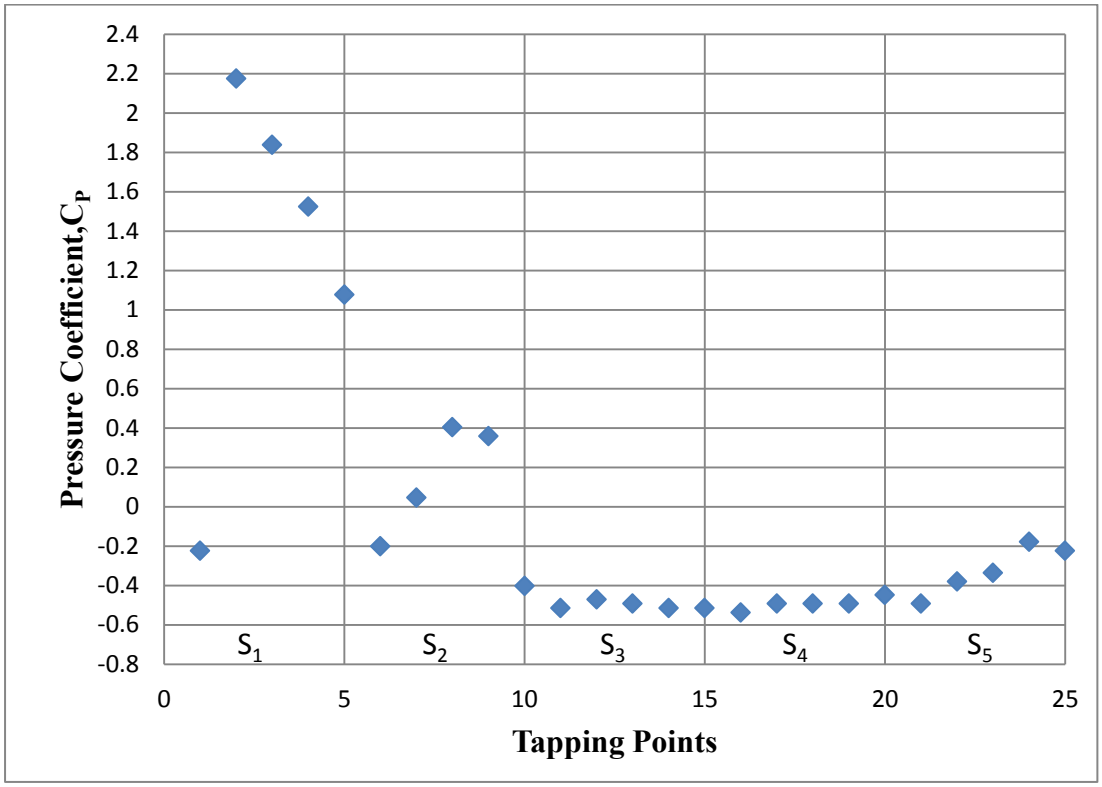

Figure 5.38: Distribution of Pressure Coefficient on Pentagonal Cylinder at L_1=6D, L_2=3D

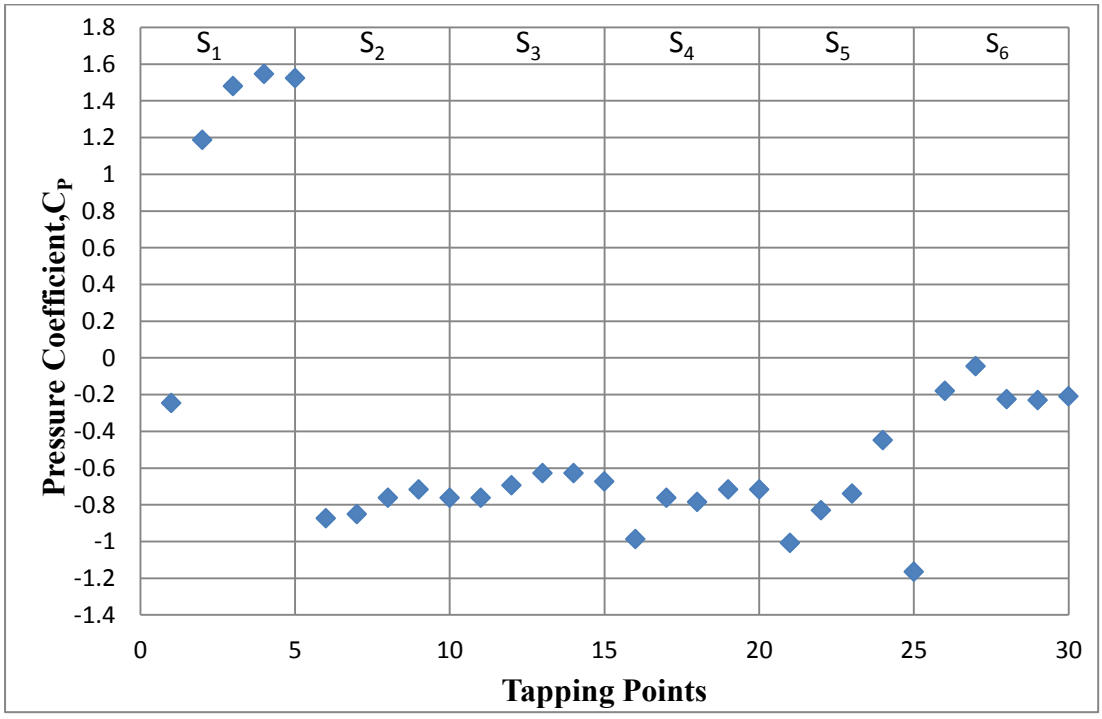

Figure 5.39: Distribution of Pressure Coefficient on Hexagonal Cylinder at L_1=4D, L_2=3D

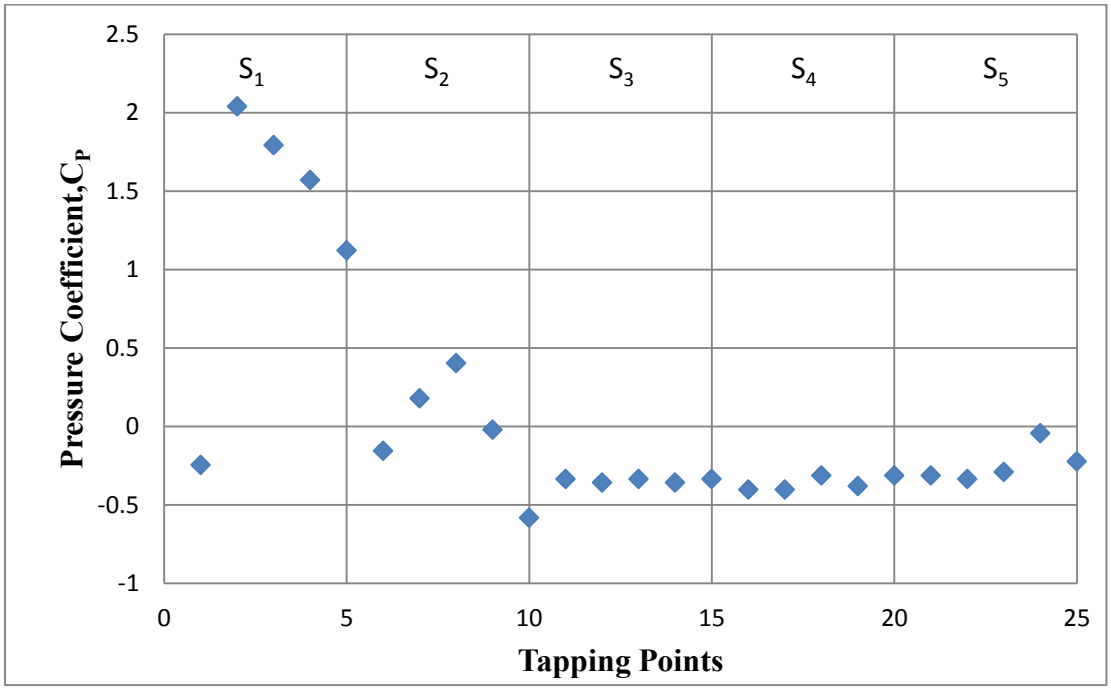

Figure 5.40: Distribution of Pressure Coefficient on Pentagonal Cylinder at L_1=4D, L_2=3D

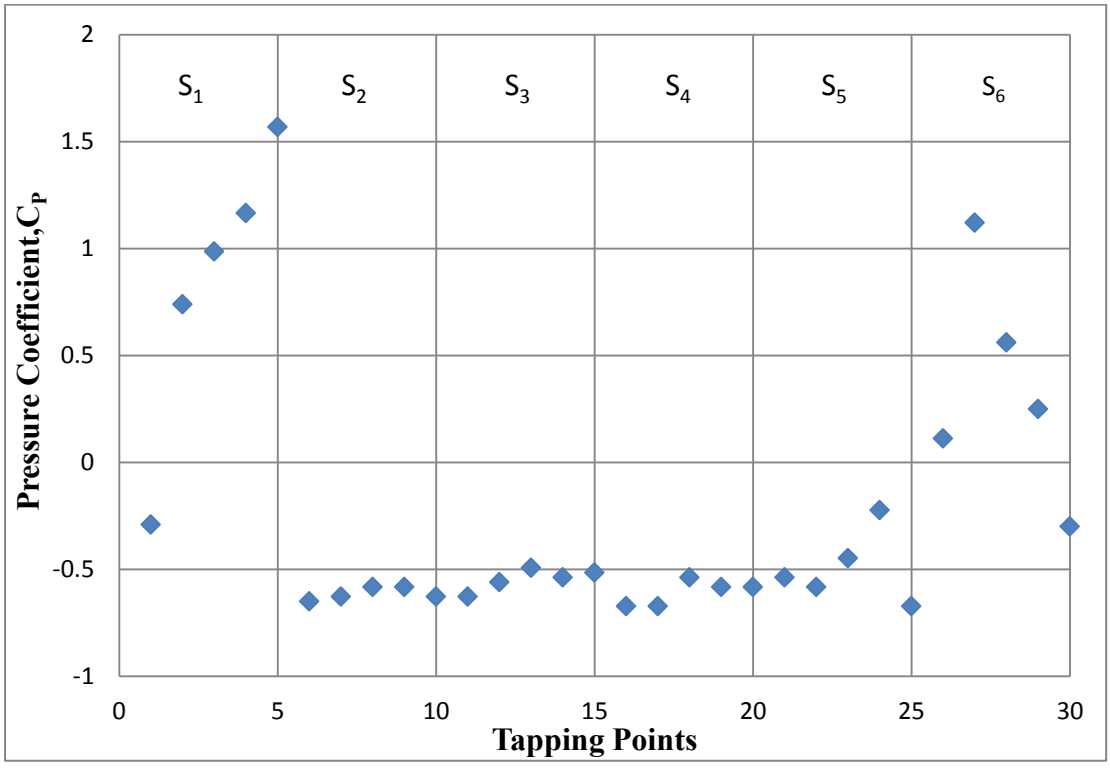

Figure 5.41: Distribution of Pressure Coefficient on Hexagonal Cylinder at L_1=2D, L_2=3D

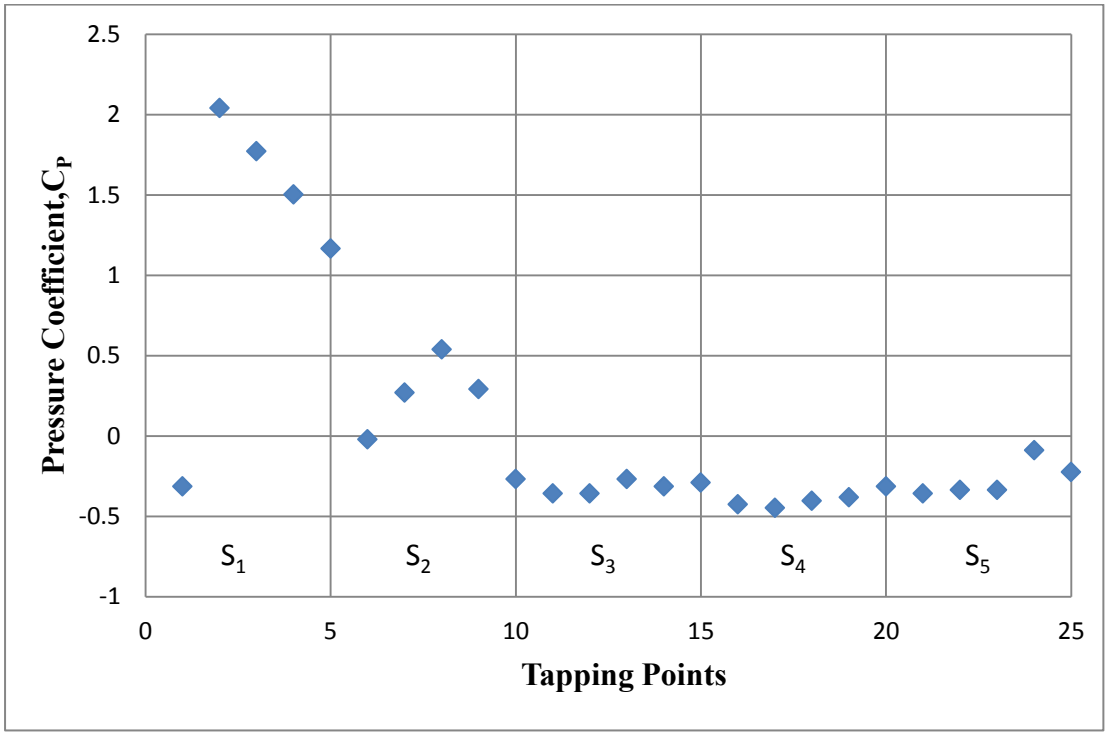

Figure 5.42: Distribution of Pressure Coefficient on Pentagonal Cylinder at L_1=2D, L_2=3D

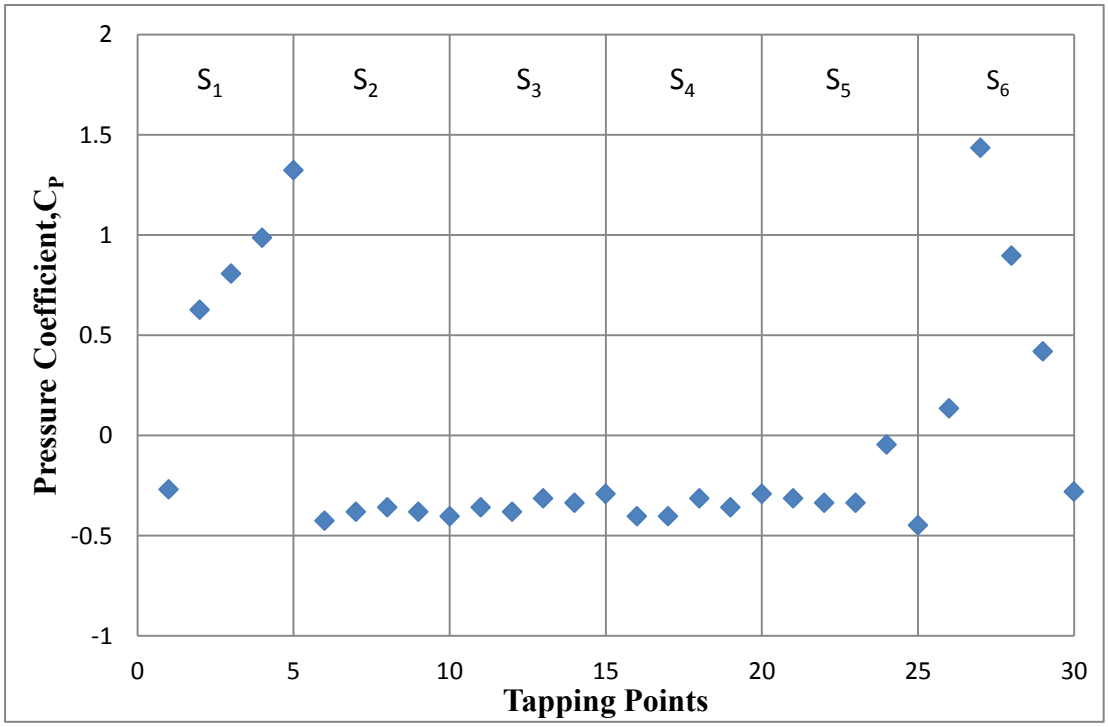

Figure 5.43: Distribution of Pressure Coefficient on Hexagonal Cylinder at L_1=1D, L_2=3D

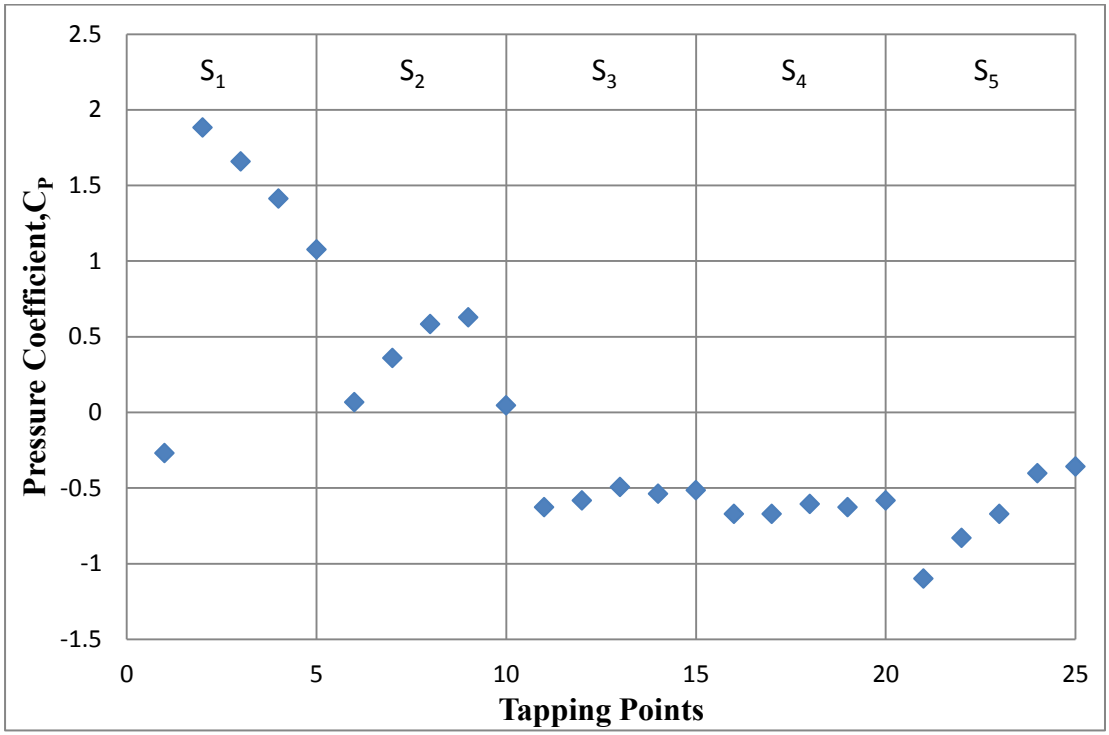

Figure 5.44: Distribution of Pressure Coefficient on Pentagonal Cylinder at L_1=1D, L_2=3D

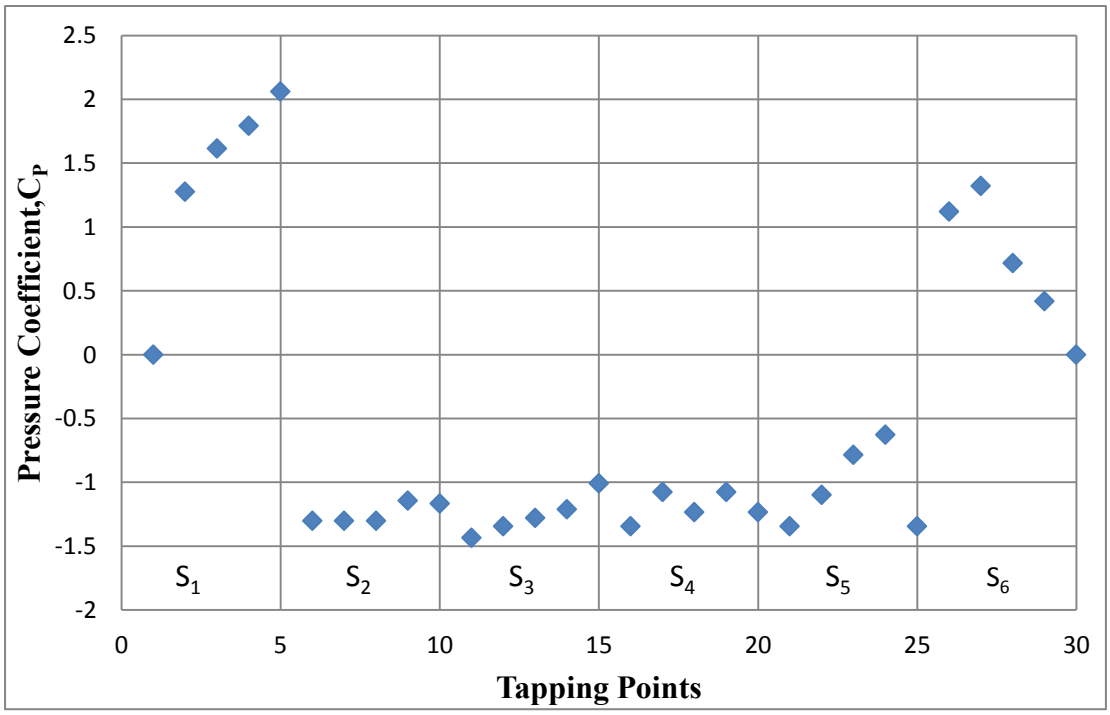

Figure 5.45: Distribution of Pressure Coefficient on Hexagonal Cylinder at L_1=8D, L_2=5D

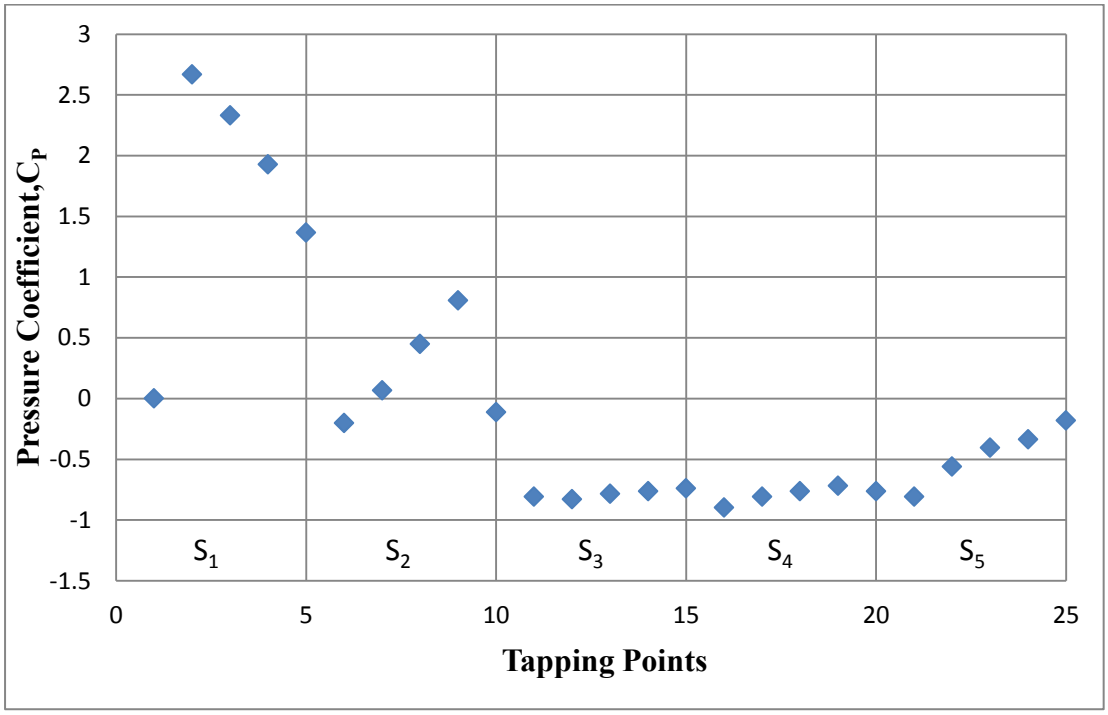

Figure 5.46: Distribution of Pressure Coefficient on Pentagonal Cylinder at L_1=8D, L_2=5D

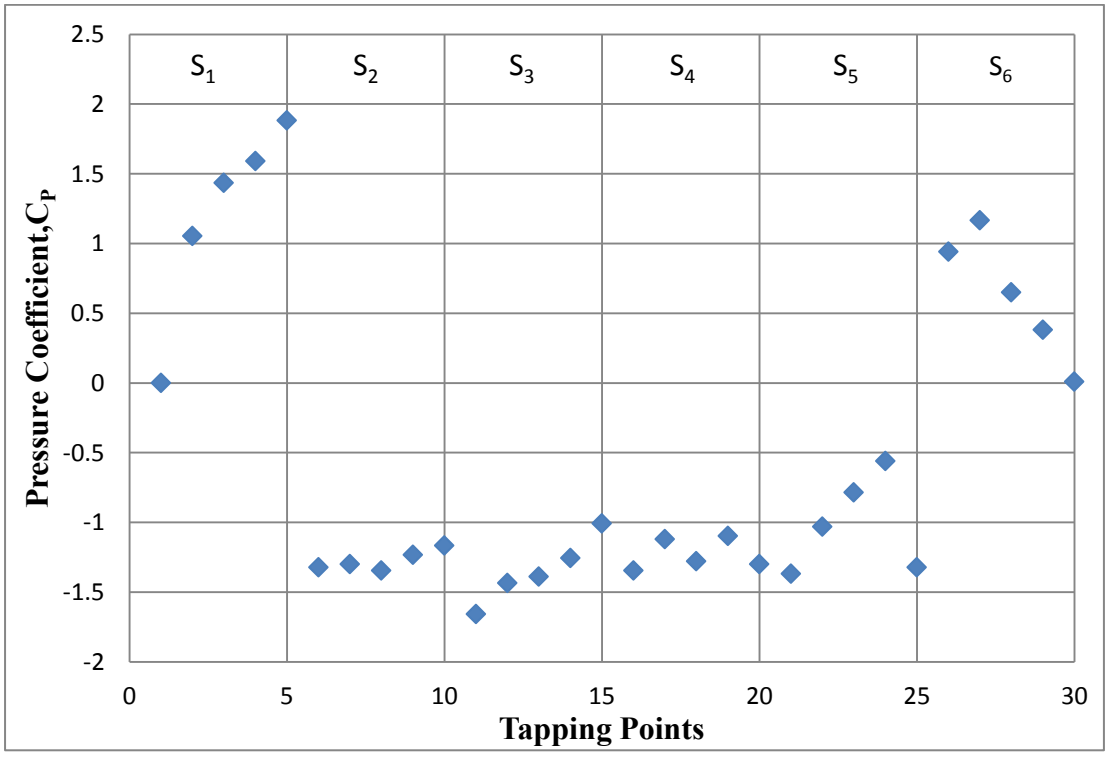

Figure 5.47: Distribution of Pressure Coefficient on Hexagonal Cylinder at L_1=6D, L_2=5D

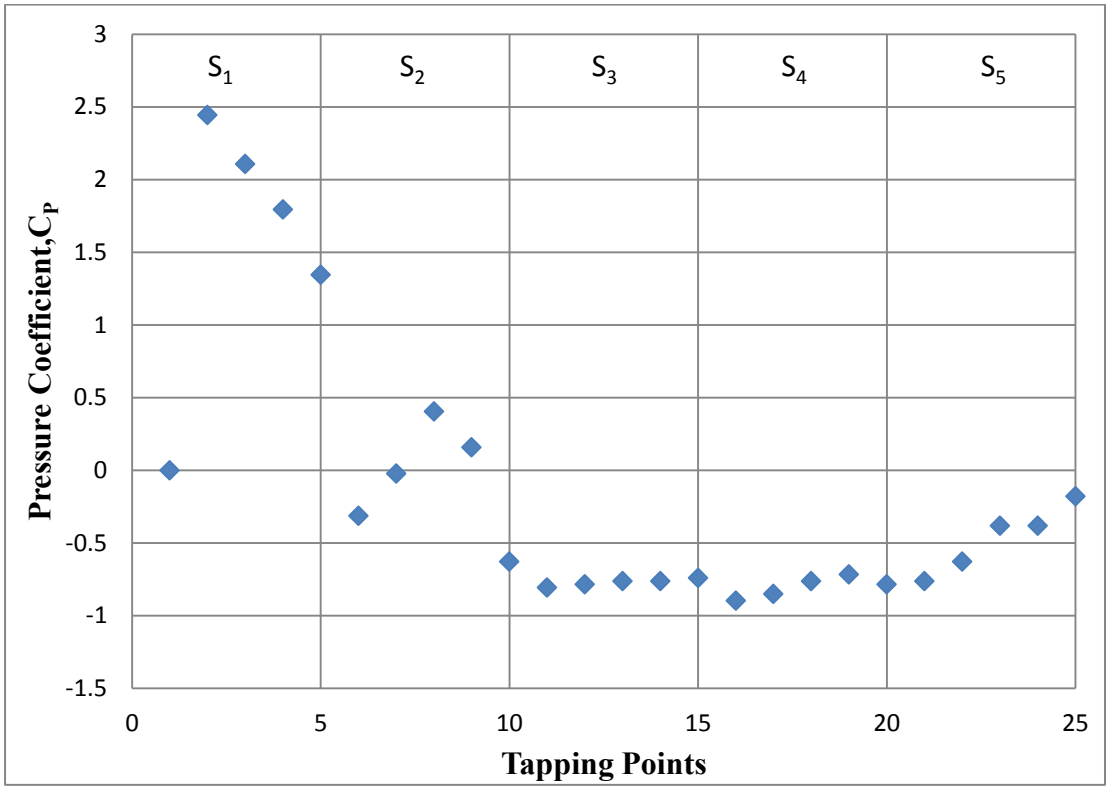

Figure 5.48: Distribution of Pressure Coefficient on Pentagonal Cylinder at L_1=6D, L_2=5D

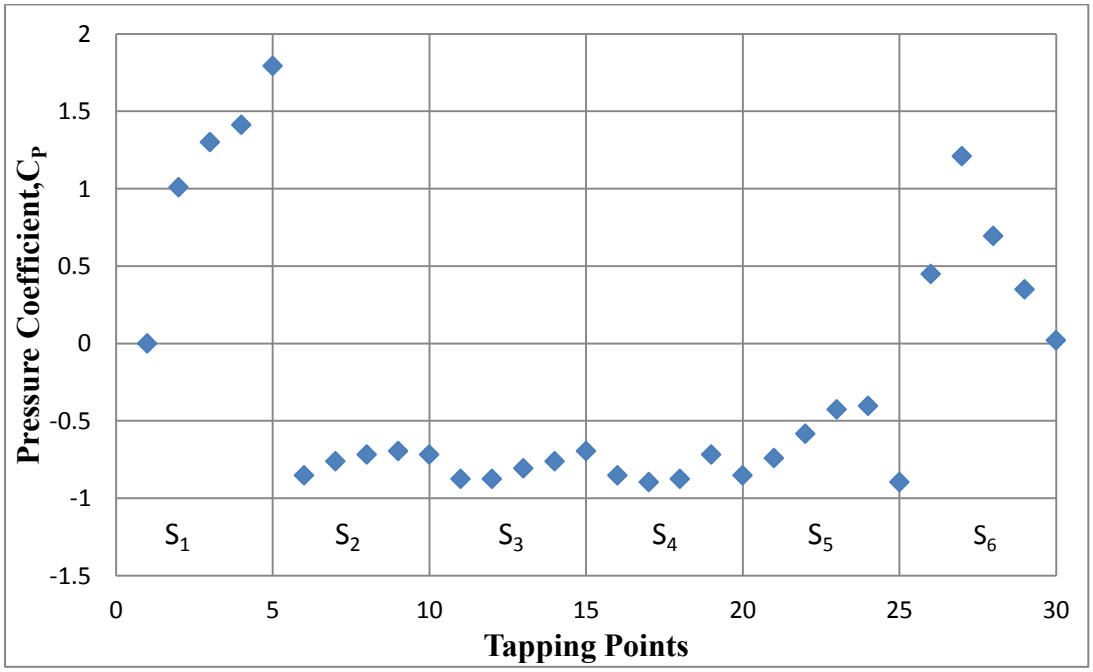

Figure 5.49: Distribution of Pressure Coefficient on Hexagonal Cylinder at L_1=4D, L_2=5D

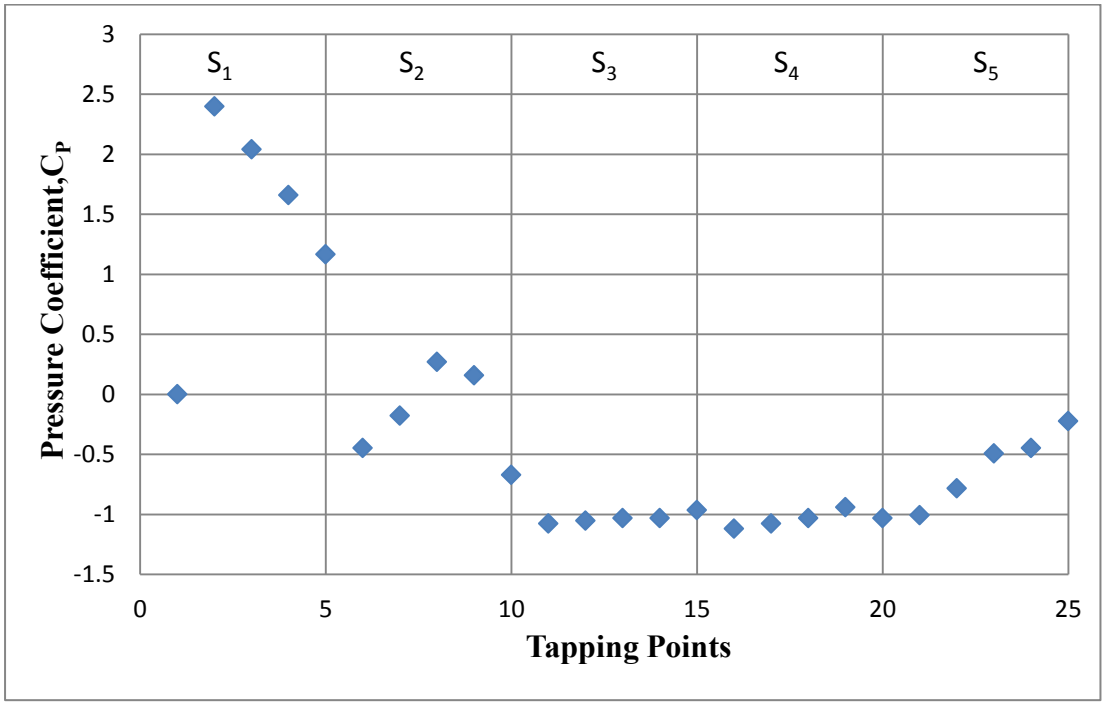

Figure 5.50: Distribution of Pressure Coefficient on Pentagonal Cylinder at L_1=4D, L_2=5D

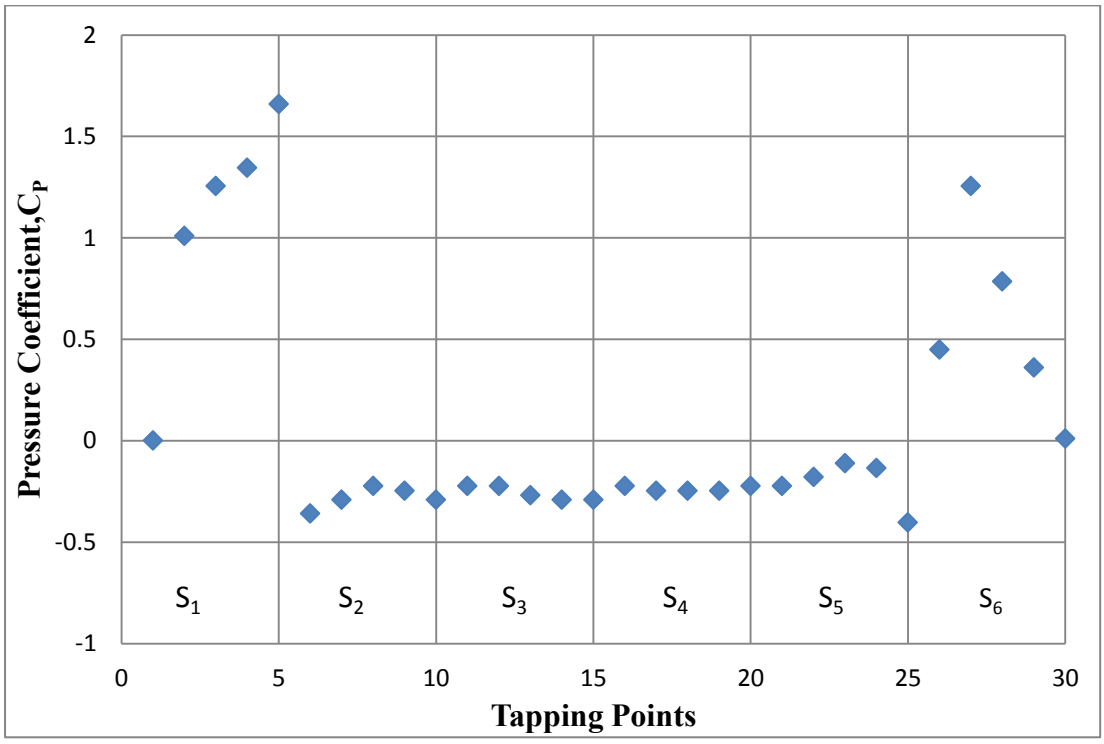

Figure 5.51: Distribution of Pressure Coefficient on Hexagonal Cylinder at L_1=2D, L_2=5D

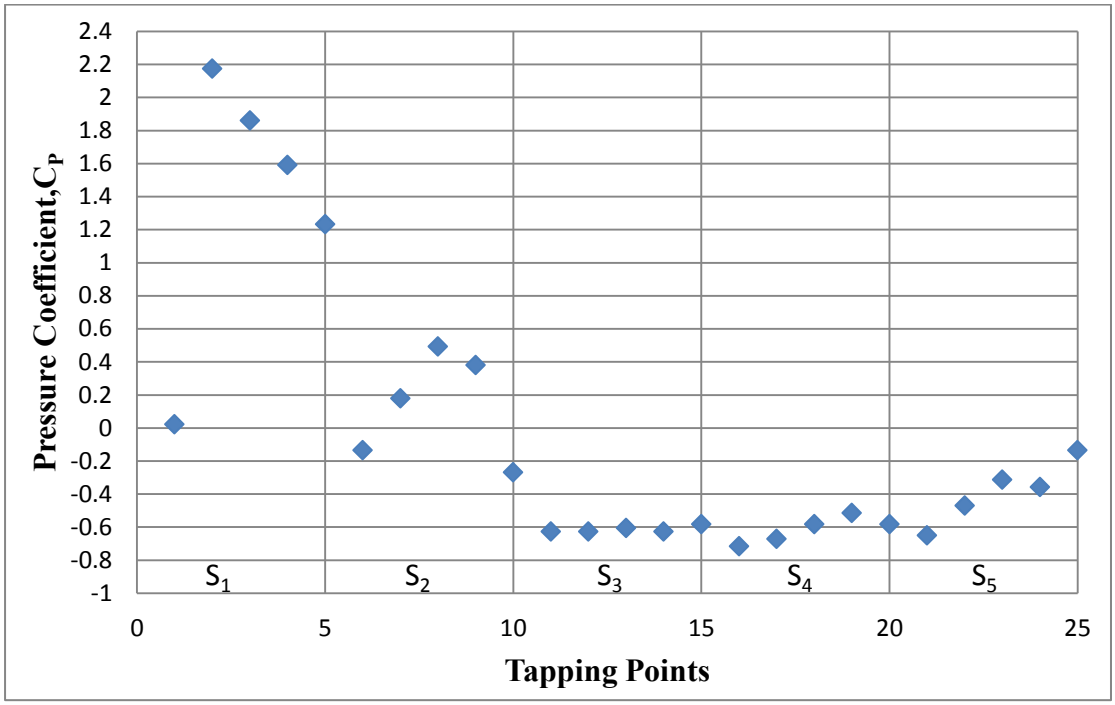

Figure 5.52: Distribution of Pressure Coefficient on Pentagonal Cylinder at L_1=2D, L_2=5D

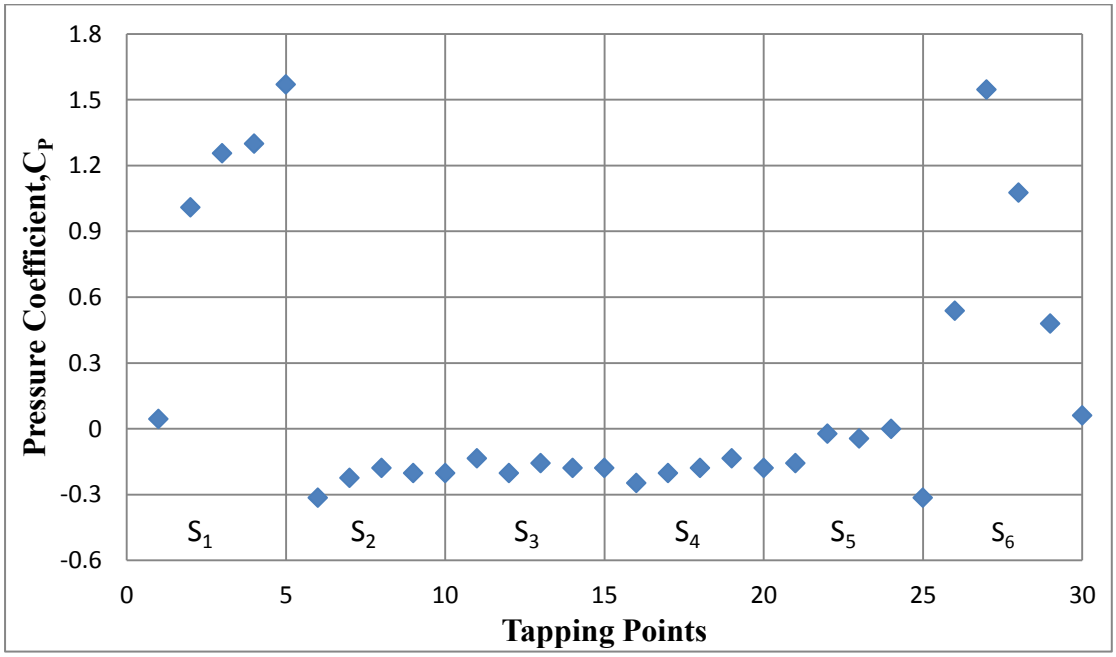

Figure 5.53: Distribution of Pressure Coefficient on Hexagonal Cylinder at L_1=1D, L_2=5D

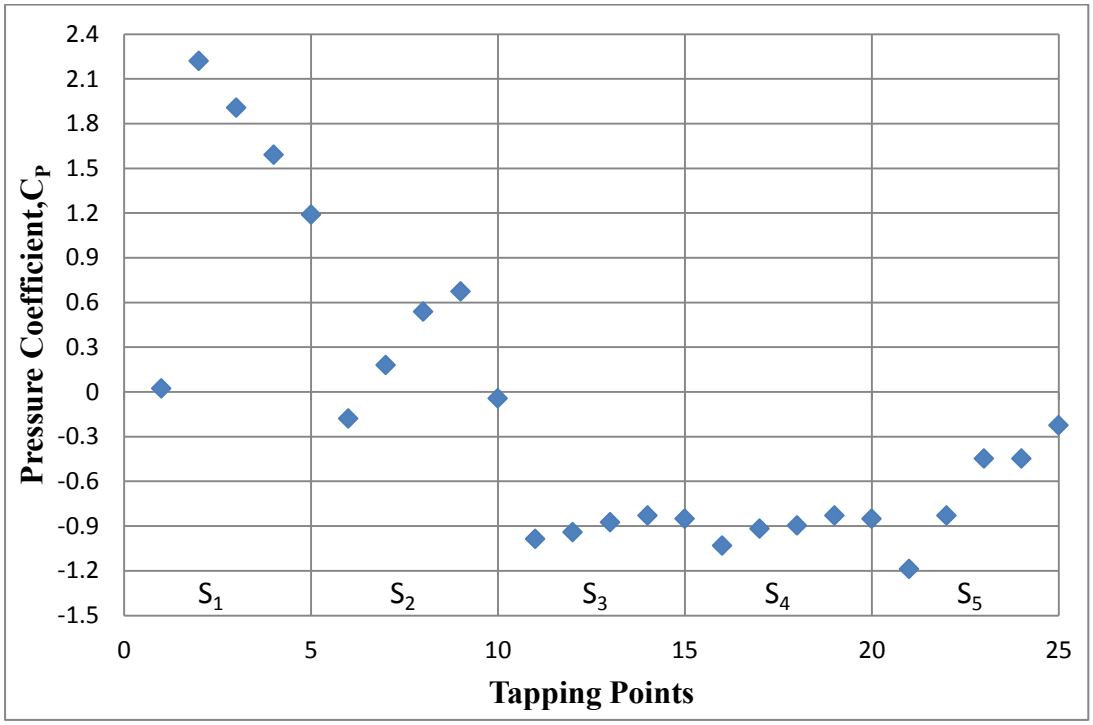

Figure 5.54: Distribution of Pressure Coefficient on Pentagonal Cylinder at L_1=1D, L_2=5D

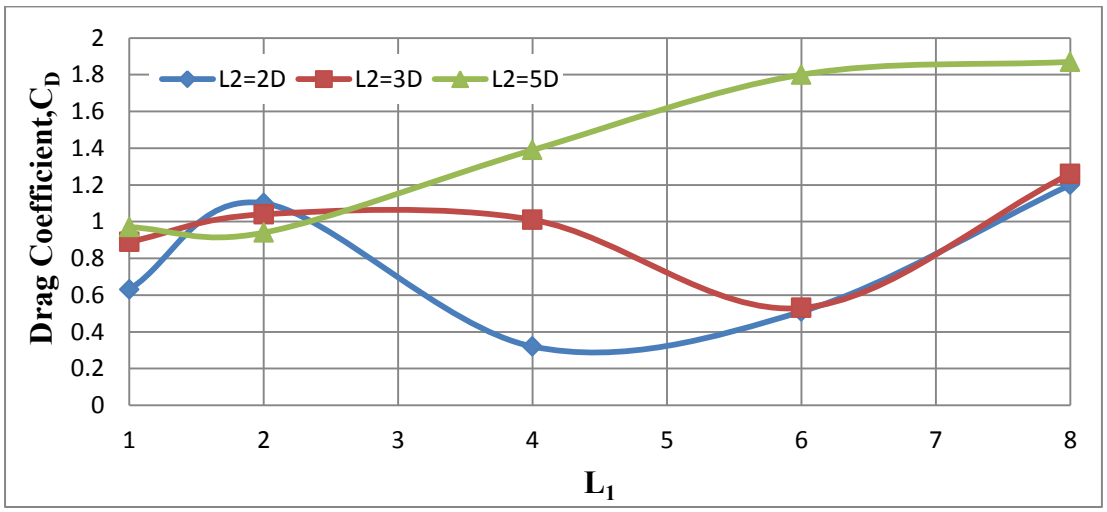

Figure 5.55: Variation of Drag Coefficients on Hexagonal Cylinder with L_1 for different values of L_2

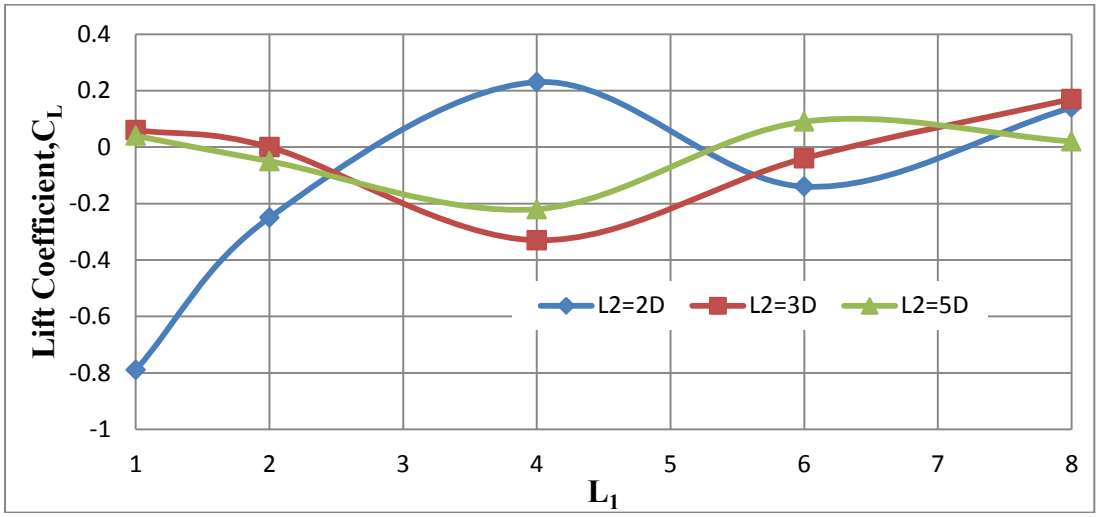

Figure 5.56: Variation of Lift Coefficients on Hexagonal Cylinder with L_1 for different values of L_2

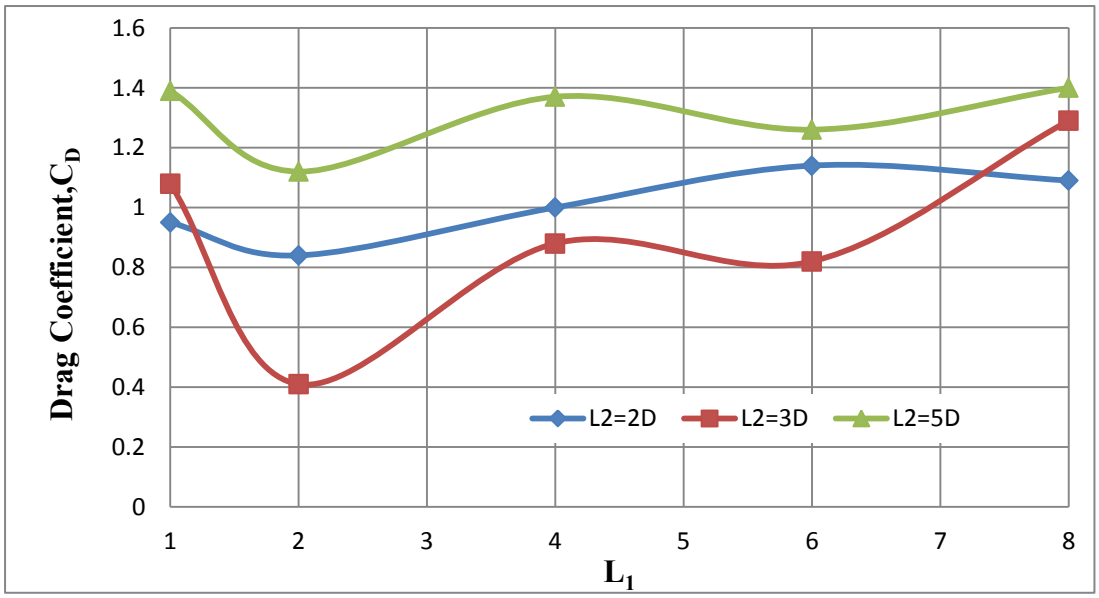

Figure 5.57: Variation of Drag Coefficients on Pentagonal Cylinder with L_1 for different values of L_2

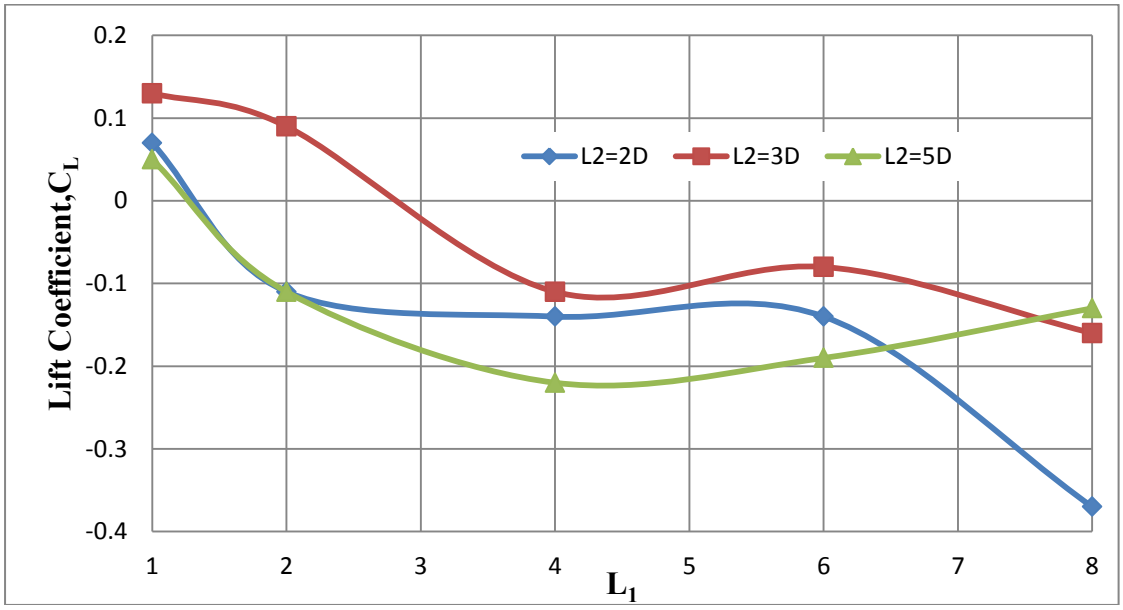

Figure 5.58: Variation of Lift Coefficients on Pentagonal Cylinder with L_1 for different values of L_2

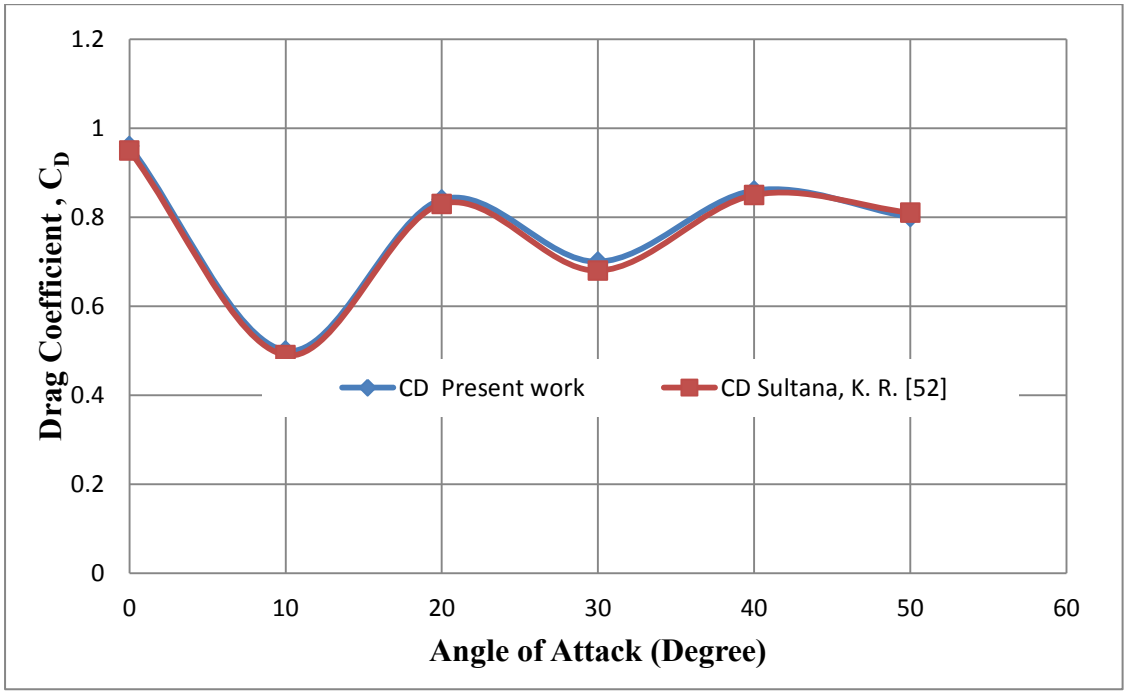

Figure 5.59: Variation of Drag Coefficient at Various Angles of Attack on Single Hexagonal Cylinder for validation

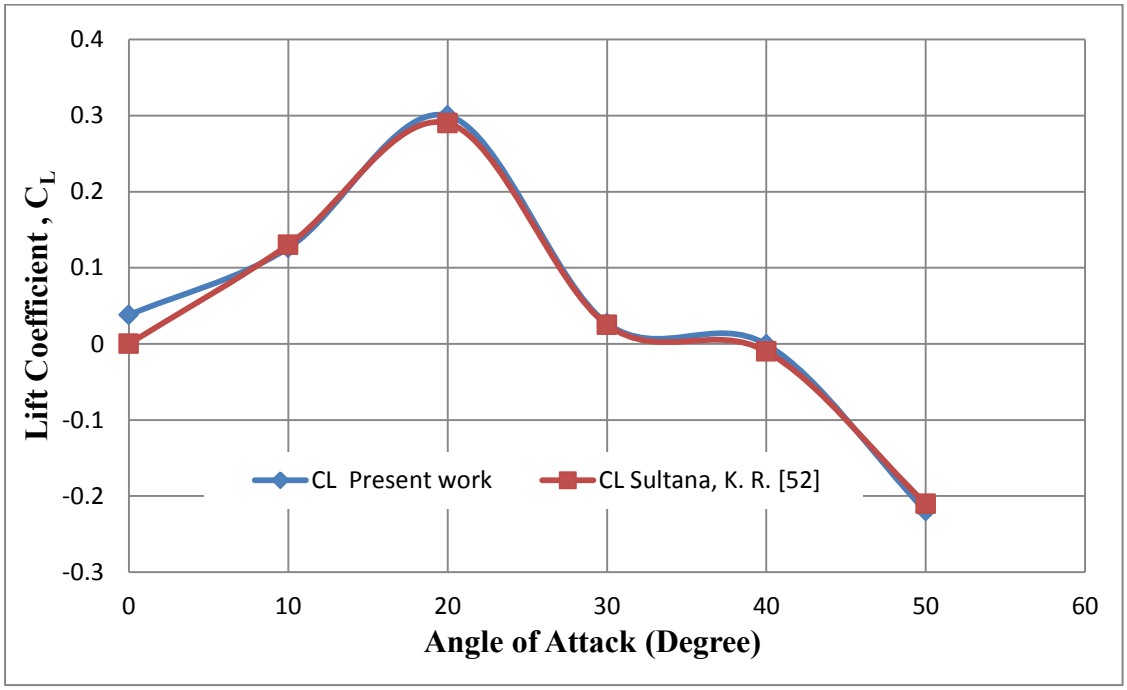

Figure 5.60: Variation of Lift Coefficient at Various Angles of Attack on Single Hexagonal Cylinder for validation

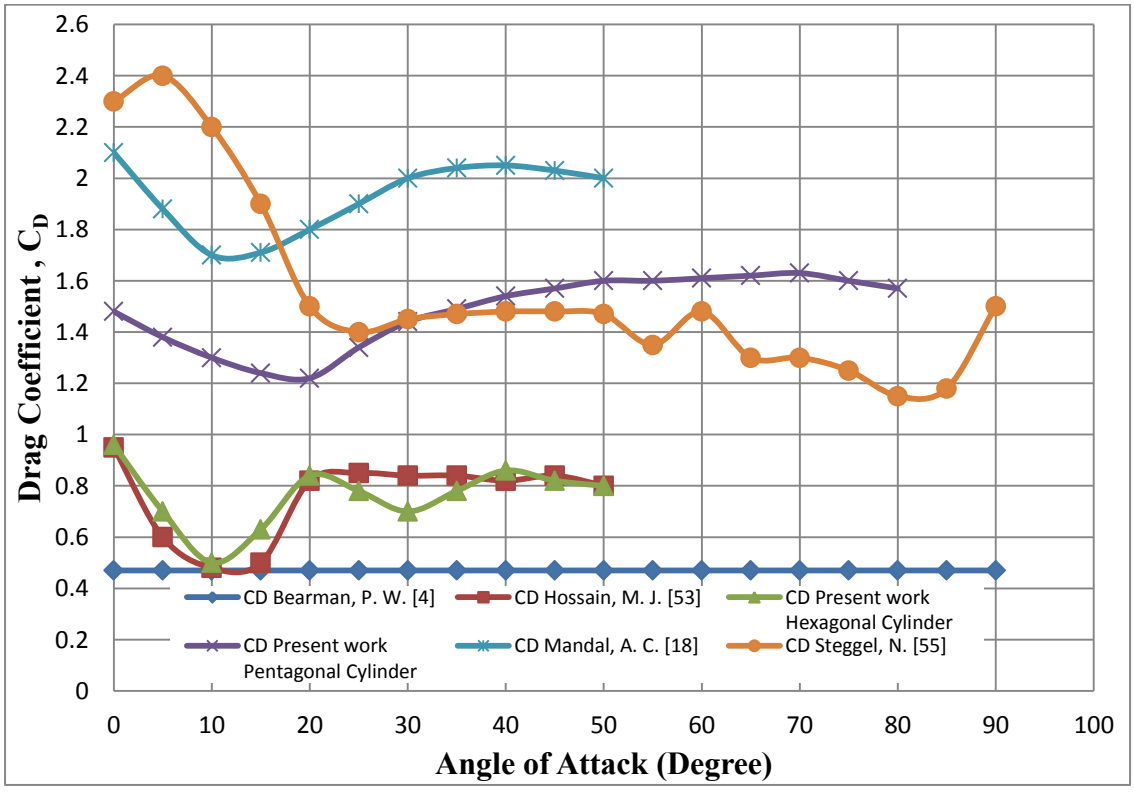

Figure 5.61: Variation of Drag Coefficient at Various Angles of Attack on different shapes of cylinder

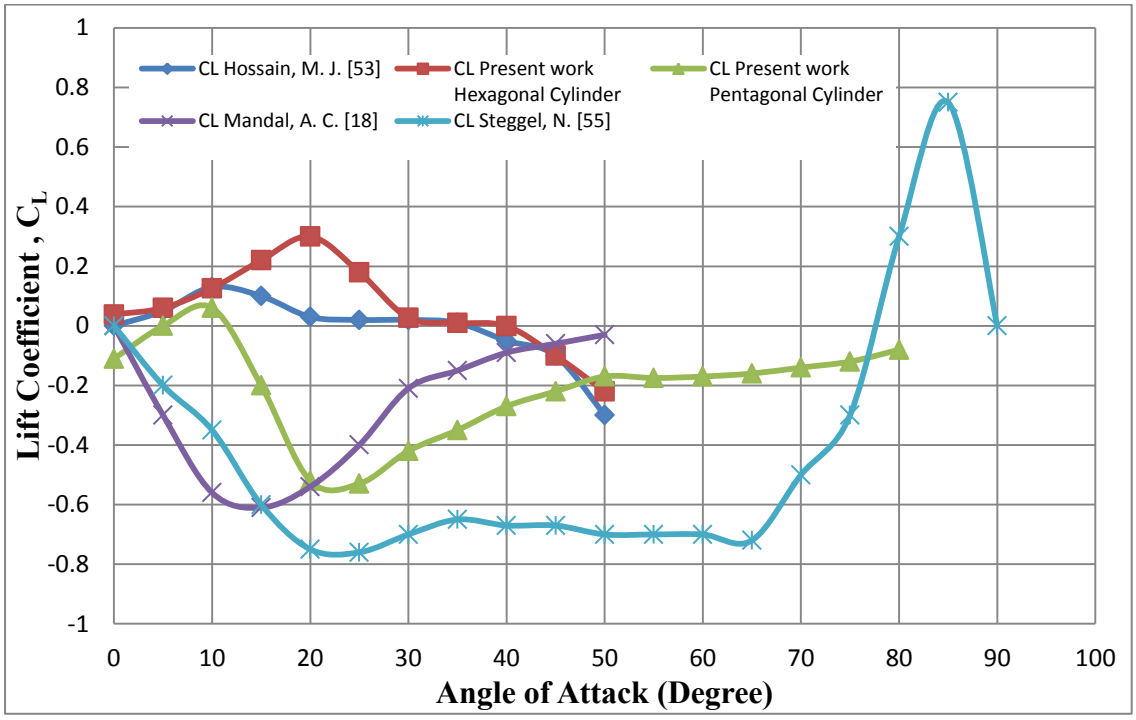

Figure 5.62: Variation of Lift Coefficient at Various Angles of Attack on different shapes of cylinder

CHAPTER-6
CONCLUSIONS AND RECOMMENDATIONS

6.1 Conclusions

The following conclusions are drawn in regard to the wind effect on the single hexagonal cylinder, single pentagonal cylinder and the two hexagonal cylinders and one pentagonal cylinder in a group

1. There is significant drop in the drag coefficient values for the single hexagonal cylinder in comparison to that of the single square cylinder and the values approaches to that of the circular cylinder.

2. The drag coefficient for a single hexagonal cylinder at zero angle of attack is about 0.95 in contrast to that of 2.0 for a single square cylinder at the same angle of attack.

3. The variation of the lift coefficient on the single hexagonal cylinder is not appreciable and they are close to zero value except at angles of attack of 10^0 and 50^0, where some insignificant values are observed.

4. There is significant drop in the drag coefficient values for the single pentagonal cylinder in comparison to that of the single square cylinder and the values is higher than the hexagonal cylinder.

5. The drag coefficient for a single pentagonal cylinder at zero angle of attack is about 1.48 in contrast to that of 2.0 for a single square cylinder at the same angle of attack.

6. The variation of the lift coefficient on the single pentagonal cylinder is shifted 9^0 and pattern is more or less similar with the variation of lift coefficient for the single square cylinder except at angle of attack of 0°.

7. The stagnation point is found on the front face of either the single hexagonal cylinder and single pentagonal cylinder or the hexagonal cylinder in the group, however, no such stagnation point is found in the pentagonal cylinder of the group.

8. As the inter-spacing L_2 increases drag coefficient also increases for the all values of inter-spacing L_1 except L_1=2D for hexagonal cylinder.

9. In group, pentagonal cylinder has lower drag coefficient than single pentagonal cylinder.
10. While wind load is to be used for the design of the free-standing building and group of building having hexagonal and pentagonal cross-section, the outcome of the present results may be applied.

6.2 **Recommendations**

For further study in relation to the present work the following recommendations are provided below.

1. The flow is considered to be uniform in the present study. The investigation may be repeated considering the different values of turbulence intensity specially the atmospheric turbulence level.
2. The flow behavior around the cylinder may be taken into consideration for the study.
3. The wind shear may be considered in performing the study to see its effect on the wind load.
4. The effect of Reynolds number may be investigation on the wind load of the single as well as cylinders in group.
5. The study in regard to the optimum inter-spacing between the tall buildings, which is suitable to the passers-by, may be investigated.
6. Building models of various shapes and sizes with different inter-spacing may be taken into consideration to find the wind load on them
7. The study has been done on the group of buildings at zero angle of attack only; the variation of the angle of attack may be taken into consideration for the study.

REFERENCES

[1] Baines, W.D., "Effects of Velocity Distribution on Wind Loads and Flow Patterns on Buildings", Procedings of a Symposium on Wind Effects on Buildings and Structures", Teddington, U.K.1963, pp.197-225.

[2] Barriga, A.R., Crowe, C.T and Roberson, J.A., "Pressure Distribution on a Square Cylinder at a Small Angle of attack in a Turbulent Cross Flow", Proceedings of the 4th International Conference on Wind Effects on Buildings, London, U.K.1975,pp.89-93.

[3] Bearman, P.W. and Truman, D.M., "An Investigation of the Flow around Rectangular Cylinders", The Eronautical Quarterly, Vol.23, 1971, pp.229-237.

[4] Bearman, P.W. and Wadcock, A.J., "The Interaction between a pair of Circular Cylinders Normal to a Stream", Journal of the Fluid mechanics", Vol.61, 1973, pp.499-511.

[5] Biswas, N., "An Experimental Investigation of Wind load on tall Buildings with Square Coss-section having Rounded Facet", A Master's Thesis Presented in Mechanical Engineering Department, BUET, Dhaka, January, 2008.

[6] Bostock, B.R and Mair, W.A., "Pressure Distributions and Forces on Rectangular and D-Shaped Cylinders", The Aero- Dynamical Quarterly, Vol.23, 1972, pp.499-511.

[7] Castro, J.P. and Fackwell, J.E., "A Note on Two- Dimensional Fence Flows with Emphasis on Wall Constant", J. Industrial. Aerodynamics, 3(1), March1978.

[8] Castro, I.P. and Robins, A.G., "The Flow around a Surface Mounted Cube in Uniform and Turbulent streams", Journal of Fluid Mechanics, Vol.79, 1977, pp.305-335.

[9] Cheung, J.C.K., "Pressures on a 1:10 Scale Model of the Texas Tech Building", J. Wind Eng. Ind. Aerodyne no.69-71, 1997, pp.529-538- Proceedings of the Journal of the Institutions of Engineers (India), Volume-83, June, 2002.

[10] Chishiom, M.P. and Lewis, J., "Cyclone- Resistance domestic Construction in Bangladesh in Implementing Hazard Resistance Housing", Proceedings of the 1st International Housing and Hazards Workshop to Explore Practical Building for Safety Solutions held in Dhaka, Bangladesh, 3-5 December, 1996,Edited by Hodgson, Seraj and Chowdhury , pp.-29-38 , NBS(1977) , 43 Rules. How Houses can better Resist High Wind, US National Bureau of Standards, Washington DC.

[11] Islam, A.T.M. and Mandal, A.C., "Experimental Analysis of Aerodynamic Forces for Cross- flow on single Rectangular Cylinder", Mechanical Engineering Research Bulletin, BUET, Dhaka, Vol.13, No.1, 1990, pp. 36-51.

[12] Farok, G.M.G., "An Experimental Investigation of Wind Effect on Rectangular Cylinders with Rounded Corners", M.Sc. thesis, BUET, 2004.

[13] Hua, C.K., "The Behavior of Lift Fluctuations on the Square Cylinders in the Wind Tunnel Test", Proceedings of the 3rd International Conference on Wind Effects on Buildings and Structures, Tokyo, Japan, 1971, pp. 911-920.

[14] Davenport, A.G., "The Relation to wind Structure to Wind Loading" "Proceedings of the Conference on Wind Effects on Buildings and Structures", Vol.1, June, 1963.

[15] Davis, R.W and Moore, E.F., "A Numerical Study of Vortex Shedding from Rectangular Cylinders". Journal of Fluid Mechanics, Vol.116, pp. 475-506.

[16] Lee, B.E., "The Effect of Turbulence on the Surface Pressure Field of a Square Prism", Journal of Fluid Mechanics, Vol.6 J.E. 9, Part 2, 1975, pp. 263-282.

[17] Lawson, T.V., "Wind Loading of Buildings, Possibilities from a Wind Tunnel Investigation", University of Bristol, U.K. Report on TVL /731A, August, 1975.

[18] Mandal, A.C., "A study of Wind Effects on Square Cylinders", M.Sc. thesis BUET, 1979.

[19] Mandal, A.C. and Farok, G.M.G., "An Experimental Investigation of Static Pressure Distributions on Square and Rectangular Cylinders with Rounded Corners", 4th International Conference on Heat Transfer, Fluids Mechanics and Thermodynamics (HEFAT), Cairo, Egypt, September. 2005, Cairo, Egypt, Paper NO. : MA5.

[20] Cochran, L.S. and Cermak, J.E., "Full and Model Scale Cladding Pressures on the Texas Tech University Experimental Building," J. Wind Eng Ind Aerodyne no.43, 1992, pp.1589-1600.

[21] Franc, N., "Model Law and Experimental technique for determination of Wind Loads on Buildings", 1st International Conferences on Wind Effects on Building and Structure, Teddington, London1963, HMSO.

[22] Hussain, H.S. and Islam, O., "Study of wind Load on Buildings and Structures", Journal of the Institution of Engineers, Bangladesh, Vol. 1. Nos.2-3, July-October,1973.

[23] Hossain, M.K.M., Islam, M.Q, Mandal, A.C and Saha, S., "Wind Effect on Staggered Square Cylinders of Square and Rectangular Sections with Variable Longitudinal Spacing", Transaction of the Mechanical Engineering Division, The Institution of Engineers, Bangladesh, Vol. ME38, Dec.2007, pp.52-57.

[24] Islam, A.M.T. and Mandal, A.C., "Static Pressure Distribution for Cross- flow on single Rectangular Cylinders", Mechanical Engineering Research Bulletin, BUET, Dhaka, Vol.14, No.1, 1991, pp.8-23.

[25] Islam, A.M.T. and Mandal, A.C., "Effect of Longitudinal Spacing on Static Pressure Distribution of Rectangular Cylinders", Mechanical Engineering Research Bulletin, BUET, Dhaka, Vol.15, No.1, 1992, pp. 22-47.

[26] Koening, K. and Roshiko, A., "An Experimental Study of Geometrical Effects on the Drag and flow Field of two Bluff Bodies Separated by a Gap", Journal of fluid Mechanics Vol.156, pp. 167-204.

[27] Lamb, H, Hydrodynamics, Cambridge University Press, 1932.

[28] Lanoville, A., Gateshore, I.S. and Parkinsoon, G.V., "An Experimental of some effects of turbulence on bluff bodies", Proceeding of the 4th international Conference on wind Effects on Buildings and Structure, London, U.K.1975, pp.333-341.

[29] Leutheusser, J., "Static wind loadings of Grouped Buildings", Proceedings of the 3rd international Conference on Wind Effects on Buildings, Tokyo, Japan, 1971, pp.211-220.

[30] Mandal, A.C. and Farok, G.M.G., "An Experimental Investigation of Static Pressure Distributions on a Group of Square and Rectangular Cylinders with Rounded Corners", Submitted for publication in the Journal of Mechanical Engineering, The Institution of Engineers, Bangladesh.

[31] Mandal, A.C. and Islam, O., "A Study of Wind Effect on a Group of Square Cylinders with Variable Transverse and Longitudinal Spacing", The Institution of Engineers, Bangladesh, Vol. 9.No.1, January,1981, pp.33-39.

[32] Mandal, A.C. and Islam, O., "A Study of Wind Effect on a Group of Square Cylinders with Variable Longitudinal Spacing", Mechanical Engineering Research Bulletin, BUET, Dhaka, Vol.3, No.1, 1980, pp. 21-26.

[33] Maskell, E.C., "A Theory of Blockage Effects on Bluff Bodies and Stalled Wings in a closed Wind Tunnel", ARC R&M No.3400, 1965, HMSO.

[34] Matsumoto, M., "The Dynamical Forces Acting on the Vibrating Square Prism in a Steady Flow", Proceedings of the 3rd international Conference on Wind Effects on Buildings and Structures, Tokyo, Japan, pp.921-930.

[35] Mchuri, F.G. et al, "Effects of the free Stream Turbulences on Drag Coefficients of Bluff sharp- Edged Cylinders", Nature, Vol.224, No. 5222, November 29, 1969,pp. 908-909

[36] Nakamura, Y. and Matsukawa, T., "Vortex Excitation of Rectangular Cylinders with a long side normal to the Flow", Journal of the Fluid Mechanics, Vol.137, 1987, pp.171-191.

[37] Nakamura, Y. and Ohya, Y., "The Effects of Turbulence on the Main Flow past Square Rods", Journal of Fluid Mechanics, Vol.137, 1983, pp.331-345.

[38] Nakamura, Y. and Yujioha, "Vortex Shedding from Square Prisms in Smooth and Turbulent Flows", Journal of Fluid Mechanics, Vol.164, 1986, pp.77-89.

[39] Pope, A and Haper, J.J., "Low Speed Wind Tunnel Testing, John Willy and Sons," New York, 1996.

[40] Parkinson, G.V. and Modi, V.J., "Recent research on Wind effects on Bluff Two Dimensional Bodies", Proceedings, international Research Seminar, Wind Effects on Buildings and Structures, Ottawa, Canada, 1967, pp.485-514.

[41] Roberson, J.A, Chi Yu Lin, Rutherford, G.S. and Stine, M.D., "Turbulence Effects on Drag of Sharp- edged Bodies", Journal of Hydraulics Division, Vol.98, No.HY7, pp.1187-1201.

[42] Roberson, J. A, Crowe , C.T and Tseng, R., " Pressure Distribution on Two and Three Dimensional Models at small Angles of Attack in Turbulent flow", Proceeding of the 2nd U.S. National Conference on wind Engineering Research, June 22-25, 1975, Colorado.

[43] Robertson, J.M., "Pressure field at Reattachment of Separated flows", Proceeding of the 2nd U .S. National Conference on wind Engineering Research, June 22-25, 1975, Colorado.

[44] Shakamoto, H and Arie, M., "Vortex Shedding from a Rectangular Prism and a Circular Cylinder Placed vertically in turbulent Boundary layer", Journal of Fluid Mechanics, Vol.126, 1983, pp.147-165.

[45] Surry, D., "Pressure Measurements on the Texas Tech buildings, Wind Tunnel Measurements and Comparison with Full Scale", J. Wind Eng. Ind. Aerodynamics.No.38, 1991, pp. 235-247.

[46] Vickery, B.J., "Fluctuating Lift and Drag on a long Cylinder of Square Cross section in a Smooth and in a Turbulent Stream", Journal of Fluid Mechanics, Vol.25, 1966, pp. 481-491.

[47] Whitbread, R.E., "Model Simulation of Wind Effects on Structures", Proceedings of a Symposium on Wind Effects on Buildings and Structures, Teddington, UK, 1963, pp. 283-301.

[48] Hayashi, M. Akirasakurai and Yujiohya., "Wake interference of a Row of Normal Flat plates Arranged Side by Side in a Uniform Flow", Journal of Fluid Mechanics, Vol.164, pp.1-25, 1986.

[49] Okajima, A., "Strouhal Numbers of Rectangular Cylinders", Journal of Fluid Mechanics, Vol.123, PP.379-398, 1982.

[50] Cochran, L.S., and Cermak, J.E., "Full and Model Scale Cladding Pressures on the Texas Tech University Experimental Building", J Wind Eng Ind Aerodyn. No.43, pp. 1589-1600, 1992.

[51] Islam, T., "An Experimental Investigation of Wind Effect on Rectangular Cylinders", M.Sc. Engg. Thesis, Department of Mechanical Engg. , BUET, 1988.

[52] Sultana, K. R., "An Experimental Investigation of Wind Load on Tall Buildings with Hexagonal Cross-Section", M.Sc. Engg. Thesis, Department of Mechanical Engg., BUET, 2009.

[53] Hossain, M.J., Islam, M.Q., and Ali, M., "An Experimental Investigation of Wind Load on Tall Buildings with Octagonal Cross-Section", International Journal of Renewable Energy Research, Vol.3, No.1, 2013.

[54] Nakamura, Y., and Yujioha., " Vortex Shedding from Square Prisms in Smooth and Turbulent Flows," Journal of Fluid Mechanics,Vol.164,1986,pp.77-89.

[55] Steggel, N., "A Numerical Investigation of the Flow around Rectangular Cylinders," Doctor of Philosophy Thesis, School of Mechanical and Materials Engg., The University of Surrey, Guildford GU2 5XH, United Kingdom, 1998.

APPENDIX

Uncertainty Analysis

Sample data: 4.34, 4.45, 4.39, 4.31, 4.39, 4.44, 4.43, 4.40, 4.40, 4.32 inch of H_2O

If our measurement result denoted by X, then,

$$X = \overline{X} \pm \Delta X \quad \text{----------} \quad (1)$$

$$\text{Or, } X = \overline{X} \pm \sigma$$

Where, $\overline{X}$ = Average value

ΔX = Uncertainty

σ = Standard deviation

$\Delta X = \sigma$

Again, from equation (1), $X = \overline{X}\left(1 \pm \frac{\Delta X}{\overline{X}}\right)$

Here, $\frac{\Delta X}{\overline{X}}$ = Fractional Uncertainty

Percent Uncertainty = Fractional Uncertainty × 100

Now, $\overline{X} = \frac{\sum_{i=1}^{N} X_i}{N}$

$$= \frac{X_1+X_2+X_3+ \text{------} +X_N}{N}$$

$$= \frac{4.34+4.45+4.39+4.31+4.39+4.44+4.43+4.40+4.40+4.32}{10}$$

$$= 4.387$$

$$\sigma = \sqrt{\frac{\sum_{i=1}^{N} (X_i-\overline{X})^2}{N-1}}$$

$$= \sqrt{\frac{(X_1-\overline{X})^2+(X_2-\overline{X})^2+\text{---------}+(X_N-\overline{X})^2}{N-1}}$$

$\Rightarrow \sigma$ or $\Delta X = 0.049$

So, $\frac{\Delta X}{\overline{X}} = \frac{0.049}{4.387}$

$$= 0.0112$$

Percent Uncertainty = 0.0112 × 100 =1.12%

$X = \overline{X} \pm \Delta X$

$= 4.387 \pm 0.049$

1.Distribution of Pressure Coefficient on hexagonal cylinder at Angle of Attack of $\alpha = 0^0$

Tapping Point	Initial Reading (inch of H_2O)	Final Reading (inch of H_2O)	Differences ,Δh_w (inch of H_2O)	Differences ,Δh_w (mm of H_2O)	Pressure Coefficient , Cp	Tapping Point	Initial Reading (inch of H_2O)	Final Reading (inch of H_2O)	Differences ,Δh_w (inch of H_2O)	Differences ,Δh_w (mm of H_2O)	Pressure Coefficient , Cp
1	4.35	4.02	0.335	8.50	0.75	16	4.30	4.60	-0.303	-7.71	-0.68
2	4.60	4.27	0.330	8.39	0.74	17	4.39	4.69	-0.299	-7.59	-0.67
3	4.38	4.09	0.286	7.25	0.64	18	3.90	4.19	-0.286	-7.25	-0.64
4	4.30	4.12	0.183	4.65	0.41	19	4.20	4.49	-0.286	-7.25	-0.64
5	4.38	4.38	0.000	0.00	0.00	20	4.19	4.48	-0.294	-7.48	-0.66
6	4.55	4.82	-0.268	-6.80	-0.60	21	4.30	4.58	-0.277	-7.03	-0.62
7	4.50	4.79	-0.290	-7.37	-0.65	22	4.33	4.62	-0.286	-7.25	-0.64
8	4.40	4.71	-0.308	-7.82	-0.69	23	4.01	4.30	-0.294	-7.48	-0.66
9	4.40	4.69	-0.290	-7.37	-0.65	24	4.00	4.29	-0.286	-7.25	-0.64
10	4.25	4.53	-0.277	-7.03	-0.62	25	4.05	4.32	-0.272	-6.91	-0.61
11	4.40	4.70	-0.299	-7.59	-0.67	26	3.95	3.95	0.004	0.11	0.01
12	4.28	4.57	-0.286	-7.25	-0.64	27	4.06	3.88	0.183	4.65	0.41
13	4.30	4.59	-0.286	-7.25	-0.64	28	4.34	4.05	0.286	7.25	0.64
14	4.00	4.30	-0.299	-7.59	-0.67	29	4.20	3.87	0.330	8.39	0.74
15	4.20	4.50	-0.303	-7.71	-0.68	30	4.01	3.68	0.335	8.50	0.75

2.Distribution of Pressure Coefficient on hexagonal cylinder at Angle of Attack of $\alpha = 10^0$

Tapping Point	Initial Reading (inch of H_2O)	Final Reading (inch of H_2O)	Differences ,Δh_w (inch of H_2O)	Differences ,Δh_w (mm of H_2O)	Pressure Coefficient , Cp	Tapping Point	Initial Reading (inch of H_2O)	Final Reading (inch of H_2O)	Differences ,Δh_w (inch of H_2O)	Differences ,Δh_w (mm of H_2O)	Pressure Coefficient , Cp
1	4.35	3.99	0.357	9.07	0.80	16	4.30	4.57	-0.272	-6.91	-0.61
2	4.60	4.22	0.379	9.63	0.85	17	4.39	4.65	-0.263	-6.69	-0.59
3	4.38	4.01	0.366	9.29	0.82	18	3.90	4.16	-0.263	-6.69	-0.59
4	4.30	4.02	0.277	7.03	0.62	19	4.20	4.44	-0.236	-6.01	-0.53
5	4.38	4.29	0.089	2.27	0.20	20	4.19	4.43	-0.241	-6.12	-0.54
6	4.55	4.82	-0.272	-6.91	-0.61	21	4.30	4.55	-0.245	-6.23	-0.55
7	4.50	4.79	-0.286	-7.25	-0.64	22	4.33	4.58	-0.245	-6.23	-0.55
8	4.40	4.69	-0.294	-7.48	-0.66	23	4.01	4.26	-0.254	-6.46	-0.57
9	4.40	4.67	-0.272	-6.91	-0.61	24	4.00	4.26	-0.263	-6.69	-0.59
10	4.25	4.52	-0.270	-6.86	-0.61	25	4.05	4.31	-0.263	-6.69	-0.59

11	4.40	4.69	-0.290	-7.37	-0.65	26	3.95	3.95	-0.004	-0.11	-0.01
12	4.28	4.55	-0.268	-6.80	-0.60	27	4.06	3.93	0.129	3.29	0.29
13	4.30	4.56	-0.263	-6.69	-0.59	28	4.34	4.12	0.219	5.55	0.49
14	4.00	4.23	-0.232	-5.89	-0.52	29	4.20	3.93	0.268	6.80	0.60
15	4.20	4.45	-0.245	-6.23	-0.55	30	4.01	3.65	0.357	9.07	0.80

3.Distribution of Pressure Coefficient on hexagonal cylinder at Angle of Attack of $\alpha = 20^0$

Tapping Point	Initial Reading (inch of H_2O)	Final Reading (inch of H_2O)	Differences ,Δh_w (inch of H_2O)	Differences ,Δh_w (mm of H_2O)	Pressure Coefficient , Cp	Tapping Point	Initial Reading (inch of H_2O)	Final Reading (inch of H_2O)	Differences ,Δh_w (inch of H_2O)	Differences ,Δh_w (mm of H_2O)	Pressure Coefficient , Cp
1	4.35	3.95	0.397	10.09	0.89	16	4.30	4.57	-0.270	-6.86	-0.61
2	4.60	4.21	0.393	9.97	0.88	17	4.39	4.65	-0.259	-6.57	-0.58
3	4.38	3.98	0.402	10.20	0.90	18	3.90	4.17	-0.268	-6.80	-0.60
4	4.30	3.97	0.326	8.27	0.73	19	4.20	4.45	-0.254	-6.46	-0.57
5	4.38	4.30	0.085	2.15	0.19	20	4.19	4.44	-0.250	-6.35	-0.56
6	4.55	5.13	-0.576	-14.62	-1.29	21	4.30	4.55	-0.254	-6.46	-0.57
7	4.50	4.94	-0.437	-11.11	-0.98	22	4.33	4.59	-0.259	-6.57	-0.58
8	4.40	4.75	-0.348	-8.84	-0.78	23	4.01	4.23	-0.223	-5.67	-0.50
9	4.40	4.63	-0.232	-5.89	-0.52	24	4.00	4.23	-0.232	-5.89	-0.52
10	4.25	4.46	-0.210	-5.33	-0.47	25	4.05	4.32	-0.272	-6.91	-0.61
11	4.40	4.68	-0.281	-7.14	-0.63	26	3.95	4.07	-0.125	-3.17	-0.28
12	4.28	4.53	-0.254	-6.46	-0.57	27	4.06	4.02	0.045	1.13	0.10
13	4.30	4.56	-0.263	-6.69	-0.59	28	4.34	4.17	0.174	4.42	0.39
14	4.00	4.27	-0.270	-6.86	-0.61	29	4.20	3.98	0.223	5.67	0.50
15	4.20	4.46	-0.263	-6.69	-0.59	30	4.01	3.74	0.272	6.91	0.61

4.Distribution of Pressure Coefficient on hexagonal cylinder at Angle of Attack of $\alpha = 30^0$

Tapping Point	Initial Reading (inch of H_2O)	Final Reading (inch of H_2O)	Differences ,Δh_w (inch of H_2O)	Differences ,Δh_w (mm of H_2O)	Pressure Coefficient , Cp	Tapping Point	Initial Reading (inch of H_2O)	Final Reading (inch of H_2O)	Differences ,Δh_w (inch of H_2O)	Differences ,Δh_w (mm of H_2O)	Pressure Coefficient , Cp
1	4.35	3.99	0.357	9.07	0.80	16	4.30	4.56	-0.263	-6.69	-0.59
2	4.60	4.19	0.410	10.43	0.92	17	4.39	4.64	-0.254	-6.46	-0.57
3	4.38	3.93	0.446	11.33	1.00	18	3.90	4.16	-0.259	-6.57	-0.58
4	4.30	3.89	0.410	10.43	0.92	19	4.20	4.41	-0.214	-5.44	-0.48
5	4.38	4.02	0.357	9.07	0.80	20	4.19	4.40	-0.214	-5.44	-0.48
6	4.55	4.93	-0.379	-9.63	-0.85	21	4.30	4.54	-0.236	-6.01	-0.53
7	4.50	4.77	-0.272	-6.91	-0.61	22	4.33	4.54	-0.205	-5.21	-0.46
8	4.40	4.58	-0.178	-4.53	-0.40	23	4.01	4.19	-0.178	-4.53	-0.40
9	4.40	4.48	-0.080	-2.04	-0.18	24	4.00	4.20	-0.201	-5.10	-0.45
10	4.25	4.38	-0.129	-3.29	-0.29	25	4.05	4.32	-0.268	-6.80	-0.60
11	4.40	4.67	-0.272	-6.91	-0.61	26	3.95	4.07	-0.125	-3.17	-0.28
12	4.28	4.51	-0.232	-5.89	-0.52	27	4.06	4.14	-0.080	-2.04	-0.18
13	4.30	4.53	-0.232	-5.89	-0.52	28	4.34	4.52	-0.183	-4.65	-0.41
14	4.00	4.23	-0.232	-5.89	-0.52	29	4.20	4.47	-0.272	-6.91	-0.61
15	4.20	4.43	-0.228	-5.78	-0.51	30	4.01	4.36	-0.352	-8.95	-0.79

5.Distribution of Pressure Coefficient on hexagonal cylinder at Angle of Attack of $\alpha = 40^0$

Tapping Point	Initial Reading (inch of H_2O)	Final Reading (inch of H_2O)	Differences ,Δh_w (inch of H_2O)	Differences ,Δh_w (mm of H_2O)	Pressure Coefficient , Cp	Tapping Point	Initial Reading (inch of H_2O)	Final Reading (inch of H_2O)	Differences ,Δh_w (inch of H_2O)	Differences ,Δh_w (mm of H_2O)	Pressure Coefficient , Cp
1	4.35	4.02	0.335	8.50	0.75	16	4.30	4.56	-0.259	-6.57	-0.58
2	4.60	4.24	0.361	9.18	0.81	17	4.39	4.64	-0.254	-6.46	-0.57
3	4.38	3.95	0.433	10.99	0.97	18	3.90	4.16	-0.259	-6.57	-0.58
4	4.30	3.85	0.446	11.33	1.00	19	4.20	4.43	-0.228	-5.78	-0.51
5	4.38	3.99	0.393	9.97	0.88	20	4.19	4.41	-0.223	-5.67	-0.50
6	4.55	4.60	-0.054	-1.36	-0.12	21	4.30	4.53	-0.228	-5.78	-0.51
7	4.50	4.34	0.156	3.97	0.35	22	4.33	4.54	-0.214	-5.44	-0.48
8	4.40	4.31	0.094	2.38	0.21	23	4.01	4.19	-0.178	-4.53	-0.40
9	4.40	4.40	0.004	0.11	0.01	24	4.00	4.19	-0.187	-4.76	-0.42
10	4.25	4.33	-0.080	-2.04	-0.18	25	4.05	4.27	-0.223	-5.67	-0.50

11	4.40	4.66	-0.263	-6.69	-0.59	26	3.95	4.10	-0.152	-3.85	-0.34
12	4.28	4.53	-0.250	-6.35	-0.56	27	4.06	4.14	-0.080	-2.04	-0.18
13	4.30	4.52	-0.223	-5.67	-0.50	28	4.34	4.44	-0.098	-2.49	-0.22
14	4.00	4.24	-0.241	-6.12	-0.54	29	4.20	4.42	-0.223	-5.67	-0.50
15	4.20	4.45	-0.254	-6.46	-0.57	30	4.01	4.28	-0.272	-6.91	-0.61

6.Distribution of Pressure Coefficient on hexagonal cylinder at Angle of Attack of α =50^0

Tapping Point	Initial Reading (inch of H_2O)	Final Reading (inch of H_2O)	Differences ,Δh_w (inch of H2O)	Differences ,Δh_w (mm of H_2O)	Pressure Coefficient , Cp	Tapping Point	Initial Reading (inch of H_2O)	Final Reading (inch of H_2O)	Differences ,Δh_w (inch of H_2O)	Differences ,Δh_w (mm of H_2O)	Pressure Coefficient , Cp
1	4.35	4.26	0.089	2.27	0.20	16	4.30	4.57	-0.268	-6.80	-0.60
2	4.60	4.42	0.183	4.65	0.41	17	4.39	4.65	-0.259	-6.57	-0.58
3	4.38	4.01	0.366	9.29	0.82	18	3.90	4.16	-0.263	-6.69	-0.59
4	4.30	3.85	0.446	11.33	1.00	19	4.20	4.38	-0.183	-4.65	-0.41
5	4.38	3.95	0.433	10.99	0.97	20	4.19	4.36	-0.174	-4.42	-0.39
6	4.55	4.33	0.223	5.67	0.50	21	4.30	4.53	-0.232	-5.89	-0.52
7	4.50	4.24	0.263	6.69	0.59	22	4.33	4.54	-0.214	-5.44	-0.48
8	4.40	4.22	0.183	4.65	0.41	23	4.01	4.21	-0.201	-5.10	-0.45
9	4.40	4.31	0.094	2.38	0.21	24	4.00	4.20	-0.201	-5.10	-0.45
10	4.25	4.28	-0.027	-0.68	-0.06	25	4.05	4.32	-0.265	-6.74	-0.60
11	4.40	4.67	-0.272	-6.91	-0.61	26	3.95	4.21	-0.263	-6.69	-0.59
12	4.28	4.48	-0.196	-4.99	-0.44	27	4.06	4.23	-0.174	-4.42	-0.39
13	4.30	4.54	-0.236	-6.01	-0.53	28	4.34	4.72	-0.379	-9.63	-0.85
14	4.00	4.25	-0.245	-6.23	-0.55	29	4.20	4.79	-0.589	-14.96	-1.32
15	4.20	4.41	-0.214	-5.44	-0.48	30	4.01	4.59	-0.576	-14.62	-1.29

7.Distribution of Pressure Coefficient on pentagonal cylinder at Angle of Attack of $\alpha = 0^0$

Tapping Point	Initial Reading (inch of H_2O)	Final Reading (inch of H_2O)	Differences ,Δh_w (inch of H_2O)	Differences ,Δh_w (mm of H_2O)	Pressure Coefficient , Cp	Tapping Point	Initial Reading (inch of H_2O)	Final Reading (inch of H_2O)	Differences ,Δh_w (inch of H_2O)	Differences ,Δh_w (mm of H_2O)	Pressure Coefficient, Cp
1	4.35	3.66	0.69	17.53	1.55	14	4.00	3.98	0.02	0.51	0.04
2	4.60	2.80	1.80	45.72	4.03	15	4.20	4.05	0.15	3.81	0.34
3	4.38	2.88	1.50	38.10	3.36	16	4.30	4.22	0.08	2.03	0.18
4	4.30	3.00	1.30	33.02	2.91	17	4.39	4.31	0.08	2.03	0.18
5	4.38	3.16	1.22	30.99	2.73	18	3.90	3.76	0.14	3.56	0.31
6	4.55	4.12	0.43	10.92	0.96	19	4.20	4.02	0.18	4.57	0.40
7	4.50	4.04	0.46	11.68	1.03	20	4.19	4.12	0.07	1.78	0.16
8	4.40	3.64	0.76	19.30	1.70	21	4.30	4.22	0.08	2.03	0.18
9	4.40	3.64	0.76	19.30	1.70	22	4.33	4.20	0.13	3.30	0.29
10	4.25	3.86	0.39	9.91	0.87	23	4.01	3.73	0.28	7.11	0.63
11	4.40	4.35	0.05	1.27	0.11	24	4.00	3.93	0.07	1.78	0.16
12	4.28	4.19	0.09	2.29	0.20	25	4.05	3.45	0.60	15.24	1.34
13	4.30	4.26	0.04	1.02	0.09						

8.Distribution of Pressure Coefficient on pentagonal cylinder at Angle of Attack of $\alpha = 9^0$

Tapping Point	Initial Reading (inch of H_2O)	Final Reading (inch of H_2O)	Differences ,Δh_w (inch of H_2O)	Differences ,Δh_w (mm of H_2O)	Pressure Coefficient , Cp	Tapping Point	Initial Reading (inch of H_2O)	Final Reading (inch of H_2O)	Differences ,Δh_w (inch of H_2O)	Differences ,Δh_w (mm of H_2O)	Pressure Coefficient , Cp
1	4.35	3.67	0.68	17.27	1.52	14	4.00	3.96	0.04	1.02	0.09
2	4.60	2.82	1.78	45.21	3.99	15	4.20	4.00	0.20	5.08	0.45
3	4.38	2.80	1.58	40.13	3.54	16	4.30	4.20	0.10	2.54	0.22
4	4.30	2.90	1.40	35.56	3.14	17	4.39	4.21	0.18	4.57	0.40
5	4.38	3.00	1.38	35.05	3.09	18	3.90	3.79	0.11	2.79	0.25
6	4.55	4.16	0.39	9.91	0.87	19	4.20	4.00	0.20	5.08	0.45
7	4.50	4.02	0.48	12.19	1.08	20	4.19	4.02	0.17	4.32	0.38
8	4.40	3.84	0.56	14.22	1.26	21	4.30	4.39	-0.09	-2.29	-0.20
9	4.40	4.33	0.07	1.78	0.16	22	4.33	4.40	-0.07	-1.78	-0.16
10	4.25	4.24	0.01	0.25	0.02	23	4.01	3.84	0.17	4.32	0.38
11	4.40	4.22	0.18	4.57	0.40	24	4.00	4.15	-0.15	-3.81	-0.34
12	4.28	4.11	0.17	4.32	0.38	25	4.05	3.49	0.56	14.22	1.26
13	4.30	4.13	0.17	4.32	0.38						

9.Distribution of Pressure Coefficient on pentagonal cylinder at Angle of Attack of $\alpha = 18^0$

Tapping Point	Initial Reading (inch of H_2O)	Final Reading (inch of H_2O)	Differences ,Δh_w (inch of H_2O)	Differences ,Δh_w (mm of H_2O)	Pressure Coefficient , Cp	Tapping Point	Initial Reading (inch of H_2O)	Final Reading (inch of H_2O)	Differences ,Δh_w (inch of H_2O)	Differences ,Δh_w (mm of H_2O)	Pressure Coefficient , Cp
1	4.35	3.66	0.69	17.53	1.55	14	4.00	3.93	0.07	1.78	0.16
2	4.60	2.90	1.70	43.18	3.81	15	4.20	3.97	0.23	5.84	0.52
3	4.38	2.80	1.58	40.13	3.54	16	4.30	4.18	0.12	3.05	0.27
4	4.30	2.80	1.50	38.10	3.36	17	4.39	4.18	0.21	5.33	0.47
5	4.38	2.81	1.57	39.88	3.52	18	3.90	3.76	0.14	3.56	0.31
6	4.55	4.49	0.06	1.52	0.13	19	4.20	3.98	0.22	5.59	0.49
7	4.50	4.70	-0.20	-5.08	-0.45	20	4.19	3.99	0.20	5.08	0.45
8	4.40	4.61	-0.21	-5.33	-0.47	21	4.30	4.39	-0.09	-2.29	-0.20
9	4.40	4.60	-0.20	-5.08	-0.45	22	4.33	4.13	0.20	5.08	0.45
10	4.25	4.40	-0.15	-3.81	-0.34	23	4.01	3.45	0.56	14.22	1.26
11	4.40	4.19	0.21	5.33	0.47	24	4.00	3.49	0.51	12.95	1.14
12	4.28	4.09	0.19	4.83	0.43	25	4.05	3.34	0.71	18.03	1.59
13	4.30	4.09	0.21	5.33	0.47						

10.Distribution of Pressure Coefficient on pentagonal cylinder at Angle of Attack of $\alpha = 27^0$

Tapping Point	Initial Reading (inch of H_2O)	Final Reading (inch of H_2O)	Differences ,Δh_w (inch of H_2O)	Differences ,Δh_w (mm of H_2O)	Pressure Coefficient , Cp	Tapping Point	Initial Reading (inch of H_2O)	Final Reading (inch of H_2O)	Differences ,Δh_w (inch of H_2O)	Differences ,Δh_w (mm of H_2O)	Pressure Coefficient , Cp
1	4.35	3.63	0.72	18.29	1.61	14	4.00	3.90	0.10	2.54	0.22
2	4.60	2.98	1.62	41.15	3.63	15	4.20	3.91	0.29	7.37	0.65
3	4.38	2.80	1.58	40.13	3.54	16	4.30	4.16	0.14	3.56	0.31
4	4.30	2.78	1.52	38.61	3.41	17	4.39	4.16	0.23	5.84	0.52
5	4.38	2.70	1.68	42.67	3.77	18	3.90	3.73	0.17	4.32	0.38
6	4.55	4.40	0.15	3.81	0.34	19	4.20	3.94	0.26	6.60	0.58
7	4.50	4.48	0.02	0.51	0.04	20	4.19	3.90	0.29	7.37	0.65
8	4.40	4.40	0.00	0.00	0.00	21	4.30	3.55	0.75	19.05	1.68
9	4.40	4.30	0.10	2.54	0.22	22	4.33	3.38	0.95	24.13	2.13
10	4.25	4.03	0.22	5.59	0.49	23	4.01	3.27	0.74	18.80	1.66
11	4.40	4.17	0.23	5.84	0.52	24	4.00	3.41	0.59	14.99	1.32
12	4.28	4.08	0.20	5.08	0.45	25	4.05	3.31	0.74	18.80	1.66
13	4.30	4.07	0.23	5.84	0.52						

11.Distribution of Pressure Coefficient on pentagonal cylinder at Angle of Attack of $\alpha = 36^0$

Tapping Point	Initial Reading (inch of H_2O)	Final Reading (inch of H_2O)	Differences ,Δh_w (inch of H_2O)	Differences ,Δh_w (mm of H_2O)	Pressure Coefficient , Cp	Tapping Point	Initial Reading (inch of H_2O)	Final Reading (inch of H_2O)	Differences ,Δh_w (inch of H_2O)	Differences ,Δh_w (mm of H_2O)	Pressure Coefficient , Cp
1	4.35	3.64	0.71	18.03	1.59	14	4.00	3.91	0.09	2.29	0.20
2	4.60	3.11	1.49	37.85	3.34	15	4.20	3.96	0.24	6.10	0.54
3	4.38	2.88	1.50	38.10	3.36	16	4.30	4.18	0.12	3.05	0.27
4	4.30	2.79	1.51	38.35	3.38	17	4.39	4.18	0.21	5.33	0.47
5	4.38	2.65	1.73	43.94	3.88	18	3.90	3.77	0.13	3.30	0.29
6	4.55	4.40	0.15	3.81	0.34	19	4.20	3.95	0.25	6.35	0.56
7	4.50	4.40	0.10	2.54	0.22	20	4.19	3.97	0.22	5.59	0.49
8	4.40	4.30	0.10	2.54	0.22	21	4.30	3.12	1.18	29.97	2.64
9	4.40	4.34	0.06	1.52	0.13	22	4.33	3.26	1.07	27.18	2.40
10	4.25	4.09	0.16	4.06	0.36	23	4.01	3.18	0.83	21.08	1.86
11	4.40	4.20	0.20	5.08	0.45	24	4.00	3.32	0.68	17.27	1.52
12	4.28	4.10	0.18	4.57	0.40	25	4.05	3.30	0.75	19.05	1.68
13	4.30	4.10	0.20	5.08	0.45						

12.Distribution of Pressure Coefficient on pentagonal cylinder at Angle of Attack of $\alpha = 45^0$

Tapping Point	Initial Reading (inch of H_2O)	Final Reading (inch of H_2O)	Differences ,Δh_w (inch of H_2O)	Differences ,Δh_w (mm of H_2O)	Pressure Coefficient , Cp	Tapping Point	Initial Reading (inch of H_2O)	Final Reading (inch of H_2O)	Differences ,Δh_w (inch of H_2O)	Differences ,Δh_w (mm of H_2O)	Pressure Coefficient , Cp
1	4.35	3.61	0.74	18.80	1.66	14	4.00	3.91	0.09	2.29	0.20
2	4.60	3.25	1.35	34.29	3.03	15	4.20	3.96	0.24	6.10	0.54
3	4.38	3.02	1.36	34.54	3.05	16	4.30	4.18	0.12	3.05	0.27
4	4.30	2.90	1.40	35.56	3.14	17	4.39	4.18	0.21	5.33	0.47
5	4.38	2.71	1.67	42.42	3.74	18	3.90	3.79	0.11	2.79	0.25
6	4.55	4.37	0.18	4.57	0.40	19	4.20	3.95	0.25	6.35	0.56
7	4.50	4.38	0.12	3.05	0.27	20	4.19	3.99	0.20	5.08	0.45
8	4.40	4.22	0.18	4.57	0.40	21	4.30	2.78	1.52	38.61	3.41
9	4.40	4.29	0.11	2.79	0.25	22	4.33	3.02	1.31	33.27	2.94
10	4.25	4.07	0.18	4.57	0.40	23	4.01	3.00	1.01	25.65	2.26
11	4.40	4.20	0.20	5.08	0.45	24	4.00	3.10	0.90	22.86	2.02
12	4.28	4.10	0.18	4.57	0.40	25	4.05	3.26	0.79	20.07	1.77
13	4.30	4.07	0.23	5.84	0.52						

13.Distribution of Pressure Coefficient on pentagonal cylinder at Angle of Attack of $\alpha = 54^0$

Tapping Point	Initial Reading (inch of H_2O)	Final Reading (inch of H_2O)	Differences ,Δh_w (inch of H_2O)	Differences ,Δh_w (mm of H_2O)	Pressure Coefficient , Cp	Tapping Point	Initial Reading (inch of H_2O)	Final Reading (inch of H_2O)	Differences ,Δh_w (inch of H_2O)	Differences ,Δh_w (mm of H_2O)	Pressure Coefficient , Cp
1	4.35	3.61	0.74	18.80	1.66	14	4.00	3.91	0.09	2.29	0.20
2	4.60	3.57	1.03	26.16	2.31	15	4.20	3.94	0.26	6.60	0.58
3	4.38	3.26	1.12	28.45	2.51	16	4.30	4.19	0.11	2.79	0.25
4	4.30	3.10	1.20	30.48	2.69	17	4.39	4.19	0.20	5.08	0.45
5	4.38	2.95	1.43	36.32	3.21	18	3.90	3.80	0.10	2.54	0.22
6	4.55	4.37	0.18	4.57	0.40	19	4.20	3.96	0.24	6.10	0.54
7	4.50	4.38	0.12	3.05	0.27	20	4.19	3.99	0.20	5.08	0.45
8	4.40	4.21	0.19	4.83	0.43	21	4.30	2.48	1.82	46.23	4.08
9	4.40	4.28	0.12	3.05	0.27	22	4.33	2.73	1.60	40.64	3.59
10	4.25	4.05	0.20	5.08	0.45	23	4.01	2.83	1.18	29.97	2.64
11	4.40	4.19	0.21	5.33	0.47	24	4.00	2.83	1.17	29.72	2.62
12	4.28	4.09	0.19	4.83	0.43	25	4.05	3.20	0.85	21.59	1.91
13	4.30	4.08	0.22	5.59	0.49						

14.Distribution of Pressure Coefficient on pentagonal cylinder at Angle of Attack of $\alpha = 63^0$

Tapping Point	Initial Reading (inch of H_2O)	Final Reading (inch of H_2O)	Differences ,Δh_w (inch of H_2O)	Differences ,Δh_w (mm of H_2O)	Pressure Coefficient , Cp	Tapping Point	Initial Reading (inch of H_2O)	Final Reading (inch of H_2O)	Differences ,Δh_w (inch of H_2O)	Differences ,Δh_w (mm of H_2O)	Pressure Coefficient , Cp
1	4.35	3.60	0.75	19.05	1.68	14	4.00	3.91	0.09	2.29	0.20
2	4.60	3.90	0.70	17.78	1.57	15	4.20	3.94	0.26	6.60	0.58
3	4.38	3.49	0.89	22.61	1.99	16	4.30	4.18	0.12	3.05	0.27
4	4.30	3.22	1.08	27.43	2.42	17	4.39	4.19	0.20	5.08	0.45
5	4.38	3.27	1.11	28.19	2.49	18	3.90	3.80	0.10	2.54	0.22
6	4.55	4.36	0.19	4.83	0.43	19	4.20	3.96	0.24	6.10	0.54
7	4.50	4.38	0.12	3.05	0.27	20	4.19	4.00	0.19	4.83	0.43
8	4.40	4.20	0.20	5.08	0.45	21	4.30	2.37	1.93	49.02	4.33
9	4.40	4.29	0.11	2.79	0.25	22	4.33	2.53	1.80	45.72	4.03
10	4.25	4.07	0.18	4.57	0.40	23	4.01	2.70	1.31	33.27	2.94
11	4.40	4.19	0.21	5.33	0.47	24	4.00	2.60	1.40	35.56	3.14
12	4.28	4.09	0.19	4.83	0.43	25	4.05	3.15	0.90	22.86	2.02
13	4.30	4.05	0.25	6.35	0.56						

15.Distribution of Pressure Coefficient on pentagonal cylinder at Angle of Attack of $\alpha = 72^0$

Tapping Point	Initial Reading (inch of H_2O)	Final Reading (inch of H_2O)	Differences Δh_w (inch of H_2O)	Differences Δh_w (mm of H_2O)	Pressure Coefficient , Cp	Tapping Point	Initial Reading (inch of H_2O)	Final Reading (inch of H_2O)	Differences Δh_w (inch of H_2O)	Differences Δh_w (mm of H_2O)	Pressure Coefficient , Cp
1	4.35	3.56	0.79	20.07	1.77	14	4.00	3.85	0.15	3.81	0.34
2	4.60	3.97	0.63	16.00	1.41	15	4.20	3.87	0.33	8.38	0.74
3	4.38	3.50	0.88	22.35	1.97	16	4.30	4.13	0.17	4.32	0.38
4	4.30	3.54	0.76	19.30	1.70	17	4.39	4.13	0.26	6.60	0.58
5	4.38	3.82	0.56	14.22	1.26	18	3.90	3.70	0.20	5.08	0.45
6	4.55	4.28	0.27	6.86	0.61	19	4.20	3.90	0.30	7.62	0.67
7	4.50	4.29	0.21	5.33	0.47	20	4.19	3.90	0.29	7.37	0.65
8	4.40	4.10	0.30	7.62	0.67	21	4.30	2.34	1.96	49.78	4.39
9	4.40	4.19	0.21	5.33	0.47	22	4.33	2.40	1.93	49.02	4.33
10	4.25	3.98	0.27	6.86	0.61	23	4.01	2.58	1.43	36.32	3.21
11	4.40	4.10	0.30	7.62	0.67	24	4.00	2.32	1.68	42.67	3.77
12	4.28	4.01	0.27	6.86	0.61	25	4.05	3.01	1.04	26.42	2.33
13	4.30	3.98	0.32	8.13	0.72						

16.Distribution of Pressure Coefficient on Hexagonal Cylinder at L_1=8D, L_2=2D

Tapping Point	Initial Reading (inch of H_2O)	Final Reading (inch of H_2O)	Differences Δh_w (inch of H_2O)	Differences Δh_w (mm of H_2O)	Pressure Coefficient, Cp	Tapping Point	Initial Reading (inch of H_2O)	Final Reading (inch of H_2O)	Differences Δh_w (inch of H_2O)	Differences Δh_w (mm of H_2O)	Pressure Coefficient, Cp
1	1.20	1.45	-0.25	-6.35	-0.56	16	1.30	2.07	-0.77	-19.56	-1.73
2	1.29	1.22	0.07	1.78	0.16	17	1.30	1.97	-0.67	-17.02	-1.50
3	1.24	1.10	0.14	3.56	0.31	18	1.06	1.75	-0.69	-17.53	-1.55
4	1.20	1.04	0.16	4.06	0.36	19	1.28	1.96	-0.68	-17.27	-1.52
5	1.20	1.00	0.20	5.08	0.45	20	1.20	1.90	-0.70	-17.78	-1.57
6	1.31	2.10	-0.79	-20.07	-1.77	21	1.36	2.52	-1.16	-29.46	-2.60
7	1.38	2.20	-0.82	-20.83	-1.84	22	1.39	2.17	-0.78	-19.81	-1.75
8	1.20	2.10	-0.90	-22.86	-2.02	23	1.15	1.80	-0.65	-16.51	-1.46
9	1.29	2.35	-1.06	-26.92	-2.38	24	1.30	1.81	-0.51	-12.95	-1.14
10	1.22	2.40	-1.18	-29.97	-2.64	25	1.30	2.02	-0.72	-18.29	-1.61
11	1.24	2.00	-0.76	-19.30	-1.70	26	1.30	1.47	-0.17	-4.32	-0.38
12	1.30	2.00	-0.70	-17.78	-1.57	27	1.44	1.41	0.03	0.76	0.07
13	1.18	1.86	-0.68	-17.27	-1.52	28	1.40	1.55	-0.15	-3.81	-0.34
14	1.26	1.90	-0.64	-16.26	-1.43	29	1.29	1.49	-0.20	-5.09	-0.45
15	1.17	1.79	-0.62	-15.75	-1.39	30	1.29	1.52	-0.23	-5.91	-0.52

17.Distribution of Pressure Coefficient on Pentagonal Cylinder at L_1=8D, L_2=2D

Tapping Point	Initial Reading (inch of H_2O)	Final Reading (inch of H_2O)	Differences Δh_w (inch of H_2O)	Differences Δh_w (mm of H_2O)	Pressure Coefficient, Cp	Tapping Point	Initial Reading (inch of H_2O)	Final Reading (inch of H_2O)	Differences Δh_w (inch of H_2O)	Differences Δh_w (mm of H_2O)	Pressure Coefficient, Cp
1	1.20	1.80	-0.60	-15.24	-1.34	14	1.26	2.02	-0.76	-19.30	-1.70
2	1.29	0.66	0.63	16.00	1.41	15	1.17	1.80	-0.63	-16.00	-1.41
3	1.24	0.82	0.42	10.67	0.94	16	1.30	2.08	-0.78	-19.81	-1.75
4	1.20	0.93	0.27	6.86	0.61	17	1.30	1.97	-0.67	-17.02	-1.50
5	1.20	1.10	0.10	2.54	0.22	18	1.06	1.78	-0.72	-18.29	-1.61
6	1.31	1.99	-0.68	-17.27	-1.52	19	1.28	1.96	-0.68	-17.27	-1.52
7	1.38	1.90	-0.52	-13.21	-1.17	20	1.20	1.90	-0.70	-17.78	-1.57
8	1.20	1.50	-0.30	-7.62	-0.67	21	1.36	2.08	-0.72	-18.29	-1.61
9	1.29	1.64	-0.35	-8.89	-0.78	22	1.39	1.96	-0.57	-14.48	-1.28
10	1.22	1.91	-0.69	-17.53	-1.55	23	1.15	1.71	-0.56	-14.22	-1.26
11	1.24	2.06	-0.82	-20.83	-1.84	24	1.30	1.66	-0.36	-9.14	-0.81
12	1.30	2.12	-0.82	-20.83	-1.84	25	1.30	1.68	-0.38	-9.65	-0.85
13	1.18	1.96	-0.78	-19.81	-1.75						

18.Distribution of Pressure Coefficient on Hexagonal Cylinder at L_1=6D, L_2=2D

Tapping Point	Initial Reading (inch of H_2O)	Final Reading (inch of H_2O)	Differences Δh_w (inch of H_2O)	Differences Δh_w (mm of H_2O)	Pressure Coefficient , Cp	Tapping Point	Initial Reading (inch of H_2O)	Final Reading (inch of H_2O)	Differences Δh_w (inch of H_2O)	Differences Δh_w (mm of H_2O)	Pressure Coefficient , Cp
1	1.20	1.45	-0.25	-6.35	-0.56	16	1.30	1.84	-0.54	-13.72	-1.21
2	1.29	1.15	0.14	3.56	0.31	17	1.30	1.82	-0.52	-13.21	-1.17
3	1.24	1.20	0.04	1.02	0.09	18	1.06	1.52	-0.46	-11.68	-1.03
4	1.20	1.30	-0.10	-2.54	-0.22	19	1.28	1.78	-0.50	-12.70	-1.12
5	1.20	1.40	-0.20	-5.08	-0.45	20	1.20	1.66	-0.46	-11.68	-1.03
6	1.31	1.76	-0.45	-11.43	-1.01	21	1.36	2.00	-0.64	-16.26	-1.43
7	1.38	1.82	-0.44	-11.18	-0.99	22	1.39	1.92	-0.53	-13.46	-1.19
8	1.20	1.63	-0.43	-10.92	-0.96	23	1.15	1.58	-0.43	-10.92	-0.96
9	1.29	1.81	-0.52	-13.21	-1.17	24	1.30	1.56	-0.26	-6.60	-0.58
10	1.22	2.05	-0.83	-21.08	-1.86	25	1.30	1.78	-0.48	-12.19	-1.08
11	1.24	1.70	-0.46	-11.68	-1.03	26	1.30	1.60	-0.30	-7.62	-0.67
12	1.30	1.76	-0.46	-11.68	-1.03	27	1.44	1.89	-0.45	-11.43	-1.01
13	1.18	1.60	-0.42	-10.67	-0.94	28	1.40	1.80	-0.40	-10.16	-0.90
14	1.26	1.70	-0.44	-11.18	-0.99	29	1.44	1.75	-0.31	-7.84	-0.69
15	1.17	1.60	-0.43	-10.92	-0.96	30	1.54	1.77	-0.23	-5.91	-0.52

19.Distribution of Pressure Coefficient on Pentagonal Cylinder at L_1=6D, L_2=2D

Tapping Point	Initial Reading (inch of H_2O)	Final Reading (inch of H_2O)	Differences Δh_w (inch of H_2O)	Differences Δh_w (mm of H_2O)	Pressure Coefficient ,Cp	Tapping Point	Initial Reading (inch of H_2O)	Final Reading (inch of H_2O)	Differences Δh_w (inch of H_2O)	Differences Δh_w (mm of H_2O)	Pressure Coefficient ,Cp
1	1.20	1.46	-0.26	-6.60	-0.58	14	1.26	1.70	-0.44	-11.18	-0.99
2	1.29	0.45	0.84	21.34	1.88	15	1.17	1.60	-0.43	-10.92	-0.96
3	1.24	0.55	0.69	17.53	1.55	16	1.30	1.79	-0.49	-12.45	-1.10
4	1.20	0.65	0.55	13.97	1.23	17	1.30	1.78	-0.48	-12.19	-1.08
5	1.20	0.82	0.38	9.65	0.85	18	1.06	1.50	-0.44	-11.18	-0.99
6	1.31	1.60	-0.29	-7.37	-0.65	19	1.28	1.76	-0.48	-12.19	-1.08
7	1.38	1.54	-0.16	-4.06	-0.36	20	1.20	1.62	-0.42	-10.67	-0.94
8	1.20	1.20	0.00	0.00	0.00	21	1.36	1.80	-0.44	-11.18	-0.99
9	1.29	1.28	0.01	0.25	0.02	22	1.39	1.80	-0.41	-10.41	-0.92
10	1.22	1.58	-0.36	-9.14	-0.81	23	1.15	1.50	-0.35	-8.89	-0.78
11	1.24	1.70	-0.46	-11.68	-1.03	24	1.30	1.55	-0.25	-6.35	-0.56
12	1.30	1.76	-0.46	-11.68	-1.03	25	1.30	1.58	-0.28	-7.11	-0.63
13	1.18	1.62	-0.44	-11.18	-0.99						

20.Distribution of Pressure Coefficient on Hexagonal Cylinder at L_1=4D, L_2=2D

Tapping Point	Initial Reading (inch of H_2O)	Final Reading (inch of H_2O)	Differences Δh_w (inch of H_2O)	Differences Δh_w (mm of H_2O)	Pressure Coefficient , Cp	Tapping Point	Initial Reading (inch of H_2O)	Final Reading (inch of H_2O)	Differences Δh_w (inch of H_2O)	Differences Δh_w (mm of H_2O)	Pressure Coefficient, Cp
1	1.20	1.46	-0.26	-6.60	-0.58	16	1.30	1.73	-0.43	-10.92	-0.96
2	1.29	1.35	-0.06	-1.52	-0.13	17	1.30	1.71	-0.41	-10.41	-0.92
3	1.24	1.30	-0.06	-1.52	-0.13	18	1.06	1.45	-0.39	-9.91	-0.87
4	1.20	1.34	-0.14	-3.56	-0.31	19	1.28	1.69	-0.41	-10.41	-0.92
5	1.20	1.43	-0.23	-5.84	-0.52	20	1.20	1.56	-0.36	-9.14	-0.81
6	1.31	1.71	-0.40	-10.16	-0.90	21	1.36	1.59	-0.23	-5.84	-0.52
7	1.38	1.80	-0.42	-10.67	-0.94	22	1.39	1.56	-0.17	-4.32	-0.38
8	1.20	1.62	-0.42	-10.67	-0.94	23	1.15	1.36	-0.21	-5.33	-0.47
9	1.29	1.83	-0.54	-13.72	-1.21	24	1.30	1.35	-0.05	-1.27	-0.11
10	1.22	2.00	-0.78	-19.81	-1.75	25	1.30	1.60	-0.30	-7.62	-0.67
11	1.24	1.60	-0.36	-9.14	-0.81	26	1.30	1.53	-0.23	-5.84	-0.52
12	1.30	1.66	-0.36	-9.14	-0.81	27	1.44	1.70	-0.26	-6.60	-0.58
13	1.18	1.52	-0.34	-8.64	-0.76	28	1.40	1.68	-0.28	-7.11	-0.63
14	1.26	1.60	-0.34	-8.64	-0.76	29	1.38	1.69	-0.31	-7.96	-0.70
15	1.17	1.50	-0.33	-8.38	-0.74	30	1.38	1.70	-0.32	-8.18	-0.72

21.Distribution of Pressure Coefficient on Pentagonal Cylinder at L_1=4D, L_2=2D

Tapping Point	Initial Reading (inch of H_2O)	Final Reading (inch of H_2O)	Differences Δh_w (inch of H_2O)	Differences Δh_w (mm of H_2O)	Pressure Coefficient ,Cp	Tapping Point	Initial Reading (inch of H_2O)	Final Reading (inch of H_2O)	Differences Δh_w (inch of H_2O)	Differences Δh_w (mm of H_2O)	Pressure Coefficient ,Cp
1	1.20	1.46	-0.26	-6.60	-0.58	14	1.26	1.62	-0.36	-9.14	-0.81
2	1.29	0.50	0.79	20.07	1.77	15	1.17	1.50	-0.33	-8.38	-0.74
3	1.24	0.56	0.68	17.27	1.52	16	1.30	1.69	-0.39	-9.91	-0.87
4	1.20	0.68	0.52	13.21	1.17	17	1.30	1.69	-0.39	-9.91	-0.87
5	1.20	0.80	0.40	10.16	0.90	18	1.06	1.40	-0.34	-8.64	-0.76
6	1.31	1.55	-0.24	-6.10	-0.54	19	1.28	1.68	-0.40	-10.16	-0.90
7	1.38	1.50	-0.12	-3.05	-0.27	20	1.20	1.55	-0.35	-8.89	-0.78
8	1.20	1.18	0.02	0.51	0.04	21	1.36	1.70	-0.34	-8.64	-0.76
9	1.29	1.30	-0.01	-0.25	-0.02	22	1.39	1.71	-0.32	-8.13	-0.72
10	1.22	1.55	-0.33	-8.38	-0.74	23	1.15	1.46	-0.31	-7.87	-0.69
11	1.24	1.60	-0.36	-9.14	-0.81	24	1.30	1.47	-0.17	-4.32	-0.38
12	1.30	1.66	-0.36	-9.14	-0.81	25	1.30	1.55	-0.25	-6.35	-0.56
13	1.18	1.54	-0.36	-9.14	-0.81						

22.Distribution of Pressure Coefficient on Hexagonal Cylinder at L_1=2D, L_2=2D

Tapping Point	Initial Reading (inch of H_2O)	Final Reading (inch of H_2O)	Differences Δh_w (inch of H_2O)	Differences Δh_w (mm of H_2O)	Pressure Coefficient ,Cp	Tapping Point	Initial Reading (inch of H_2O)	Final Reading (inch of H_2O)	Differences Δh_w (inch of H_2O)	Differences Δh_w (mm of H_2O)	Pressure Coefficient ,Cp
1	1.20	1.46	-0.26	-6.60	-0.58	16	1.30	1.92	-0.62	-15.75	-1.39
2	1.29	0.76	0.53	13.46	1.19	17	1.30	1.89	-0.59	-14.99	-1.32
3	1.24	0.60	0.64	16.26	1.43	18	1.06	1.60	-0.54	-13.72	-1.21
4	1.20	0.60	0.60	15.24	1.34	19	1.28	1.80	-0.52	-13.21	-1.17
5	1.20	0.66	0.54	13.72	1.21	20	1.20	1.72	-0.52	-13.21	-1.17
6	1.31	1.88	-0.57	-14.48	-1.28	21	1.36	1.95	-0.59	-14.99	-1.32
7	1.38	1.90	-0.52	-13.21	-1.17	22	1.39	1.87	-0.48	-12.19	-1.08
8	1.20	1.69	-0.49	-12.45	-1.10	23	1.15	1.45	-0.30	-7.62	-0.67
9	1.29	1.80	-0.51	-12.95	-1.14	24	1.30	1.36	-0.06	-1.52	-0.13
10	1.22	1.71	-0.49	-12.45	-1.10	25	1.30	1.58	-0.28	-7.11	-0.63
11	1.24	1.72	-0.48	-12.19	-1.08	26	1.30	1.53	-0.23	-5.84	-0.52
12	1.30	1.76	-0.46	-11.68	-1.03	27	1.44	1.70	-0.26	-6.60	-0.58
13	1.18	1.63	-0.45	-11.43	-1.01	28	1.40	1.70	-0.30	-7.62	-0.67
14	1.26	1.70	-0.44	-11.18	-0.99	29	1.34	1.65	-0.31	-7.95	-0.70
15	1.17	1.60	-0.43	-10.92	-0.96	30	1.31	1.63	-0.32	-8.18	-0.72

23.Distribution of Pressure Coefficient on Pentagonal Cylinder at L_1=2D, L_2=2D

Tapping Point	Initial Reading (inch of H_2O)	Final Reading (inch of H_2O)	Differences Δh_w (inch of H_2O)	Differences Δh_w (mm of H_2O)	Pressure Coefficient ,Cp	Tapping Point	Initial Reading (inch of H_2O)	Final Reading (inch of H_2O)	Differences Δh_w (inch of H_2O)	Differences Δh_w (mm of H_2O)	Pressure Coefficient ,Cp
1	1.20	1.46	-0.26	-6.60	-0.58	14	1.26	1.49	-0.23	-5.84	-0.52
2	1.29	0.50	0.79	20.07	1.77	15	1.17	1.39	-0.22	-5.59	-0.49
3	1.24	0.58	0.66	16.76	1.48	16	1.30	1.55	-0.25	-6.35	-0.56
4	1.20	0.67	0.53	13.46	1.19	17	1.30	1.55	-0.25	-6.35	-0.56
5	1.20	0.80	0.40	10.16	0.90	18	1.06	1.28	-0.22	-5.59	-0.49
6	1.31	1.44	-0.13	-3.30	-0.29	19	1.28	1.50	-0.22	-5.59	-0.49
7	1.38	1.39	-0.01	-0.25	-0.02	20	1.20	1.40	-0.20	-5.08	-0.45
8	1.20	1.09	0.11	2.79	0.25	21	1.36	1.57	-0.21	-5.33	-0.47
9	1.29	1.27	0.02	0.51	0.04	22	1.39	1.60	-0.21	-5.33	-0.47
10	1.22	1.45	-0.23	-5.84	-0.52	23	1.15	1.40	-0.25	-6.35	-0.56
11	1.24	1.49	-0.25	-6.35	-0.56	24	1.30	1.40	-0.10	-2.54	-0.22
12	1.30	1.54	-0.24	-6.10	-0.54	25	1.30	1.52	-0.22	-5.59	-0.49
13	1.18	1.40	-0.22	-5.59	-0.49						

24.Distribution of Pressure Coefficient on Hexagonal Cylinder at L_1=1D, L_2=2D

Tapping Point	Initial Reading (inch of H_2O)	Final Reading (inch of H_2O)	Differences Δh_w (inch of H_2O)	Differences Δh_w (mm of H_2O)	Pressure Coefficient, Cp	Tapping Point	Initial Reading (inch of H_2O)	Final Reading (inch of H_2O)	Differences Δh_w (inch of H_2O)	Differences Δh_w (mm of H_2O)	Pressure Coefficient , Cp
1	1.20	1.34	-0.14	-3.56	-0.31	16	1.30	1.90	-0.60	-15.24	-1.34
2	1.29	0.89	0.40	10.16	0.90	17	1.30	1.75	-0.45	-11.43	-1.01
3	1.24	0.68	0.56	14.22	1.26	18	1.06	1.50	-0.44	-11.18	-0.99
4	1.20	0.53	0.67	17.02	1.50	19	1.28	1.70	-0.42	-10.67	-0.94
5	1.20	0.40	0.80	20.32	1.79	20	1.20	1.60	-0.40	-10.16	-0.90
6	1.31	1.70	-0.39	-9.91	-0.87	21	1.36	2.20	-0.84	-21.34	-1.88
7	1.38	1.75	-0.37	-9.40	-0.83	22	1.39	2.07	-0.68	-17.27	-1.52
8	1.20	1.52	-0.32	-8.13	-0.72	23	1.15	1.72	-0.57	-14.48	-1.28
9	1.29	1.60	-0.31	-7.87	-0.69	24	1.30	1.56	-0.26	-6.60	-0.58
10	1.22	1.55	-0.33	-8.38	-0.74	25	1.30	1.61	-0.31	-7.87	-0.69
11	1.24	1.62	-0.38	-9.65	-0.85	26	1.30	1.21	0.09	2.29	0.20
12	1.30	1.66	-0.36	-9.14	-0.81	27	1.44	1.10	0.34	8.64	0.76
13	1.18	1.50	-0.32	-8.13	-0.72	28	1.40	1.40	0.00	0.00	0.00
14	1.26	1.56	-0.30	-7.62	-0.67	29	1.36	1.45	-0.09	-2.27	-0.20
15	1.17	1.47	-0.30	-7.62	-0.67	30	1.33	1.44	-0.11	-2.84	-0.25

25.Distribution of Pressure Coefficient on Pentagonal Cylinder at L_1=1D, L_2=2D

Tapping Point	Initial Reading (inch of H_2O)	Final Reading (inch of H_2O)	Differences ,Δh_w (inch of H_2O)	Differences ,Δh_w (mm of H_2O)	Pressure Coefficient, Cp	Tapping Point	Initial Reading (inch of H_2O)	Final Reading (inch of H_2O)	Differences ,Δh_w (inch of H_2O)	Differences ,Δh_w (mm of H_2O)	Pressure Coefficient , Cp
1	1.20	1.34	-0.14	-3.56	-0.31	14	1.26	1.40	-0.14	-3.56	-0.31
2	1.29	0.45	0.84	21.34	1.88	15	1.17	1.30	-0.13	-3.30	-0.29
3	1.24	0.55	0.69	17.53	1.55	16	1.30	1.47	-0.17	-4.32	-0.38
4	1.20	0.62	0.58	14.73	1.30	17	1.30	1.47	-0.17	-4.32	-0.38
5	1.20	0.77	0.43	10.92	0.96	18	1.06	1.19	-0.13	-3.30	-0.29
6	1.31	1.17	0.14	3.56	0.31	19	1.28	1.38	-0.10	-2.54	-0.22
7	1.38	1.15	0.23	5.84	0.52	20	1.20	1.25	-0.05	-1.27	-0.11
8	1.20	0.88	0.32	8.13	0.72	21	1.36	1.50	-0.14	-3.56	-0.31
9	1.29	0.87	0.42	10.67	0.94	22	1.39	1.50	-0.11	-2.79	-0.25
10	1.22	0.98	0.24	6.10	0.54	23	1.15	1.28	-0.13	-3.30	-0.29
11	1.24	1.39	-0.15	-3.81	-0.34	24	1.30	1.30	0.00	0.00	0.00
12	1.30	1.45	-0.15	-3.81	-0.34	25	1.30	1.45	-0.15	-3.81	-0.34
13	1.18	1.30	-0.12	-3.05	-0.27						

26.Distribution of Pressure Coefficient on Hexagonal Cylinder at L_1=8D, L_2=3D

Tapping Point	Initial Reading (inch of H_2O)	Final Reading (inch of H_2O)	Differences ,Δh_w (inch of H_2O)	Differences ,Δh_w (mm of H_2O)	Pressure Coefficient, Cp	Tapping Point	Initial Reading (inch of H_2O)	Final Reading (inch of H_2O)	Differences ,Δh_w (inch of H_2O)	Differences ,Δh_w (mm of H_2O)	Pressure Coefficient ,Cp
1	1.20	1.30	-0.10	-2.54	-0.22	16	1.30	1.84	-0.54	-13.72	-1.21
2	1.29	0.99	0.30	7.62	0.67	17	1.30	1.73	-0.43	-10.92	-0.96
3	1.24	0.80	0.44	11.18	0.99	18	1.06	1.55	-0.49	-12.45	-1.10
4	1.20	0.72	0.48	12.19	1.08	19	1.28	1.70	-0.42	-10.67	-0.94
5	1.20	0.70	0.50	12.70	1.12	20	1.20	1.69	-0.49	-12.45	-1.10
6	1.31	1.88	-0.57	-14.48	-1.28	21	1.36	2.12	-0.76	-19.30	-1.70
7	1.38	1.97	-0.59	-14.99	-1.32	22	1.39	1.93	-0.54	-13.72	-1.21
8	1.20	1.92	-0.72	-18.29	-1.61	23	1.15	1.55	-0.40	-10.16	-0.90
9	1.29	2.16	-0.87	-22.10	-1.95	24	1.30	1.58	-0.28	-7.11	-0.63
10	1.22	2.15	-0.93	-23.62	-2.08	25	1.30	1.88	-0.58	-14.73	-1.30
11	1.24	1.75	-0.51	-12.95	-1.14	26	1.30	1.30	0.00	0.00	0.00
12	1.30	1.80	-0.50	-12.70	-1.12	27	1.44	1.20	0.24	6.10	0.54
13	1.18	1.66	-0.48	-12.19	-1.08	28	1.40	1.32	0.08	2.03	0.18
14	1.26	1.74	-0.48	-12.19	-1.08	29	1.38	1.34	0.04	1.14	0.10
15	1.17	1.60	-0.43	-10.92	-0.96	30	1.30	1.35	-0.05	-1.36	-0.12

27.Distribution of Pressure Coefficient on Pentagonal Cylinder at L_1=8D, L_2=3D

Tapping Point	Initial Reading (inch of H_2O)	Final Reading (inch of H_2O)	Differences ,Δh_w (inch of H_2O)	Differences ,Δh_w (mm of H_2O)	Pressure Coefficient, Cp	Tapping Point	Initial Reading (inch of H_2O)	Final Reading (inch of H_2O)	Differences ,Δh_w (inch of H_2O)	Differences ,Δh_w (mm of H_2O)	Pressure Coefficient , Cp
1	1.20	1.30	-0.10	-2.54	-0.22	14	1.26	1.62	-0.36	-9.14	-0.81
2	1.29	0.20	1.09	27.69	2.44	15	1.17	1.52	-0.35	-8.89	-0.78
3	1.24	0.30	0.94	23.88	2.11	16	1.30	1.70	-0.40	-10.16	-0.90
4	1.20	0.40	0.80	20.32	1.79	17	1.30	1.69	-0.39	-9.91	-0.87
5	1.20	0.70	0.50	12.70	1.12	18	1.06	1.41	-0.35	-8.89	-0.78
6	1.31	1.50	-0.19	-4.83	-0.43	19	1.28	1.64	-0.36	-9.14	-0.81
7	1.38	1.40	-0.02	-0.51	-0.04	20	1.20	1.56	-0.36	-9.14	-0.81
8	1.20	1.05	0.15	3.81	0.34	21	1.36	1.73	-0.37	-9.40	-0.83
9	1.29	1.15	0.14	3.56	0.31	22	1.39	1.70	-0.31	-7.87	-0.69
10	1.22	1.48	-0.26	-6.60	-0.58	23	1.15	1.40	-0.25	-6.35	-0.56
11	1.24	1.66	-0.42	-10.67	-0.94	24	1.30	1.48	-0.18	-4.57	-0.40
12	1.30	1.68	-0.38	-9.65	-0.85	25	1.30	1.45	-0.15	-3.81	-0.34
13	1.18	1.54	-0.36	-9.14	-0.81						

28.Distribution of Pressure Coefficient on Hexagonal Cylinder at L_1=6D, L_2=3D

Tapping Point	Initial Reading (inch of H_2O)	Final Reading (inch of H_2O)	Differences ,Δh_w (inch of H_2O)	Differences ,Δh_w (mm of H_2O)	Pressure Coefficient,Cp	Tapping Point	Initial Reading (inch of H_2O)	Final Reading (inch of H_2O)	Differences ,Δh_w (inch of H_2O)	Differences ,Δh_w (mm of H_2O)	Pressure Coefficient,Cp
1	1.20	1.30	-0.10	-2.54	-0.22	16	1.30	1.62	-0.32	-8.13	-0.72
2	1.29	0.95	0.34	8.64	0.76	17	1.30	1.60	-0.30	-7.62	-0.67
3	1.24	0.89	0.35	8.89	0.78	18	1.06	1.36	-0.30	-7.62	-0.67
4	1.20	0.90	0.30	7.62	0.67	19	1.28	1.56	-0.28	-7.11	-0.63
5	1.20	0.92	0.28	7.11	0.63	20	1.20	1.48	-0.28	-7.11	-0.63
6	1.31	1.62	-0.31	-7.87	-0.69	21	1.36	1.72	-0.36	-9.14	-0.81
7	1.38	1.70	-0.32	-8.13	-0.72	22	1.39	1.69	-0.30	-7.62	-0.67
8	1.20	1.58	-0.38	-9.65	-0.85	23	1.15	1.38	-0.23	-5.84	-0.52
9	1.29	1.89	-0.60	-15.24	-1.34	24	1.30	1.39	-0.09	-2.29	-0.20
10	1.22	2.05	-0.83	-21.08	-1.86	25	1.30	1.60	-0.30	-7.62	-0.67
11	1.24	1.50	-0.26	-6.60	-0.58	26	1.30	1.40	-0.10	-2.54	-0.22
12	1.30	1.56	-0.26	-6.60	-0.58	27	1.44	1.53	-0.09	-2.29	-0.20
13	1.18	1.40	-0.22	-5.59	-0.49	28	1.40	1.50	-0.10	-2.54	-0.22
14	1.26	1.50	-0.24	-6.10	-0.54	29	1.41	1.52	-0.11	-2.73	-0.24
15	1.17	1.46	-0.29	-7.37	-0.65	30	1.38	1.49	-0.11	-2.84	-0.25

29.Distribution of Pressure Coefficient on Pentagonal Cylinder at L_1=6D, L_2=3D

Tapping Point	Initial Reading (inch of H_2O)	Final Reading (inch of H_2O)	Differences Δh_w (inch of H_2O)	Differences Δh_w (mm of H_2O)	Pressure Coefficient ,Cp	Tapping Point	Initial Reading (inch of H_2O)	Final Reading (inch of H_2O)	Differences Δh_w (inch of H_2O)	Differences Δh_w (mm of H_2O)	Pressure Coefficient ,Cp
1	1.20	1.30	-0.10	-2.54	-0.22	14	1.26	1.49	-0.23	-5.84	-0.52
2	1.29	0.32	0.97	24.64	2.17	15	1.17	1.40	-0.23	-5.84	-0.52
3	1.24	0.42	0.82	20.83	1.84	16	1.30	1.54	-0.24	-6.10	-0.54
4	1.20	0.52	0.68	17.27	1.52	17	1.30	1.52	-0.22	-5.59	-0.49
5	1.20	0.72	0.48	12.19	1.08	18	1.06	1.28	-0.22	-5.59	-0.49
6	1.31	1.40	-0.09	-2.29	-0.20	19	1.28	1.50	-0.22	-5.59	-0.49
7	1.38	1.36	0.02	0.51	0.04	20	1.20	1.40	-0.20	-5.08	-0.45
8	1.20	1.02	0.18	4.57	0.40	21	1.36	1.58	-0.22	-5.59	-0.49
9	1.29	1.13	0.16	4.06	0.36	22	1.39	1.56	-0.17	-4.32	-0.38
10	1.22	1.40	-0.18	-4.57	-0.40	23	1.15	1.30	-0.15	-3.81	-0.34
11	1.24	1.47	-0.23	-5.84	-0.52	24	1.30	1.38	-0.08	-2.03	-0.18
12	1.30	1.51	-0.21	-5.33	-0.47	25	1.30	1.40	-0.10	-2.54	-0.22
13	1.18	1.40	-0.22	-5.59	-0.49						

30.Distribution of Pressure Coefficient on Hexagonal Cylinder at L_1=4D, L_2=3D

Tapping Point	Initial Reading (inch of H_2O)	Final Reading (inch of H_2O)	Differences Δh_w (inch of H_2O)	Differences Δh_w (mm of H_2O)	Pressure Coefficient ,Cp	Tapping Point	Initial Reading (inch of H_2O)	Final Reading (inch of H_2O)	Differences Δh_w (inch of H_2O)	Differences Δh_w (mm of H_2O)	Pressure Coefficient ,Cp
1	1.20	1.31	-0.11	-2.79	-0.25	16	1.30	1.74	-0.44	-11.18	-0.99
2	1.29	0.76	0.53	13.46	1.19	17	1.30	1.64	-0.34	-8.64	-0.76
3	1.24	0.58	0.66	16.76	1.48	18	1.06	1.41	-0.35	-8.89	-0.78
4	1.20	0.51	0.69	17.53	1.55	19	1.28	1.60	-0.32	-8.13	-0.72
5	1.20	0.52	0.68	17.27	1.52	20	1.20	1.52	-0.32	-8.13	-0.72
6	1.31	1.70	-0.39	-9.91	-0.87	21	1.36	1.81	-0.45	-11.43	-1.01
7	1.38	1.76	-0.38	-9.65	-0.85	22	1.39	1.76	-0.37	-9.40	-0.83
8	1.20	1.54	-0.34	-8.64	-0.76	23	1.15	1.48	-0.33	-8.38	-0.74
9	1.29	1.61	-0.32	-8.13	-0.72	24	1.30	1.50	-0.20	-5.08	-0.45
10	1.22	1.56	-0.34	-8.64	-0.76	25	1.30	1.82	-0.52	-13.21	-1.17
11	1.24	1.58	-0.34	-8.64	-0.76	26	1.30	1.38	-0.08	-2.03	-0.18
12	1.30	1.61	-0.31	-7.87	-0.69	27	1.44	1.46	-0.02	-0.51	-0.04
13	1.18	1.46	-0.28	-7.11	-0.63	28	1.40	1.50	-0.10	-2.54	-0.22
14	1.26	1.54	-0.28	-7.11	-0.63	29	1.38	1.48	-0.10	-2.61	-0.23
15	1.17	1.47	-0.30	-7.62	-0.67	30	1.37	1.46	-0.09	-2.39	-0.21

31.Distribution of Pressure Coefficient on Pentagonal Cylinder at L_1=4D, L_2=3D

Tapping Point	Initial Reading (inch of H_2O)	Final Reading (inch of H_2O)	Differences Δh_w (inch of H_2O)	Differences Δh_w (mm of H_2O)	Pressure Coefficient ,Cp	Tapping Point	Initial Reading (inch of H_2O)	Final Reading (inch of H_2O)	Differences Δh_w (inch of H_2O)	Differences Δh_w (mm of H_2O)	Pressure Coefficient ,Cp
1	1.20	1.31	-0.11	-2.79	-0.25	14	1.26	1.42	-0.16	-4.06	-0.36
2	1.29	0.38	0.91	23.11	2.04	15	1.17	1.32	-0.15	-3.81	-0.34
3	1.24	0.44	0.80	20.32	1.79	16	1.30	1.48	-0.18	-4.57	-0.40
4	1.20	0.50	0.70	17.78	1.57	17	1.30	1.48	-0.18	-4.57	-0.40
5	1.20	0.70	0.50	12.70	1.12	18	1.06	1.20	-0.14	-3.56	-0.31
6	1.31	1.38	-0.07	-1.78	-0.16	19	1.28	1.45	-0.17	-4.32	-0.38
7	1.38	1.30	0.08	2.03	0.18	20	1.20	1.34	-0.14	-3.56	-0.31
8	1.20	1.02	0.18	4.57	0.40	21	1.36	1.50	-0.14	-3.56	-0.31
9	1.29	1.30	-0.01	-0.25	-0.02	22	1.39	1.54	-0.15	-3.81	-0.34
10	1.22	1.48	-0.26	-6.60	-0.58	23	1.15	1.28	-0.13	-3.30	-0.29
11	1.24	1.39	-0.15	-3.81	-0.34	24	1.30	1.32	-0.02	-0.51	-0.04
12	1.30	1.46	-0.16	-4.06	-0.36	25	1.30	1.40	-0.10	-2.54	-0.22
13	1.18	1.33	-0.15	-3.81	-0.34						

32.Distribution of Pressure Coefficient on Hexagonal Cylinder at L_1=2D, L_2=3D

Tapping Point	Initial Reading (inch of H_2O)	Final Reading (inch of H_2O)	Differences Δh_w (inch of H_2O)	Differences Δh_w (mm of H_2O)	Pressure Coefficient ,Cp	Tapping Point	Initial Reading (inch of H_2O)	Final Reading (inch of H_2O)	Differences Δh_w (inch of H_2O)	Differences Δh_w (mm of H_2O)	Pressure Coefficient ,Cp
1	1.20	1.33	-0.13	-3.30	-0.29	16	1.30	1.60	-0.30	-7.62	-0.67
2	1.29	0.96	0.33	8.38	0.74	17	1.30	1.60	-0.30	-7.62	-0.67
3	1.24	0.80	0.44	11.18	0.99	18	1.06	1.30	-0.24	-6.10	-0.54
4	1.20	0.68	0.52	13.21	1.17	19	1.28	1.54	-0.26	-6.60	-0.58
5	1.20	0.50	0.70	17.78	1.57	20	1.20	1.46	-0.26	-6.60	-0.58
6	1.31	1.60	-0.29	-7.37	-0.65	21	1.36	1.60	-0.24	-6.10	-0.54
7	1.38	1.66	-0.28	-7.11	-0.63	22	1.39	1.65	-0.26	-6.60	-0.58
8	1.20	1.46	-0.26	-6.60	-0.58	23	1.15	1.35	-0.20	-5.08	-0.45
9	1.29	1.55	-0.26	-6.60	-0.58	24	1.30	1.40	-0.10	-2.54	-0.22
10	1.22	1.50	-0.28	-7.11	-0.63	25	1.30	1.60	-0.30	-7.62	-0.67
11	1.24	1.52	-0.28	-7.11	-0.63	26	1.30	1.25	0.05	1.27	0.11
12	1.30	1.55	-0.25	-6.35	-0.56	27	1.44	0.94	0.50	12.70	1.12
13	1.18	1.40	-0.22	-5.59	-0.49	28	1.40	1.15	0.25	6.35	0.56
14	1.26	1.50	-0.24	-6.10	-0.54	29	1.37	1.26	0.11	2.84	0.25
15	1.17	1.40	-0.23	-5.84	-0.52	30	1.32	1.45	-0.13	-3.41	-0.30

33.Distribution of Pressure Coefficient on Pentagonal Cylinder at L_1=2D, L_2=3D

Tapping Point	Initial Reading (inch of H_2O)	Final Reading (inch of H_2O)	Differences Δh_w (inch of H_2O)	Differences Δh_w (mm of H_2O)	Pressure Coefficient ,Cp	Tapping Point	Initial Reading (inch of H_2O)	Final Reading (inch of H_2O)	Differences Δh_w (inch of H_2O)	Differences Δh_w (mm of H_2O)	Pressure Coefficient ,Cp
1	1.20	1.34	-0.14	-3.56	-0.31	14	1.26	1.40	-0.14	-3.56	-0.31
2	1.29	0.38	0.91	23.11	2.04	15	1.17	1.30	-0.13	-3.30	-0.29
3	1.24	0.45	0.79	20.07	1.77	16	1.30	1.49	-0.19	-4.83	-0.43
4	1.20	0.53	0.67	17.02	1.50	17	1.30	1.50	-0.20	-5.08	-0.45
5	1.20	0.68	0.52	13.21	1.17	18	1.06	1.24	-0.18	-4.57	-0.40
6	1.31	1.32	-0.01	-0.25	-0.02	19	1.28	1.45	-0.17	-4.32	-0.38
7	1.38	1.26	0.12	3.05	0.27	20	1.20	1.34	-0.14	-3.56	-0.31
8	1.20	0.96	0.24	6.10	0.54	21	1.36	1.52	-0.16	-4.06	-0.36
9	1.29	1.16	0.13	3.30	0.29	22	1.39	1.54	-0.15	-3.81	-0.34
10	1.22	1.34	-0.12	-3.05	-0.27	23	1.15	1.30	-0.15	-3.81	-0.34
11	1.24	1.40	-0.16	-4.06	-0.36	24	1.30	1.34	-0.04	-1.02	-0.09
12	1.30	1.46	-0.16	-4.06	-0.36	25	1.30	1.40	-0.10	-2.54	-0.22
13	1.18	1.30	-0.12	-3.05	-0.27						

34.Distribution of Pressure Coefficient on Hexagonal Cylinder at L_1=1D, L_2=3D

Tapping Point	Initial Reading (inch of H_2O)	Final Reading (inch of H_2O)	Differences Δh_w (inch of H_2O)	Differences Δh_w (mm of H_2O)	Pressure Coefficient ,Cp	Tapping Point	Initial Reading (inch of H_2O)	Final Reading (inch of H_2O)	Differences Δh_w (inch of H_2O)	Differences Δh_w (mm of H_2O)	Pressure Coefficient ,Cp
1	1.20	1.32	-0.12	-3.05	-0.27	16	1.30	1.48	-0.18	-4.57	-0.40
2	1.29	1.01	0.28	7.11	0.63	17	1.30	1.48	-0.18	-4.57	-0.40
3	1.24	0.88	0.36	9.14	0.81	18	1.06	1.20	-0.14	-3.56	-0.31
4	1.20	0.76	0.44	11.18	0.99	19	1.28	1.44	-0.16	-4.06	-0.36
5	1.20	0.61	0.59	14.99	1.32	20	1.20	1.33	-0.13	-3.30	-0.29
6	1.31	1.50	-0.19	-4.83	-0.43	21	1.36	1.50	-0.14	-3.56	-0.31
7	1.38	1.55	-0.17	-4.32	-0.38	22	1.39	1.54	-0.15	-3.81	-0.34
8	1.20	1.36	-0.16	-4.06	-0.36	23	1.15	1.30	-0.15	-3.81	-0.34
9	1.29	1.46	-0.17	-4.32	-0.38	24	1.30	1.32	-0.02	-0.51	-0.04
10	1.22	1.40	-0.18	-4.57	-0.40	25	1.30	1.50	-0.20	-5.08	-0.45
11	1.24	1.40	-0.16	-4.06	-0.36	26	1.30	1.24	0.06	1.52	0.13
12	1.30	1.47	-0.17	-4.32	-0.38	27	1.44	0.80	0.64	16.26	1.43
13	1.18	1.32	-0.14	-3.56	-0.31	28	1.40	1.00	0.40	10.16	0.90
14	1.26	1.41	-0.15	-3.81	-0.34	29	1.34	1.15	0.19	4.77	0.42
15	1.17	1.30	-0.13	-3.30	-0.29	30	1.18	1.30	-0.13	-3.18	-0.28

35.Distribution of Pressure Coefficient on Pentagonal Cylinder at L_1=1D, L_2=3D

Tapping Point	Initial Reading (inch of H_2O)	Final Reading (inch of H_2O)	Differences Δh_w (inch of H_2O)	Differences Δh_w (mm of H_2O)	Pressure Coefficient ,Cp	Tapping Point	Initial Reading (inch of H_2O)	Final Reading (inch of H_2O)	Differences Δh_w (inch of H_2O)	Differences Δh_w (mm of H_2O)	Pressure Coefficient ,Cp
1	1.20	1.32	-0.12	-3.05	-0.27	14	1.26	1.50	-0.24	-6.10	-0.54
2	1.29	0.45	0.84	21.34	1.88	15	1.17	1.40	-0.23	-5.84	-0.52
3	1.24	0.50	0.74	18.80	1.66	16	1.30	1.60	-0.30	-7.62	-0.67
4	1.20	0.57	0.63	16.00	1.41	17	1.30	1.60	-0.30	-7.62	-0.67
5	1.20	0.72	0.48	12.19	1.08	18	1.06	1.33	-0.27	-6.86	-0.61
6	1.31	1.28	0.03	0.76	0.07	19	1.28	1.56	-0.28	-7.11	-0.63
7	1.38	1.22	0.16	4.06	0.36	20	1.20	1.46	-0.26	-6.60	-0.58
8	1.20	0.94	0.26	6.60	0.58	21	1.36	1.85	-0.49	-12.45	-1.10
9	1.29	1.01	0.28	7.11	0.63	22	1.39	1.76	-0.37	-9.40	-0.83
10	1.22	1.20	0.02	0.51	0.04	23	1.15	1.45	-0.30	-7.62	-0.67
11	1.24	1.52	-0.28	-7.11	-0.63	24	1.30	1.48	-0.18	-4.57	-0.40
12	1.30	1.56	-0.26	-6.60	-0.58	25	1.30	1.46	-0.16	-4.06	-0.36
13	1.18	1.40	-0.22	-5.59	-0.49						

36.Distribution of Pressure Coefficient on Hexagonal Cylinder at L_1=8D, L_2=5D

Tapping Point	Initial Reading (inch of H_2O)	Final Reading (inch of H_2O)	Differences Δh_w (inch of H_2O)	Differences Δh_w (mm of H_2O)	Pressure Coefficient , Cp	Tapping Point	Initial Reading (inch of H_2O)	Final Reading (inch of H_2O)	Differences Δh_w (inch of H_2O)	Differences Δh_w (mm of H_2O)	Pressure Coefficient , Cp
1	1.20	1.20	0.00	0.00	0.00	16	1.30	1.90	-0.60	-15.24	-1.34
2	1.29	0.72	0.57	14.48	1.28	17	1.30	1.78	-0.48	-12.19	-1.08
3	1.24	0.52	0.72	18.29	1.61	18	1.06	1.61	-0.55	-13.97	-1.23
4	1.20	0.40	0.80	20.32	1.79	19	1.28	1.76	-0.48	-12.19	-1.08
5	1.20	0.28	0.92	23.37	2.06	20	1.20	1.75	-0.55	-13.97	-1.23
6	1.31	1.89	-0.58	-14.73	-1.30	21	1.36	1.96	-0.60	-15.24	-1.34
7	1.38	1.96	-0.58	-14.73	-1.30	22	1.39	1.88	-0.49	-12.45	-1.10
8	1.20	1.78	-0.58	-14.73	-1.30	23	1.15	1.50	-0.35	-8.89	-0.78
9	1.29	1.80	-0.51	-12.95	-1.14	24	1.30	1.58	-0.28	-7.11	-0.63
10	1.22	1.74	-0.52	-13.21	-1.17	25	1.30	1.90	-0.60	-15.24	-1.34
11	1.24	1.88	-0.64	-16.26	-1.43	26	1.30	0.80	0.50	12.70	1.12
12	1.30	1.90	-0.60	-15.24	-1.34	27	1.44	0.85	0.59	14.99	1.32
13	1.18	1.75	-0.57	-14.48	-1.28	28	1.40	1.08	0.32	8.13	0.72
14	1.26	1.80	-0.54	-13.72	-1.21	29	1.34	1.15	0.19	4.77	0.42
15	1.17	1.62	-0.45	-11.43	-1.01	30	1.25	1.25	0.00	0.00	0.00

37.Distribution of Pressure Coefficient on Pentagonal Cylinder at L_1=8D, L_2=5D

Tapping Point	Initial Reading (inch of H_2O)	Final Reading (inch of H_2O)	Differences Δh_w (inch of H_2O)	Differences Δh_w (mm of H_2O)	Pressure Coefficient ,Cp	Tapping Point	Initial Reading (inch of H_2O)	Final Reading (inch of H_2O)	Differences Δh_w (inch of H_2O)	Differences Δh_w (mm of H_2O)	Pressure Coefficient ,Cp
1	1.20	1.20	0.00	0.00	0.00	14	1.26	1.60	-0.34	-8.64	-0.76
2	1.29	0.10	1.19	30.23	2.67	15	1.17	1.50	-0.33	-8.38	-0.74
3	1.24	0.20	1.04	26.42	2.33	16	1.30	1.70	-0.40	-10.16	-0.90
4	1.20	0.34	0.86	21.84	1.93	17	1.30	1.66	-0.36	-9.14	-0.81
5	1.20	0.59	0.61	15.49	1.37	18	1.06	1.40	-0.34	-8.64	-0.76
6	1.31	1.40	-0.09	-2.29	-0.20	19	1.28	1.60	-0.32	-8.13	-0.72
7	1.38	1.35	0.03	0.76	0.07	20	1.20	1.54	-0.34	-8.64	-0.76
8	1.20	1.00	0.20	5.08	0.45	21	1.36	1.72	-0.36	-9.14	-0.81
9	1.29	0.93	0.36	9.14	0.81	22	1.39	1.64	-0.25	-6.35	-0.56
10	1.22	1.27	-0.05	-1.27	-0.11	23	1.15	1.33	-0.18	-4.57	-0.40
11	1.24	1.60	-0.36	-9.14	-0.81	24	1.30	1.45	-0.15	-3.81	-0.34
12	1.30	1.67	-0.37	-9.40	-0.83	25	1.30	1.38	-0.08	-2.03	-0.18
13	1.18	1.53	-0.35	-8.89	-0.78						

38.Distribution of Pressure Coefficient on Hexagonal Cylinder at L_1=6D, L_2=5D

Tapping Point	Initial Reading (inch of H_2O)	Final Reading (inch of H_2O)	Differences Δh_w (inch of H_2O)	Differences Δh_w (mm of H_2O)	Pressure Coefficient ,Cp	Tapping Point	Initial Reading (inch of H_2O)	Final Reading (inch of H_2O)	Differences Δh_w (inch of H_2O)	Differences Δh_w (mm of H_2O)	Pressure Coefficient ,Cp
1	1.20	1.20	0.00	0.00	0.00	16	1.30	1.90	-0.60	-15.24	-1.34
2	1.29	0.82	0.47	11.94	1.05	17	1.30	1.80	-0.50	-12.70	-1.12
3	1.24	0.60	0.64	16.26	1.43	18	1.06	1.63	-0.57	-14.48	-1.28
4	1.20	0.49	0.71	18.03	1.59	19	1.28	1.77	-0.49	-12.45	-1.10
5	1.20	0.36	0.84	21.34	1.88	20	1.20	1.78	-0.58	-14.73	-1.30
6	1.31	1.90	-0.59	-14.99	-1.32	21	1.36	1.97	-0.61	-15.49	-1.37
7	1.38	1.96	-0.58	-14.73	-1.30	22	1.39	1.85	-0.46	-11.68	-1.03
8	1.20	1.80	-0.60	-15.24	-1.34	23	1.15	1.50	-0.35	-8.89	-0.78
9	1.29	1.84	-0.55	-13.97	-1.23	24	1.30	1.55	-0.25	-6.35	-0.56
10	1.22	1.74	-0.52	-13.21	-1.17	25	1.30	1.89	-0.59	-14.99	-1.32
11	1.24	1.98	-0.74	-18.80	-1.66	26	1.30	0.88	0.42	10.67	0.94
12	1.30	1.94	-0.64	-16.26	-1.43	27	1.44	0.92	0.52	13.21	1.17
13	1.18	1.80	-0.62	-15.75	-1.39	28	1.40	1.11	0.29	7.37	0.65
14	1.26	1.82	-0.56	-14.22	-1.26	29	1.37	1.20	0.17	4.32	0.38
15	1.17	1.62	-0.45	-11.43	-1.01	30	1.25	1.245	0.005	0.13	0.01

39.Distribution of Pressure Coefficient on Pentagonal Cylinder at L_1=6D, L_2=5D

Tapping Point	Initial Reading (inch of H_2O)	Final Reading (inch of H_2O)	Differences ,Δh_w (inch of H_2O)	Differences ,Δh_w (mm of H_2O)	Pressure Coefficient , Cp	Tapping Point	Initial Reading (inch of H_2O)	Final Reading (inch of H_2O)	Differences ,Δh_w (inch of H_2O)	Differences ,Δh_w (mm of H_2O)	Pressure Coefficient , Cp
1	1.20	1.20	0.00	0.00	0.00	14	1.26	1.60	-0.34	-8.64	-0.76
2	1.29	0.20	1.09	27.69	2.44	15	1.17	1.50	-0.33	-8.38	-0.74
3	1.24	0.30	0.94	23.88	2.11	16	1.30	1.70	-0.40	-10.16	-0.90
4	1.20	0.40	0.80	20.32	1.79	17	1.30	1.68	-0.38	-9.65	-0.85
5	1.20	0.60	0.60	15.24	1.34	18	1.06	1.40	-0.34	-8.64	-0.76
6	1.31	1.45	-0.14	-3.56	-0.31	19	1.28	1.60	-0.32	-8.13	-0.72
7	1.38	1.39	-0.01	-0.25	-0.02	20	1.20	1.55	-0.35	-8.89	-0.78
8	1.20	1.02	0.18	4.57	0.40	21	1.36	1.70	-0.34	-8.64	-0.76
9	1.29	1.22	0.07	1.78	0.16	22	1.39	1.67	-0.28	-7.11	-0.63
10	1.22	1.50	-0.28	-7.11	-0.63	23	1.15	1.32	-0.17	-4.32	-0.38
11	1.24	1.60	-0.36	-9.14	-0.81	24	1.30	1.47	-0.17	-4.32	-0.38
12	1.30	1.65	-0.35	-8.89	-0.78	25	1.30	1.38	-0.08	-2.03	-0.18
13	1.18	1.52	-0.34	-8.64	-0.76						

40.Distribution of Pressure Coefficient on Hexagonal Cylinder at L_1=4D, L_2=5D

Tapping Point	Initial Reading (inch of H_2O)	Final Reading (inch of H_2O)	Differences ,Δh_w (inch of H_2O)	Differences ,Δh_w (mm of H_2O)	Pressure Coefficient, Cp	Tapping Point	Initial Reading (inch of H_2O)	Final Reading (inch of H_2O)	Differences ,Δh_w (inch of H_2O)	Differences ,Δh_w (mm of H_2O)	Pressure Coefficient ,Cp
1	1.20	1.20	0.00	0.00	0.00	16	1.30	1.68	-0.38	-9.65	-0.85
2	1.29	0.84	0.45	11.43	1.01	17	1.30	1.70	-0.40	-10.16	-0.90
3	1.24	0.66	0.58	14.73	1.30	18	1.06	1.45	-0.39	-9.91	-0.87
4	1.20	0.57	0.63	16.00	1.41	19	1.28	1.60	-0.32	-8.13	-0.72
5	1.20	0.40	0.80	20.32	1.79	20	1.20	1.58	-0.38	-9.65	-0.85
6	1.31	1.69	-0.38	-9.65	-0.85	21	1.36	1.69	-0.33	-8.38	-0.74
7	1.38	1.72	-0.34	-8.64	-0.76	22	1.39	1.65	-0.26	-6.60	-0.58
8	1.20	1.52	-0.32	-8.13	-0.72	23	1.15	1.34	-0.19	-4.83	-0.43
9	1.29	1.60	-0.31	-7.87	-0.69	24	1.30	1.48	-0.18	-4.57	-0.40
10	1.22	1.54	-0.32	-8.13	-0.72	25	1.30	1.70	-0.40	-10.16	-0.90
11	1.24	1.63	-0.39	-9.91	-0.87	26	1.30	1.10	0.20	5.08	0.45
12	1.30	1.69	-0.39	-9.91	-0.87	27	1.44	0.90	0.54	13.72	1.21
13	1.18	1.54	-0.36	-9.14	-0.81	28	1.40	1.09	0.31	7.87	0.69
14	1.26	1.60	-0.34	-8.64	-0.76	29	1.31	1.15	0.16	3.98	0.35
15	1.17	1.48	-0.31	-7.87	-0.69	30	1.20	1.19	0.01	0.25	0.02

41.Distribution of Pressure Coefficient on Pentagonal Cylinder at L_1=4D, L_2=5D

Tapping Point	Initial Reading (inch of H_2O)	Final Reading (inch of H_2O)	Differences Δh_w (inch of H_2O)	Differences Δh_w (mm of H_2O)	Pressure Coefficient ,Cp	Tapping Point	Initial Reading (inch of H_2O)	Final Reading (inch of H_2O)	Differences Δh_w (inch of H_2O)	Differences Δh_w (mm of H_2O)	Pressure Coefficient ,Cp
1	1.20	1.20	0.00	0.00	0.00	14	1.26	1.72	-0.46	-11.68	-1.03
2	1.29	0.22	1.07	27.18	2.40	15	1.17	1.60	-0.43	-10.92	-0.96
3	1.24	0.33	0.91	23.11	2.04	16	1.30	1.80	-0.50	-12.70	-1.12
4	1.20	0.46	0.74	18.80	1.66	17	1.30	1.78	-0.48	-12.19	-1.08
5	1.20	0.68	0.52	13.21	1.17	18	1.06	1.52	-0.46	-11.68	-1.03
6	1.31	1.51	-0.20	-5.08	-0.45	19	1.28	1.70	-0.42	-10.67	-0.94
7	1.38	1.46	-0.08	-2.03	-0.18	20	1.20	1.66	-0.46	-11.68	-1.03
8	1.20	1.08	0.12	3.05	0.27	21	1.36	1.81	-0.45	-11.43	-1.01
9	1.29	1.22	0.07	1.78	0.16	22	1.39	1.74	-0.35	-8.89	-0.78
10	1.22	1.52	-0.30	-7.62	-0.67	23	1.15	1.37	-0.22	-5.59	-0.49
11	1.24	1.72	-0.48	-12.19	-1.08	24	1.30	1.50	-0.20	-5.08	-0.45
12	1.30	1.77	-0.47	-11.94	-1.05	25	1.30	1.40	-0.10	-2.54	-0.22
13	1.18	1.64	-0.46	-11.68	-1.03						

42.Distribution of Pressure Coefficient on Hexagonal Cylinder at L_1=2D, L_2=5D

Tapping Point	Initial Reading (inch of H_2O)	Final Reading (inch of H_2O)	Differences Δh_w (inch of H_2O)	Differences Δh_w (mm of H_2O)	Pressure Coefficient ,Cp	Tapping Point	Initial Reading (inch of H_2O)	Final Reading (inch of H_2O)	Differences Δh_w (inch of H_2O)	Differences Δh_w (mm of H_2O)	Pressure Coefficient ,Cp
1	1.20	1.20	0.00	0.00	0.00	16	1.30	1.40	-0.10	-2.54	-0.22
2	1.29	0.84	0.45	11.43	1.01	17	1.30	1.41	-0.11	-2.79	-0.25
3	1.24	0.68	0.56	14.22	1.26	18	1.06	1.17	-0.11	-2.79	-0.25
4	1.20	0.60	0.60	15.24	1.34	19	1.28	1.39	-0.11	-2.79	-0.25
5	1.20	0.46	0.74	18.80	1.66	20	1.20	1.30	-0.10	-2.54	-0.22
6	1.31	1.47	-0.16	-4.06	-0.36	21	1.36	1.46	-0.10	-2.54	-0.22
7	1.38	1.51	-0.13	-3.30	-0.29	22	1.39	1.47	-0.08	-2.03	-0.18
8	1.20	1.30	-0.10	-2.54	-0.22	23	1.15	1.20	-0.05	-1.27	-0.11
9	1.29	1.40	-0.11	-2.79	-0.25	24	1.30	1.36	-0.06	-1.52	-0.13
10	1.22	1.35	-0.13	-3.30	-0.29	25	1.30	1.48	-0.18	-4.57	-0.40
11	1.24	1.34	-0.10	-2.54	-0.22	26	1.30	1.10	0.20	5.08	0.45
12	1.30	1.40	-0.10	-2.54	-0.22	27	1.44	0.88	0.56	14.22	1.26
13	1.18	1.30	-0.12	-3.05	-0.27	28	1.40	1.05	0.35	8.89	0.78
14	1.26	1.39	-0.13	-3.30	-0.29	29	1.30	1.14	0.16	4.09	0.36
15	1.17	1.30	-0.13	-3.30	-0.29	30	1.25	1.245	0.005	0.13	0.01

43.Distribution of Pressure Coefficient on Pentagonal Cylinder at L_1=2D, L_2=5D

Tapping Point	Initial Reading (inch of H_2O)	Final Reading (inch of H_2O)	Differences Δh_w (inch of H_2O)	Differences Δh_w (mm of H_2O)	Pressure Coefficient ,Cp	Tapping Point	Initial Reading (inch of H_2O)	Final Reading (inch of H_2O)	Differences Δh_w (inch of H_2O)	Differences Δh_w (mm of H_2O)	Pressure Coefficient ,Cp
1	1.20	1.19	0.01	0.25	0.02	14	1.26	1.54	-0.28	-7.11	-0.63
2	1.29	0.32	0.97	24.64	2.17	15	1.17	1.43	-0.26	-6.60	-0.58
3	1.24	0.41	0.83	21.08	1.86	16	1.30	1.62	-0.32	-8.13	-0.72
4	1.20	0.49	0.71	18.03	1.59	17	1.30	1.60	-0.30	-7.62	-0.67
5	1.20	0.65	0.55	13.97	1.23	18	1.06	1.32	-0.26	-6.60	-0.58
6	1.31	1.37	-0.06	-1.52	-0.13	19	1.28	1.51	-0.23	-5.84	-0.52
7	1.38	1.30	0.08	2.03	0.18	20	1.20	1.46	-0.26	-6.60	-0.58
8	1.20	0.98	0.22	5.59	0.49	21	1.36	1.65	-0.29	-7.37	-0.65
9	1.29	1.12	0.17	4.32	0.38	22	1.39	1.60	-0.21	-5.33	-0.47
10	1.22	1.34	-0.12	-3.05	-0.27	23	1.15	1.29	-0.14	-3.56	-0.31
11	1.24	1.52	-0.28	-7.11	-0.63	24	1.30	1.46	-0.16	-4.06	-0.36
12	1.30	1.58	-0.28	-7.11	-0.63	25	1.30	1.36	-0.06	-1.52	-0.13
13	1.18	1.45	-0.27	-6.86	-0.61						

44.Distribution of Pressure Coefficient on Hexagonal Cylinder at L_1=1D, L_2=5D

Tapping Point	Initial Reading (inch of H_2O)	Final Reading (inch of H_2O)	Differences Δh_w (inch of H_2O)	Differences Δh_w (mm of H_2O)	Pressure Coefficient ,Cp	Tapping Point	Initial Reading (inch of H_2O)	Final Reading (inch of H_2O)	Differences Δh_w (inch of H_2O)	Differences Δh_w (mm of H_2O)	Pressure Coefficient , Cp
1	1.20	1.18	0.02	0.51	0.04	16	1.30	1.41	-0.11	-2.79	-0.25
2	1.29	0.84	0.45	11.43	1.01	17	1.30	1.39	-0.09	-2.29	-0.20
3	1.24	0.68	0.56	14.22	1.26	18	1.06	1.14	-0.08	-2.03	-0.18
4	1.20	0.62	0.58	14.73	1.30	19	1.28	1.34	-0.06	-1.52	-0.13
5	1.20	0.50	0.70	17.78	1.57	20	1.20	1.28	-0.08	-2.03	-0.18
6	1.31	1.45	-0.14	-3.56	-0.31	21	1.36	1.43	-0.07	-1.78	-0.16
7	1.38	1.48	-0.10	-2.54	-0.22	22	1.39	1.40	-0.01	-0.25	-0.02
8	1.20	1.28	-0.08	-2.03	-0.18	23	1.15	1.17	-0.02	-0.51	-0.04
9	1.29	1.38	-0.09	-2.29	-0.20	24	1.30	1.30	0.00	0.00	0.00
10	1.22	1.31	-0.09	-2.29	-0.20	25	1.30	1.44	-0.14	-3.56	-0.31
11	1.24	1.30	-0.06	-1.52	-0.13	26	1.30	1.06	0.24	6.10	0.54
12	1.30	1.39	-0.09	-2.29	-0.20	27	1.44	0.75	0.69	17.53	1.55
13	1.18	1.25	-0.07	-1.78	-0.16	28	1.40	0.92	0.48	12.19	1.08

14	1.26	1.34	-0.08	-2.03	-0.18	29	1.34	1.12	0.22	5.46	0.48
15	1.17	1.25	-0.08	-2.03	-0.18	30	1.31	1.28	0.03	0.68	0.06

45.Distribution of Pressure Coefficient on Pentagonal Cylinder at L_1=1D, L_2=5D

Tapping Point	Initial Reading (inch of H_2O)	Final Reading (inch of H_2O)	Differences ,Δh_w (inch of H_2O)	Differences ,Δh_w (mm of H_2O)	Pressure Coefficient ,Cp	Tapping Point	Initial Reading (inch of H_2O)	Final Reading (inch of H_2O)	Differences ,Δh_w (inch of H_2O)	Differences ,Δh_w (mm of H_2O)	Pressure Coefficient ,Cp
1	1.20	1.19	0.01	0.25	0.02	14	1.26	1.63	-0.37	-9.40	-0.83
2	1.29	0.30	0.99	25.15	2.22	15	1.17	1.55	-0.38	-9.65	-0.85
3	1.24	0.39	0.85	21.59	1.91	16	1.30	1.76	-0.46	-11.68	-1.03
4	1.20	0.49	0.71	18.03	1.59	17	1.30	1.71	-0.41	-10.41	-0.92
5	1.20	0.67	0.53	13.46	1.19	18	1.06	1.46	-0.40	-10.16	-0.90
6	1.31	1.39	-0.08	-2.03	-0.18	19	1.28	1.65	-0.37	-9.40	-0.83
7	1.38	1.30	0.08	2.03	0.18	20	1.20	1.58	-0.38	-9.65	-0.85
8	1.20	0.96	0.24	6.10	0.54	21	1.36	1.89	-0.53	-13.46	-1.19
9	1.29	0.99	0.30	7.62	0.67	22	1.39	1.76	-0.37	-9.40	-0.83
10	1.22	1.24	-0.02	-0.51	-0.04	23	1.15	1.35	-0.20	-5.08	-0.45
11	1.24	1.68	-0.44	-11.18	-0.99	24	1.30	1.50	-0.20	-5.08	-0.45
12	1.30	1.72	-0.42	-10.67	-0.94	25	1.30	1.40	-0.10	-2.54	-0.22
13	1.18	1.57	-0.39	-9.91	-0.87						

46. Variation of Drag and Lift Coefficient at Various Angles of Attack on Single Hexagonal Cylinder

Angle of Attack ,degree( )	0^0	10^0	20^0	30^0	40^0	50^0
Drag	0.96	0.5	0.84	0.7	0.86	0.8
Lift	0.038	0.126	0.3	0.027	-0.0008	-0.22

47. Variation of Drag and Lift Coefficient at Various Angles of Attack on Single Pentagonal Cylinder

Angle of Attack ,degree( )	0^0	9^0	18^0	27^0	36^0	45^0	54^0	63^0	72^0
Drag	1.48	1.30	1.22	1.44	1.54	1.60	1.61	1.63	1.57
Lift	-0.11	0.06	-0.52	-0.42	-0.27	-0.17	-0.17	-0.14	-0.08

48. Variation of Drag Coefficients on Hexagonal Cylinder with L_1 for different values of L_2

L_1	C_D for L_2=2D	C_D for L_2=3D	C_D for L_2=5D
1D	0.63	0.89	0.97
2D	1.10	1.04	0.94
4D	0.32	1.01	1.39
6D	0.51	0.53	1.80
8D	1.20	1.26	1.87

49. Variation of Lift Coefficients on Hexagonal Cylinder with L_1 for different values of L_2

L_1	C_L for L_2=2D	C_L for L_2=3D	C_L for L_2=5D
1D	-0.79	0.06	0.04
2D	-0.25	0	-0.05
4D	0.23	-0.33	-0.22
6D	-0.14	-0.04	0.09
8D	0.14	0.17	0.02

50. Variation of Drag Coefficients on Pentagonal Cylinder with L_1 for different values of L_2

L_1	C_D for L_2=2D	C_D for L_2=3D	C_D for L_2=5D
1D	0.95	1.08	1.39
2D	0.84	0.41	1.12
4D	1.00	0.88	1.37
6D	1.14	0.82	1.26
8D	1.09	1.29	1.40

51. Variation of Lift Coefficients on Pentagonal Cylinder with L_1 for different values of L_2

L_1	C_L for L_2=2D	C_L for L_2=3D	C_L for L_2=5D
1D	0.07	0.13	0.05
2D	-0.11	0.09	-0.11
4D	-0.14	-0.11	-0.22
6D	-0.14	-0.08	-0.19
8D	-0.37	-0.16	-0.13